nature synthesis

Supplementary information

https://doi.org/10.1038/s44160-025-00876-7

Dual C–H functionalization of polyolefins for covalent adaptable network formation via cooperative electrolysis

In the format provided by the authors and unedited

Table of Contents

General Experimental Details

All reagents were purchased from commercial suppliers and used as received unless otherwise indicated. Dicyclopentadiene (DCPD) was purchased from Sigma-Aldrich; Grubbs' 2nd generation catalyst (G2) was purchased from Sigma-Aldrich, and tributyl phosphite (TBP) was purchased from TCI chemicals. *N*-tetrabutylammonium hexafluorophosphate 98% was purchased from Thermo Scientific Chemicals; *N*-hydroxyphthalimide 97%, *N*-Hydroxysuccinimide 98%, *N*-Hydroxytetrachlorophthalimide, pyridine ACS reagent, ≥99%, Tetrabutylammonium fluoride solution (1.0 M in THF), Hydrazine monohydrate reagent grade, ≥97% were purchased from Sigma-Aldrich. All solvents were purchased from commercial suppliers and used without further purification. TLC plates with fluorescent indicator F254 were used and visualized with UV lamps or KMnO4 Stain. Duocel® reticulated vitreous carbon (RVC) foam (100 pores per inch) was purchased from ERG Materials & Aerospace. The measured surface area of the Duocel® foam can be found at: https://ergaerospace.com/duocel-foam-surface-area/.

Deuterated solvents were obtained from Cambridge Isotope Laboratories, Inc. and used without further modification. Nuclear magnetic resonance (NMR) spectra were recorded on either a Varian Unity Inova 500 MHz spectrometer or a Bruker CB500 spectrometer. ^{1}H chemical shifts are reported in parts per million (ppm) relative to tetramethylsilane (TMS) and referenced to the residual solvent peak ($CHCl_3$; δH = 7.26 ppm). Column chromatography was performed using a Biotage Isolera system with Silicycle SiliaSep HP flash cartridges. Infrared (IR) spectra were acquired using a PerkinElmer Spectrum 2 instrument equipped with an attenuated total reflection (ATR) sampler. Low-resolution mass spectrometry (LRMS) data were collected at the UIUC Mass Spectrometry Laboratory using electrospray ionization (ESI) or electron ionization (EI) methods. Gas chromatography-mass spectrometry (GC-MS) analyses were conducted with an Agilent 7820A GC system coupled to a 5977E mass selective detector (MSD), equipped with an Agilent J&W DB-5MS-U1 column (length = 30 m, diameter = 0.25 mm, film thickness = 0.25 µm). The GC oven was programmed to hold at 80 °C for 2 minutes, ramp at 20 °C/min to 280 °C, and hold at 280 °C for 5 minutes. Size exclusion chromatography (SEC) was performed using an Agilent 1260 Infinity system, equipped with an isocratic pump, degasser, autosampler, and a series of four Waters HR Styragel columns (7.8 × 300 mm; HR1, HR3, HR4, and HR5) in tetrahydrofuran (THF) at 25 °C with a flow rate of 1 mL min^{-1}. The system incorporated a triple-detection setup, including an Agilent 1200 series G1362A Infinity Refractive Index Detector (RID), a Wyatt ViscoStar II viscometer, and a Wyatt MiniDAWN Treos multi-angle light-scattering detector. Molecular weights and dispersities (Đ) were determined using a 12-point calibration curve based on narrow-dispersity polystyrene standards ranging from 980 to 1,013,000 kDa. Dynamic mechanical analysis (DMA) was performed on a TA Instruments RSA II using tensile grips under a nitrogen environment. The gauge length was set to 4-10 mm, with a dynamic loading frequency of 1 Hz and a strain amplitude of 0.1%. The temperature was increased at a rate of 3 °C/min.

General Procedure for the Preparation of Deconstructed pDCPD Oligomers

General FROMP Procedure of pDCPD & pH_2DCPD:

The second-generation Grubbs catalyst (GC2[1], 5.1 mg) was weighed in a 20 mL vial, and tributyl phosphite (TBP, 1.64 μL) was added to this vial to wet the GC2 powder. Then the monomer mixture (4.0 g DCPD with 319 mg iPrSi7 or 4.0 g exo-H2DCPD with 314 mg iPrSi7) was weighted into this vial, and the mixture was subjected to sonication for 5 minutes until all catalyst was dissolved to obtain a clear resin for FROMP. The resin was transformed into a test tube, and a soldering iron was used to initiate the FROMP to give the resulting materials for deconstruction.

General Procedure of Deconstruction of pDCPD & pH_2DCPD Oligomers:

The materials obtained via FROMP, a drop of ethyl vinyl ether, and dry THF (20 mL per gram of the material) were added to a round bottle flask. TBAF solution (1.0 M in THF, 2.2 equiv regards to iPrSi7) was added and the mixture was stirred slowly at room temperature until all solid material was dissolved. The reaction mixture was added dropwise to a stirred methanol solution (100 mL per gram of the material) and the oligomers precipitated out, which was then separated by a Buchner funnel. The solid was washed with methanol. The oligomer sample was air-dried for 1 hour and then transferred to a flask for vacuum dry to give the oligomers as a white powder. The synthesized deconstructed oligo-DCPD exhibited molecular weights (M_n) ranging from 3.3 to 8.7 kDa, with the corresponding SEC traces provided on page 4.

SEC Traces of Deconstructed Oligo-DCPD with Various MW

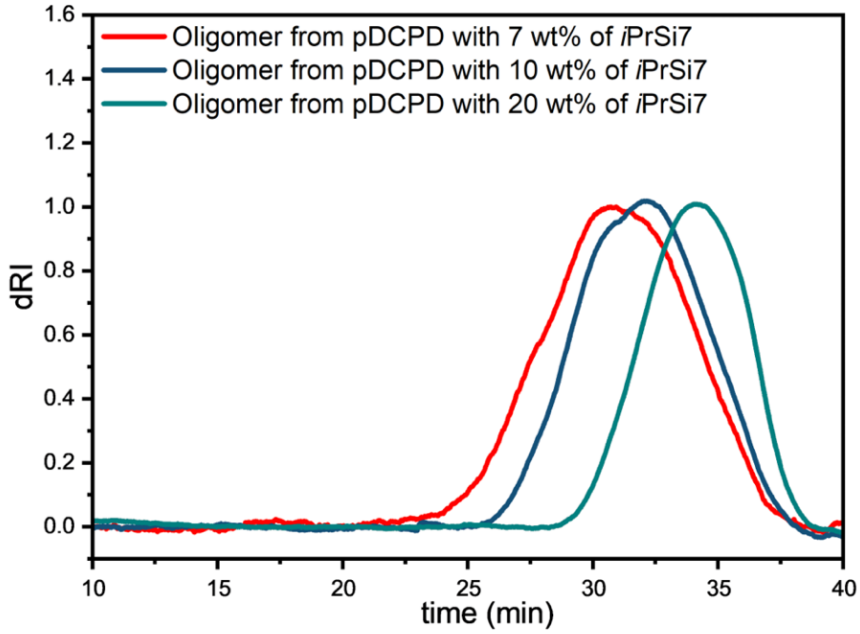

Supplementary Fig. 1 Comparison of SEC traces of oligo-DCPD with varying molecular weights. The synthesized deconstructed oligo-DCPD exhibited number-average molecular weights (Mn) ranging from 3.3 to 8.7 kDa. Specifically, samples prepared with 20 wt% *i*PrSi7 had an M_n of 3.3 kDa, those with 10 wt% *i*PrSi7 reached 6.6 kDa, and 7 wt% *i*PrSi7 yielded an M_n of 8.7 kDa.

Monomer Synthesis

Synthesis of Exo-H_2DCPD:

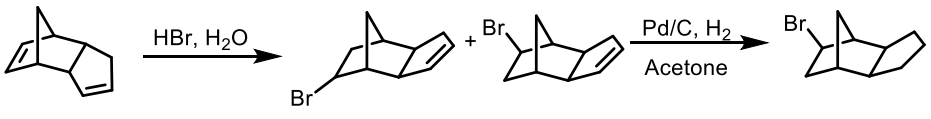

Exo-H_2DCPD was synthesized based on reported procedures[2]. In a 2 L round-bottom flask, DCPD (132.2 g, 1.0 mol, 1.0 equiv.) and HBr (238 mL, 2.1 mol, 2.1 equiv.) were added. The mixture was heated at 80 °C for 20 h. After cooling, the reaction mixture was extracted with Et_2O, and the organic layer was washed with saturated $NaHCO_3$ solution and dried over Na_2SO_4. The solvent was removed under reduced pressure to afford a crude product, which was used directly in the next step. In a 1 L round-bottom flask, the crude DCPD-HBr, Pd/C (3.0 g, 10 wt%), and acetone (300 mL) were combined. The flask was purged with hydrogen using balloons, and the mixture was

stirred at 40 °C, while the reaction progress was monitored by GC-MS. When the reaction stopped, with residual DCPD-HBr still present, the mixture was filtered through Celite to remove the Pd/C, and the solvent was removed under reduced pressure. The resulting crude product was passed through a pad of silica gel and washed with DCM. The solvent was removed under reduced pressure, and the crude product was subjected to hydrogenation again until no alkene signals remained. H_2DCPD-HBr, was purified by distillation to yield 181.6 g of a colorless liquid.

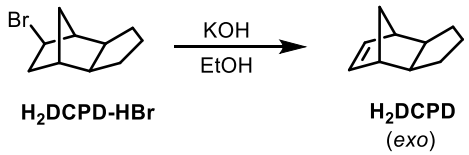

Next, 181.6 g of H_2DCPD-HBr was dissolved in 500 mL EtOH in a 2 L round-bottom flask. KOH (112 g, 2.0 mol) was added, and the mixture was refluxed using an oil bath maintained at 120 °C for 3 days. After cooling, the reaction was diluted with water, extracted with Et_2O, and the organic phase was dried over Na_2SO_4. The solvent was removed under reduced pressure, and the crude product was purified by distillation to afford 90.4 g of a colorless liquid. The overall yield of the three-step synthesis was 67%.

^{1}H NMR spectrum is consistent with the reported spectrum.[2] The ratio of exo/endo is 12.4:1. ^{1}H NMR (500 MHz, $CDCl_3$) δ 6.12 – 6.07 (m, 2H), 2.47 (t, J = 1.9 Hz, 2H), 1.91 (ddt, J = 18.6, 12.8, 6.2 Hz, 3H), 1.83 – 1.72 (m, 2H), 1.64 – 1.40 (m, 2H), 1.34 (dt, J = 8.9, 1.8 Hz, 1H), 1.03 – 0.91 (m, 2H).

Synthesis of Endo-H_2DCPD:

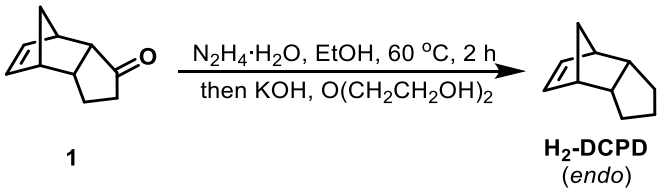

To a 1 L round-bottom flask were added cyclopentadiene (30.15 g, 457 mmol, 1.5 eq.), 2-cyclopentenone (25.0 g, 305 mmol, 1.0 eq.), and anhydrous diethyl ether (300 mL). The reaction mixture was cooled to 0 °C in an ice-water bath, and $BF_3 \cdot Et_2O$ (17.3 g, 122 mmol, 0.4 equiv) was added dropwise. The reaction was then stirred at room temperature for 24 h. After completion, saturated aqueous $NaHCO_3$ (100 mL) was added slowly, and the mixture was stirred for an additional 30 min. The aqueous phase was diluted with water, and the organic layer was separated. The organic layer was washed with water and brine, dried over Na_2SO_4, and concentrated under reduced pressure. The crude product was purified by silica gel column chromatography (hexanes/ethyl acetate = 95:5) to afford compound **1** as a colorless crystalline solid (36.12 g, 80% yield).[3] **1** (10.00 g, 66.7 mmol, 1.0 eq.) was dissolved in 100 mL EtOH, then $N_2H_4 \cdot H_2O$ (10.0 g,

9.72 mL, 200 mmol, 3 eq.) was added to the reaction and stirred at 60 °C for 2 h. The solvent was removed under reduced pressure, and the residue was subjected to a high vacuum to remove the remaining water and excess hydrazine. The residue was dissolved by 100 mL diethylene glycol, KOH (14.9 g, 267 mmol, 4 eq.) was added and the solution was heated at 180 °C for 12 h. Water was added to dilute the reaction, and ethyl ether was used to extract the aqueous phase three times. The combined organic phase was washed with brine and dried with Na_2SO_4. The solvent was removed by evaporation under reduced pressure, and the residue was subjected to distillation to give the product as a colorless liquid. 4.12 g, 46% yield. The final product is a mixture of endo and exo isomers in a ratio of 11.7:1. ^{1}H NMR (500 MHz, $CDCl_3$) δ 6.11 (t, J = 2.1 Hz, 2H), 2.77 – 2.69 (m, 2H), 2.60 (d, J = 3.1 Hz, 2H), 1.65 – 1.54 (m, 4H), 1.48 – 1.40 (m, 2H), 0.98 (ddd, J = 12.5, 6.5, 2.8 Hz, 2H). ^{13}C NMR (126 MHz, $CDCl_3$) δ 136.52, 53.90, 47.50, 46.26, 30.57, 29.01.

Synthesis of Cleavable Comonomer:

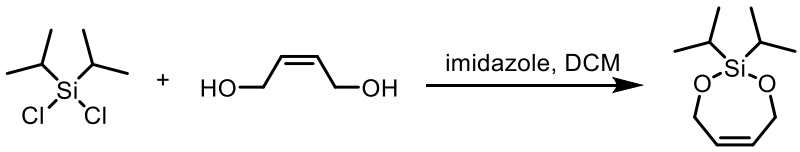

iPrSi7 was prepared according to the literature and used after distillation[4]. Diol (8.81 g, 8.22 mL, 100 mmol, 1.0 eq.) and imidazole (14.98 g, 220 mmol, 2.2 eq.) were dissolved in 500 mL of dry DCM. A solution of dichlorodiisopropylsilane (18.52 g, 18.06 mL, 100 mmol, 1.0 eq.) in 100 mL DCM was added dropwise into the reaction solution and the reaction was stirred for an additional 1 h. Then the cloudy mixture was filtered through a silica pad. The solvent was removed under reduced pressure, and the residue was distilled to afford the product as a colorless liquid. 14.93 g, 75 % yield. ^{1}H NMR (500 MHz, $CDCl_3$) δ 5.66 (d, J = 2.1 Hz, 2H), 4.50 (d, J = 1.9 Hz, 4H), 1.18 – 0.93 (m, 14H).

pDCPD Model Compound Synthesis

Synthesis of 1,2-Dicyclohexylethylene

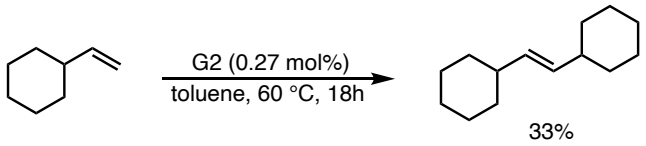

In a 100 mL round-bottom flask, 50 mg (0.27 mol%) of Grubbs II catalyst was weighed and added. A solution of 3 mL of vinylcyclohexane in 50 mL of toluene was then added to the flask under a nitrogen atmosphere. The reaction mixture was stirred at 60 °C overnight. After completion, the solvent was removed under reduced pressure. The resulting residue was purified by column chromatography using 100% hexanes as the eluent, yielding 760 mg (33%) of 1,2-dicyclohexylethylene (E:Z = 94:6) as a colorless oil. ^{1}H NMR (500 MHz, $CDCl_3$) δ 5.30 (dd, J = 3.8, 1.7 Hz, 2H), 1.91 – 1.81 (m, 2H), 1.75 – 1.57 (m, 10H), 1.36 – 0.95 (m, 10H).

General Synthetic Procedure of pDCPD/p-H_2-DCPD Monomer, Dimer, Trimer and Tetramer:

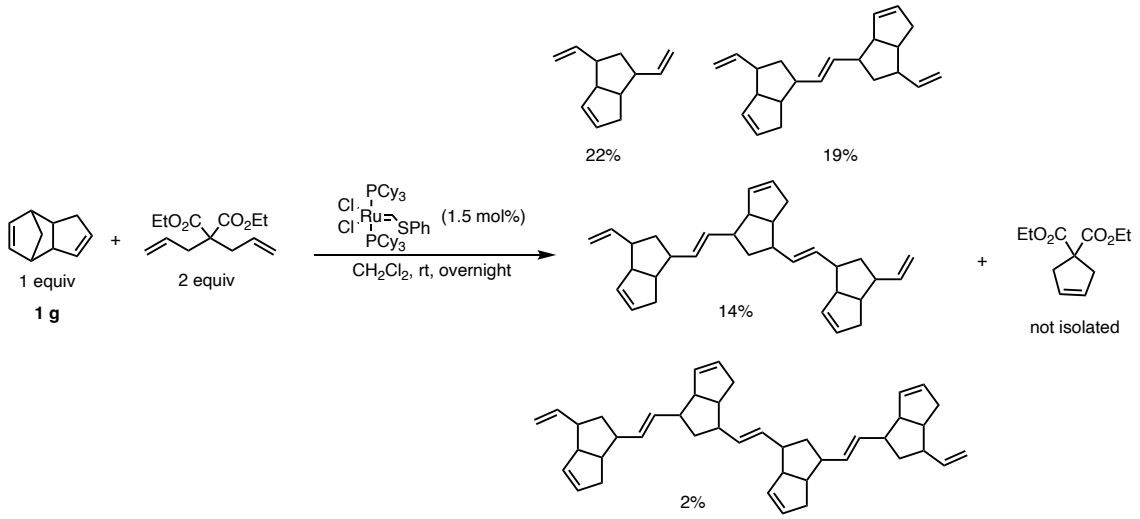

In a 100 mL round-bottom flask, 100 mg of Grubbs I type catalyst was weighed and added. A solution of 1.00 g of dicyclopentadiene (DCPD) and 5.486 mL of diethyl diallylmalonate in 70 mL of dichloromethane (DCM) was then added to the flask under a nitrogen atmosphere. The reaction mixture was stirred at room temperature overnight. After completion, the solvent was removed under reduced pressure. The resulting residue was purified by column chromatography using 100% hexanes as the eluent, yielding the following products: monomer (270 mg, 22% yield, colorless

oil), dimer (205 mg, 19% yield, oily solid), trimer (153 mg, 14% yield, white solid), and tetramer (18 mg, 2% yield, white solid).

Adjusted Reaction Conditions for **5g** Scale: monomer (2.48 g), dimer (1.83 g), trimer (0.53 g)

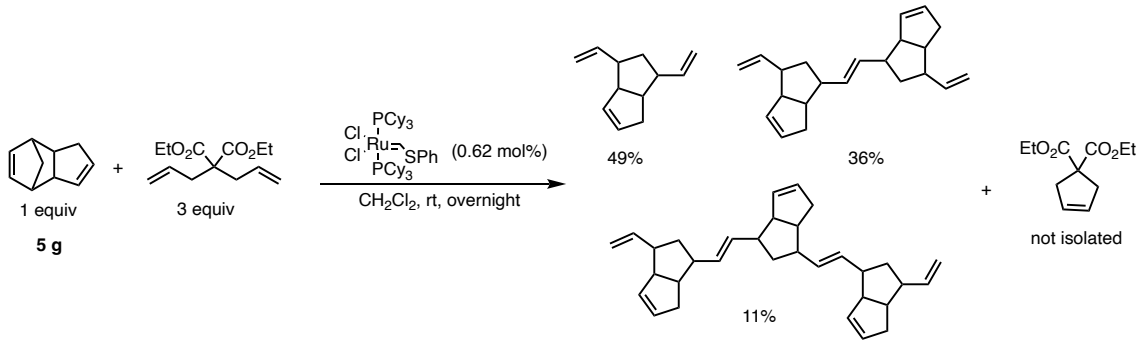

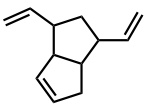

1,3-divinyl-1,2,3,3a,4,6a-hexahydropentalene (**Monomer**): ^{1}H NMR (500 MHz, $CDCl_3$) δ 5.95 – 5.75 (m, 2H), 5.71 (dt, *J* = 6.3, 2.3 Hz, 1H), 5.52 (dp, *J* = 4.9, 2.5 Hz, 1H), 5.13 – 4.84 (m, 4H), 3.31 (tt, *J* = 8.4, 2.3 Hz, 1H), 2.93 – 2.82 (m, 1H), 2.75 – 2.59 (m, 2H), 2.36 – 2.22 (m, 2H), 1.66 (dt, *J* = 11.1, 5.3 Hz, 1H), 1.34 (q, *J* = 12.2 Hz, 1H). MS: EI (GCMS) m/z 160.2

1-vinyl-3-(2-(3-vinyl-1,2,3,3a,4,6a-hexahydropentalen-1-yl)vinyl)-1,2,3,3a,4,6a-

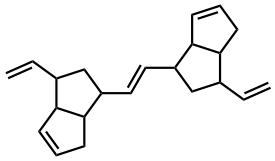

hexahydropentalene (**Dimer**): ^{1}H NMR (500 MHz, $CDCl_3$) δ 5.96 – 5.76 (m, 2H), 5.71 (ddt, *J* = 9.8, 5.8, 2.3 Hz, 2H), 5.62 – 5.29 (m, 4H), 5.15 – 4.91 (m, 4H), 3.46 – 3.18 (m, 2H), 2.86-2.57 (dtd, *J* = 13.9, 6.7, 3.8 Hz, 6H), 2.28 (dh, *J* = 7.9, 2.5 Hz, 4H), 1.69 – 1.56 (m, 2H), 1.31 (q, *J* = 12.2 Hz, 2H). MS: EI (GCMS) m/z 292.5

1-vinyl-3-(2-(3-(2-(3-vinyl-1,2,3,3a,4,6a-hexahydropentalen-1-yl)vinyl)-1,2,3,3a,4,6a-

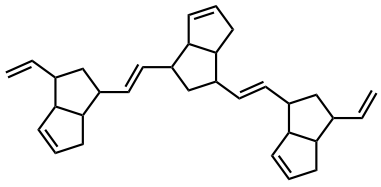

hexahydropentalen-1-yl)vinyl)-1,2,3,3a,4,6a-hexahydropentalene (**Trimer**): ^{1}H NMR (500 MHz, $CDCl_3$) δ 5.86 (dddd, *J* = 40.5, 17.6, 10.4, 6.9 Hz, 2H), 5.76 – 5.66 (m, 3H), 5.61 – 5.27 (m, 7H), 5.15 – 4.91 (m, 4H), 3.33 – 3.20 (m, 3H), 2.91 – 2.77 (m, 3H), 2.72 – 2.56 (m, 6H), 2.28 (dh, *J* = 7.2, 2.4 Hz, 6H), 1.63 (dt, *J* = 11.2, 5.4 Hz, 3H), 1.36 – 1.21 (m, 3H). LSMS: EI m/z 424.3

1-vinyl-3-(2-(3-(2-(3-(2-(3-vinyl-1,2,3,3a,4,6a-hexahydropentalen-1-yl)vinyl)-1,2,3,3a,4,6a-

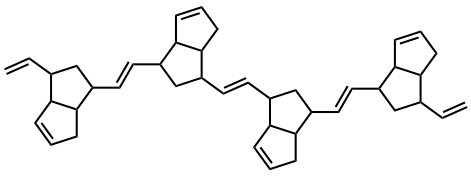

hexahydropentalen-1-yl)vinyl)-1,2,3,3a,4,6a-hexahydropentalen-1-yl)vinyl)-1,2,3,3a,4,6a-hexahydropentalene (**Tetramer**): ^{1}H NMR (500 MHz, $CDCl_3$) δ 5.86 (dddd, *J* = 40.5, 17.5, 10.4, 6.9 Hz, 2H), 5.70

(d, J = 7.0 Hz, 4H), 5.64 – 5.28 (m, 10H), 5.08 – 4.96 (m, 4H), 3.27 (dt, J = 16.8, 8.5 Hz, 4H), 3.07 – 2.54 (m, 12H), 2.29 (d, J = 7.1 Hz, 8H), 1.63 (tt, J = 11.3, 5.5 Hz, 4H), 1.39 – 1.23 (m, 4H). LSMS: EI m/z 556.4

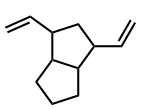

1,3-divinyloctahydropentalene (**pH$_2$DCPD Monomer**): ^{1}H NMR (500 MHz, $CDCl_3$) δ 5.91 (ddd, J = 17.0, 10.4, 6.4 Hz, 2H), 5.08 – 4.97 (m, 4H), 2.66 – 2.48 (m, 4H), 1.61-1.1 (m, 8H). MS: EI (GCMS) m/z 162.2

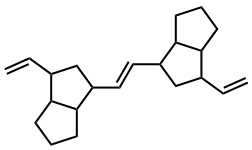

1,2-bis(3-vinyloctahydropentalen-1-yl) ethene (**pH$_2$DCPD Dimer**): ^{1}H NMR (500 MHz, $CDCl_3$) δ 5.87 (dddd, J = 43.5, 17.3, 10.3, 7.1 Hz, 2H), 5.52 – 5.36 (m, 2H), 5.06 – 4.97 (m, 4H), 2.55 (ddq, J = 40.4, 13.8, 7.3 Hz, 8H), 1.60-1.20 (m, 16H). MS: EI (GCMS) m/z 296.5

General Procedure of Model Compound Terminal Alkene Reduction:

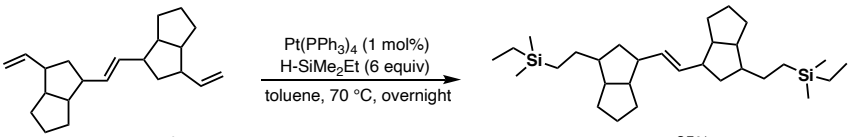

In a 50 mL round-bottom flask, 14 mg of $Pt(PPh_3)_4$ was added. Next, a solution of 330 mg of pH$_2$DCPD dimer in 10 mL of toluene was introduced into the flask, followed by the addition of 0.882 mL of H-SiMe_2Et under a nitrogen atmosphere. The reaction mixture was then stirred at room temperature overnight. Upon completion, the solvent was removed under reduced pressure, and the residue was purified by column chromatography using 100% hexanes, yielding 448 mg (85%) of the **silane-reduced pH$_2$DCPD dimer** compound as a colorless, oily solid. ^{1}H NMR (500 MHz, $CDCl_3$) δ 5.57 – 5.21 (m, 2H), 2.42 (dh, J = 16.2, 7.2 Hz, 6H), 1.76 (qt, J = 12.6, 6.4 Hz, 2H), 1.56 (d, J = 6.4 Hz, 10H), 1.30 (q, J = 8.2 Hz, 5H), 1.23 – 1.07 (m, 4H), 1.00 (t, J = 11.8 Hz, 1H), 0.91 (t, J = 7.9 Hz, 6H), 0.57 – 0.42 (m, 8H), -0.06 (s, 12H). HREI: calculated for $(C_{30}H_{56}Si_2)^+$ 472.39151, found 472.39227.

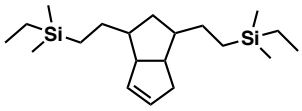

Silane-reduced pDCPD monomer (1.0 g, 95% yield , colorless oil): ^{1}H NMR (500 MHz, $CDCl_3$) δ 5.68 (dq, J = 4.7, 2.3 Hz, 1H), 5.53 (dt, J = 5.7, 2.5 Hz, 1H), 3.22 – 3.14 (m, 1H), 2.77 (qd, J = 8.4, 5.4 Hz, 1H), 2.29 – 2.14 (m, 2H), 1.79 (qq, J = 13.4, 6.2 Hz, 2H), 1.68 – 1.55 (m, 2H), 1.38 – 1.13 (m, 4H), 0.92 (t, J = 7.9 Hz, 6H), 0.63 – 0.28 (m, 8H), -0.01 (s, 12H). HREI: calculated for $(C_{20}H_{40}Si)^+$ 336.26609, found 336.26631.

General Procedure of Electro-catalyzed C-H Functionalization of Deconstructed pDCPD Oligomers

Screening Scale (100 mg of deconstructed pDCPD oligomers):

All bulk electrolysis was conducted under ambient conditions without precautions to exclude air or moisture. A 20 mL scintillation vial was prepared with a stir bar, NHPI (20 mol%), and $TBAPF_6$ (0.1 M). Then, 8 mL of dichloromethane (DCM) was added, and the solution was stirred until the solids was fully dissolved. A solution of 100 mg deconstructed pDCPD oligomers in 2 mL of DCM was introduced, followed by the addition of pyridine (2 equiv.) and 70% aqueous tert-butyl hydroperoxide (1 equiv.). Reticulated vitreous carbon (RVC) foam anodes and cathodes (dimensions: 18 mm x 10 mm x 6 mm) were submerged in the solution. The electrolysis was carried out at a constant cell potential of 3.5 V at room temperature, supplied by an external power source, with a stable current of approximately 10 mA, monitored using a multimeter integrated into the circuit.

Aliquots (0.5 mL, containing approximately 5 mg of oligomers) were collected at 2-hour, 4-hour, and 6-hour intervals for ^1H NMR analysis. Each aliquot was purified by precipitating in methanol, followed by centrifugation and filtration, with each step repeated twice. The functionalized oligomers were subsequently dried under reduced pressure.

After 6 hours, the electrolysis was stopped. The remaining reaction mixture was purified by precipitating the oligomers in methanol three times and then drying under reduced pressure to give the functionalized pDCPD oligomers with an average isolated mass 79 mg (±8 mg).

Scale Up Procedure (10-15 g of deconstructed pDCPD Oligomers):

All bulk electrolysis was conducted under ambient conditions without precautions to exclude air or moisture. An 800 mL bottle was prepared with a stir bar, NHPI (40 mol%), and $TBAPF_6$ (0.1 M). Then, 500 mL of dichloromethane (DCM) was added, and the solution was stirred until the solids fully dissolved. A solution of 10.0 g deconstructed pDCPD oligomers in 100 mL of DCM was introduced, followed by the addition of pyridine (2 equiv.) and 70% aqueous tert-butyl hydroperoxide (1.5 equiv.). Reticulated vitreous carbon (RVC) foam anodes and cathodes (dimensions: 950 mm x 550 mm x 6 mm) were submerged in the solution. The electrolysis was carried out at a constant cell potential of 3.5 V at room temperature, supplied by an external power source, with a stable current of approximately 40 mA, monitored using a multimeter integrated into the circuit. The reaction was monitored by ^1H NMR analysis. After 18 hours, the electrolysis was stopped. The reaction mixture was purified by precipitating the oligomers in methanol three times and then drying under reduced pressure to give the functionalized pDCPD oligomers with an average isolated mass 9.03g (±0.6 g).

Electrolysis at 15 g scale was also conducted using the same setup, 12.41 g of functionalized oligomers was purified after three times of precipitation in methanol.

Reduction of E-Functionalized Oligomers using Pd/C (Peroxide Residues Removal)

To remove peroxide residues from E-functionalized oligomers, 2 grams of the oligomers was dissolved in 40 mL of THF in a round-bottom flask. Next, 100 mg of Pd/C (10 wt%, containing approximately 50% water) was added. The flask was evacuated and refilled with hydrogen three times using a hydrogen balloon, and the reaction was stirred at 40 °C for 8 hours. After completion, the mixture was filtered through a Celite pad, and the solvent was removed via rotary evaporation, yielding peroxide-free oligomers.

Amine Deprotection of E-Functionalized Oligomers (Ing–Manske procedure)

To deprotect the amine groups of E-functionalized oligomers, 800 mg of the oligomers (post-peroxide removal) was dissolved in 30 mL of dichloromethane (DCM) in a round-bottom flask. To this solution, 10 mL of ethanol and 1 mL of hydrazine monohydrate were added. The reaction mixture was stirred at 50 °C under a nitrogen atmosphere for 1 hour. After completion, the solvent was removed under reduced pressure, and the resulting polymer was purified by triple re-precipitation in methanol. This yielded the final amine-functionalized oligomers (632 mg), ready for film casting.

Solvent Casting Procedure for Preparing pDCPD Films for DMA Measurements

400 mg of the final amine-functionalized oligomers was added to a 20 mL vial, followed by the addition of 4 mL of DCM. The mixture was sonicated until the solid was fully dissolved. This solution was then transferred into a PTFE-lined petri dish and placed in a DCM-saturated chamber under nitrogen for 16 hours to enable slow solvent evaporation. The resulting film was subsequently dried under vacuum at room temperature for 6 hours, followed by an additional 12 hours at 70 °C.

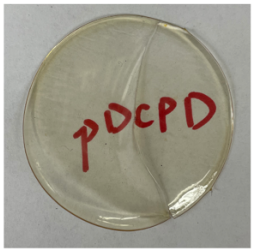

casted film from unfunctionalized oligo-DCPD

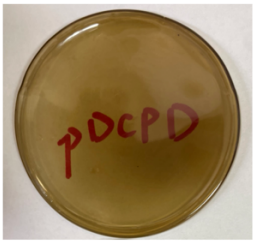

casted film from E-functionalized oligo-DCPD

DMA Measurement

DMA was measured on a TA Instruments RSA II with supplied tensile grips under a nitrogen environment, the gauge length was maintained at 4-10 mm, a dynamic loading was applied for temperature ramp at 1 Hz and 0.1% strain amplitude to measure storage moduli and the T_g, and the temperature ramp is 3 °C/min.

DMA Results

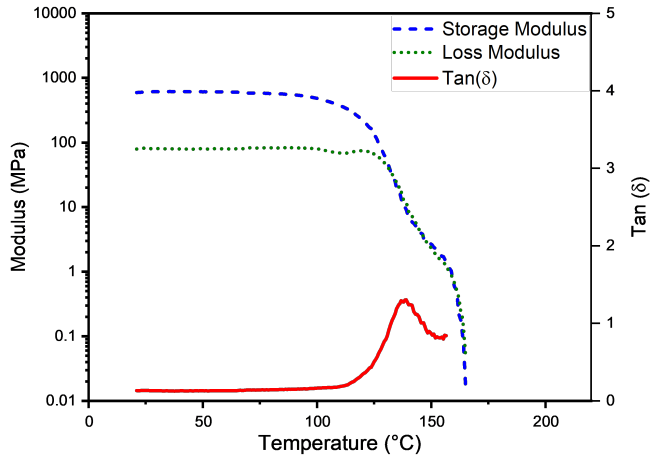

Supplementary Fig. 2 Representative DMA plot for temperature ramp of the material made from unfunctionalized deconstructed pDCPD oligomers.

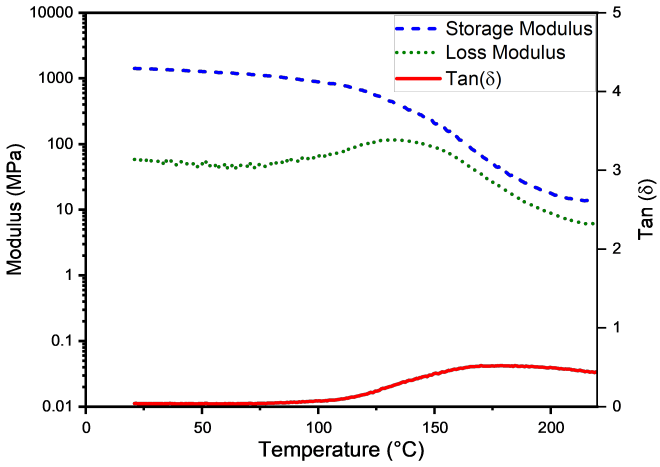

Supplementary Fig. 3 Representative DMA plot for temperature ramp of the material made from E-functionalized deconstructed pDCPD oligomers.

IR Spectra of E-functionalized Deconstructed pDCPD oligomers

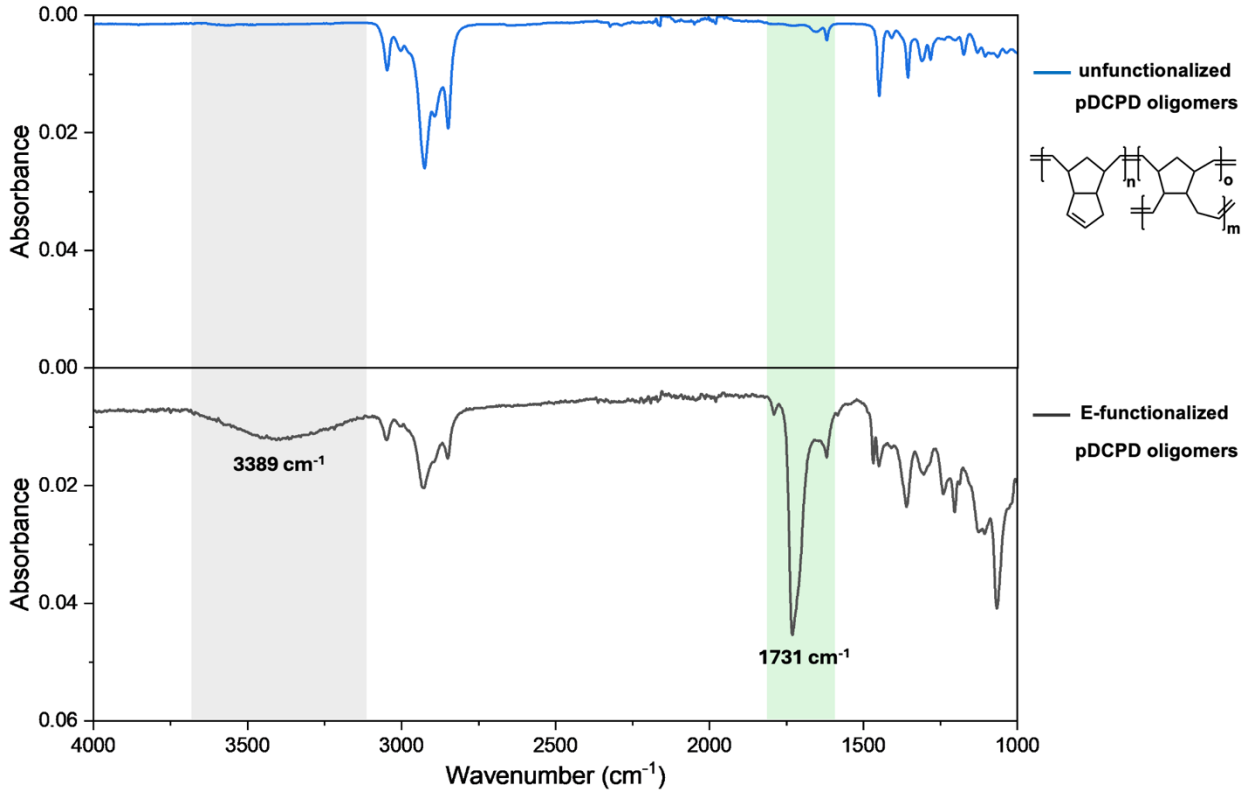

Supplementary Fig. 4 IR spectra of unfunctionalized deconstructed pDCPD oligomers and E-functionalized deconstructed pDCPD oligomers at 6 h. New carbonyl peak observed at 1731 cm^{-1} and new hydroxyl peak observed at 3389 cm^{-1}.

Note, the E-functionalization process is also monitored by ^{1}H NMR, see **Supplementary Fig. 9**.

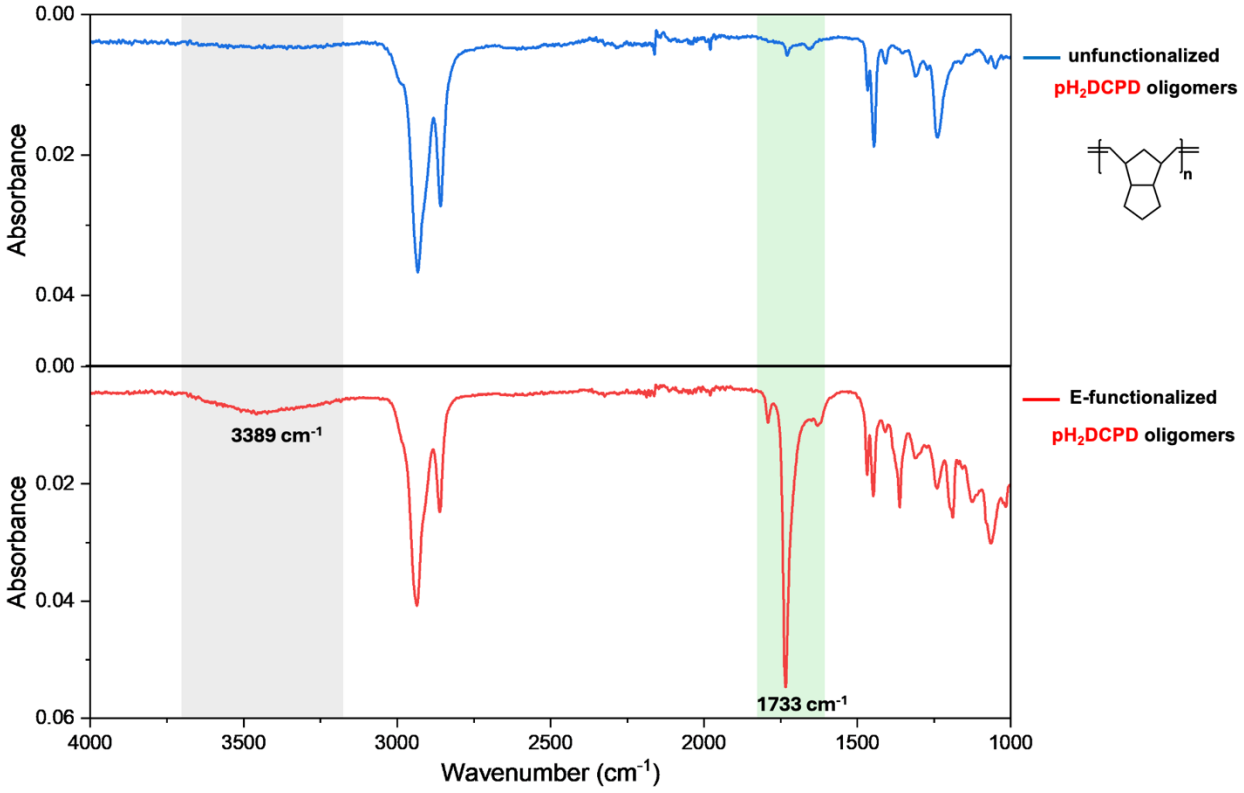

Supplementary Fig. 5 IR spectra of unfunctionalized deconstructed pH_2DCPD oligomers and E-functionalized deconstructed pH_2DCPD oligomers at 6 h. New carbonyl peak observed at 1733 cm^{-1} and new hydroxyl peak observed at 3389 cm^{-1}. IR result of the linear pH_2DCPD oligomers is similar as the branched pDCPD.

For stacked ^1H NMR spectra of linear pH_2DCPD oligomers before and after E-functionalization, see **Supplementary Fig. 59**.

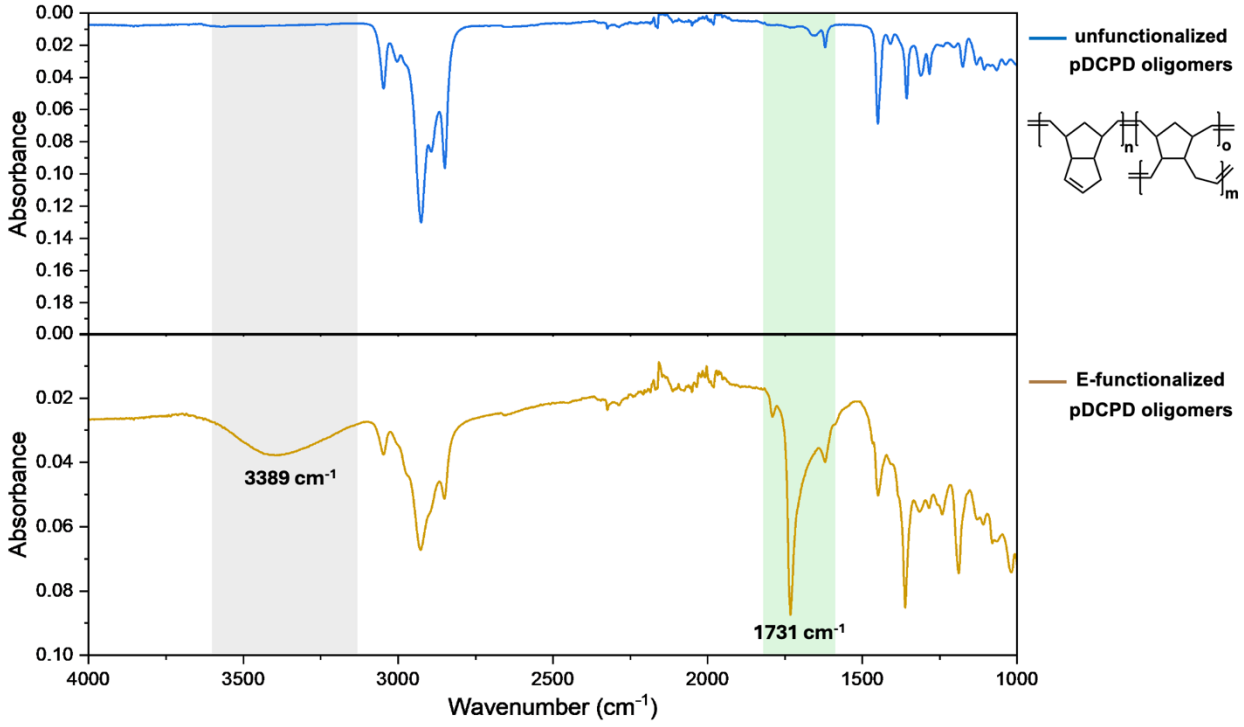

Supplementary Fig. 6 IR spectra of unfunctionalized deconstructed pDCPD oligomers and E-functionalized deconstructed pDCPD oligomers at **24 h (10 g scale)**. New carbonyl peak observed at 1731 cm^{-1} and new hydroxyl peak observed at 3389 cm^{-1}.

IR Spectra of E-Functionalized pDCPD Oligomers after Amine Deprotection

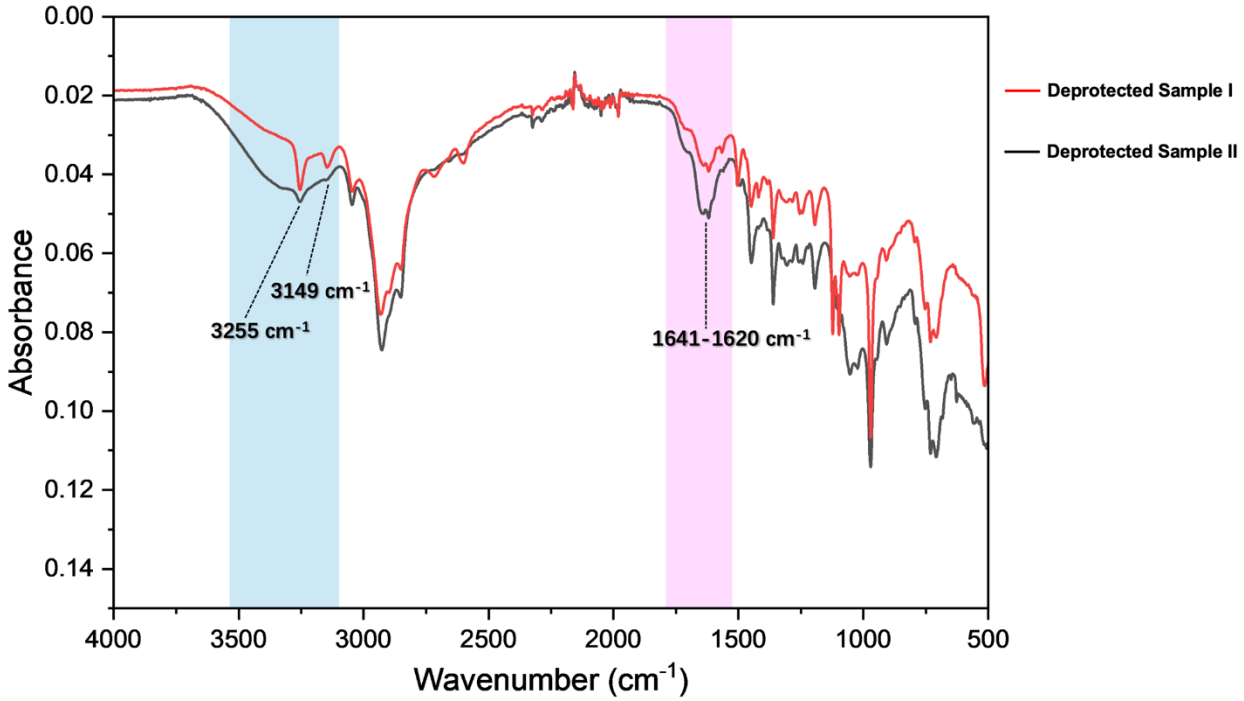

Supplementary Fig. 7 IR spectra of E-functionalized deconstructed pDCPD oligomers amine deprotection. A new C=N peak appears at ~1641 cm^{-1}, consistent with previously reported values,[5,6] along with new amine peaks at 3255 and 3149 cm^{-1}.

Note, the amine deprotection reaction is also monitored by ^{1}H NMR, see **Supplementary Fig. 10**.

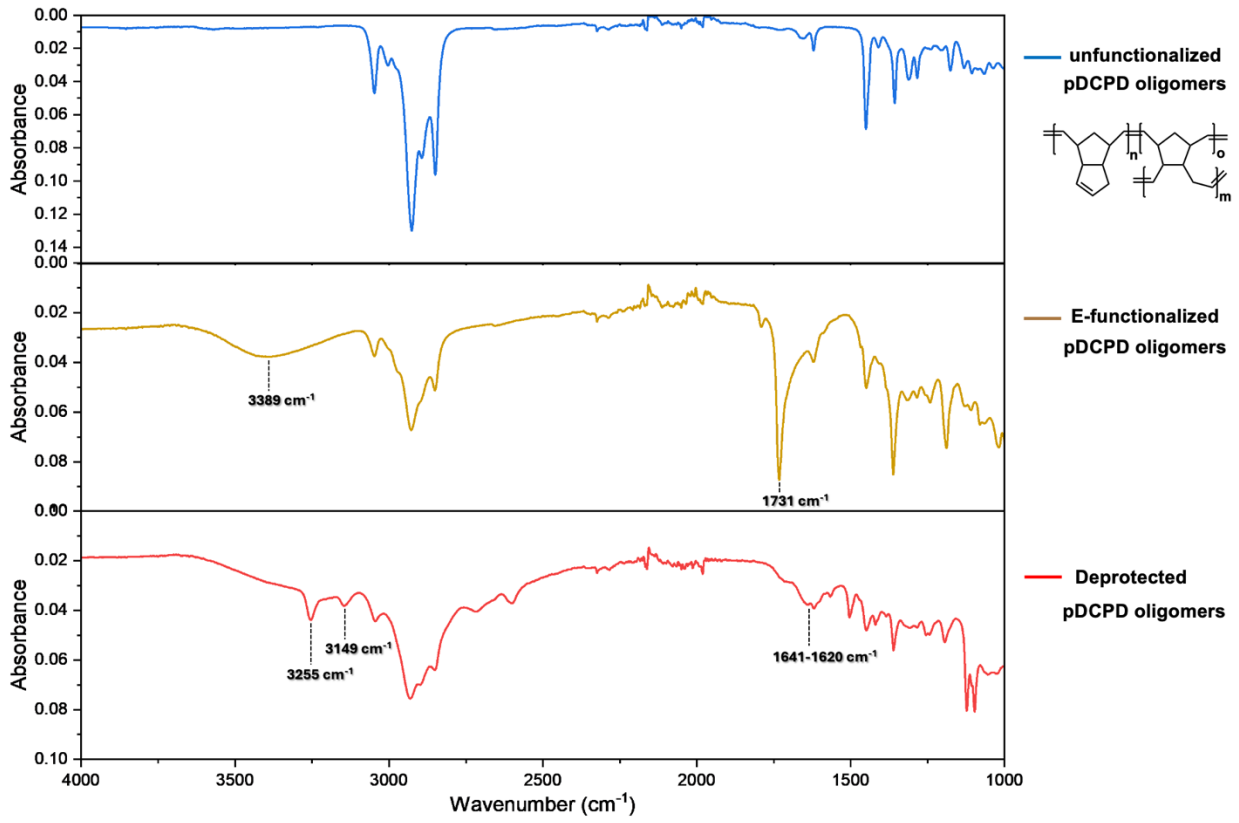

Supplementary Fig. 8 Stacked IR spectra of unfunctionalized deconstructed pDCPD oligomers (top), E-functionalized deconstructed pDCPD oligomers (middle), and deprotected E-functionalized pDCPD network (bottom). Upon deprotection, the E-functionalized sample spontaneously forms a covalent imine-linked network, which can be reversibly de-crosslinked by introducing small-molecule amines during film casting.

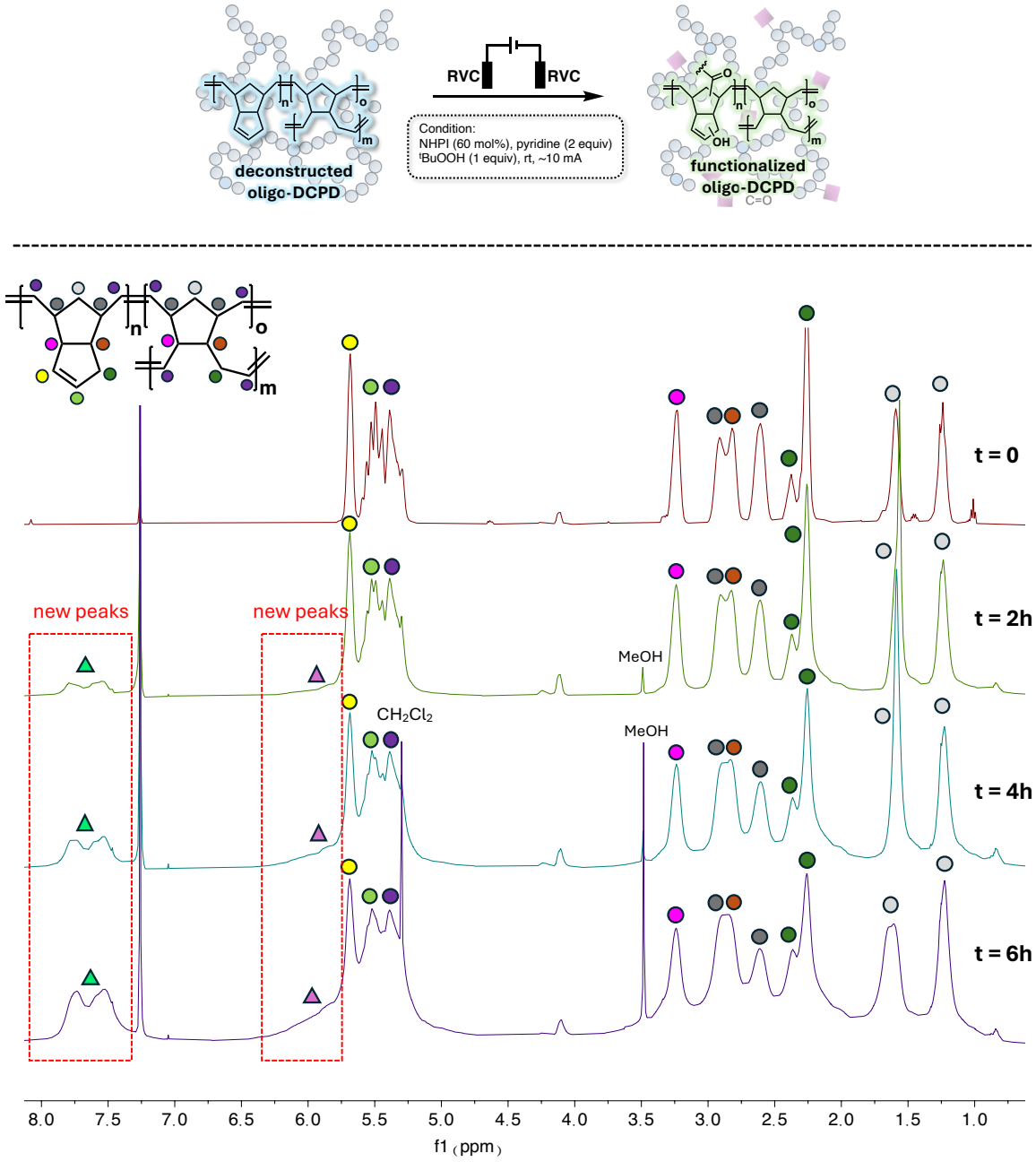

Supplementary Fig. 9 ^{1}H NMR spectra of the unfunctionalized and the electro-functionalized deconstructed oligo-DCPD. ^{1}H NMR spectra of unfunctionalized oligo-DCPD and the isolated E-functionalized oligo-DCPD at different reaction time points. New H peaks (highlight in red box) are detected at 5.0-6.5 ppm (pink triangle) and 7.5-7.8 ppm (green triangle). Notably, the alkene C–H region (5.0–6.5 ppm) exhibits significant peak overlap.

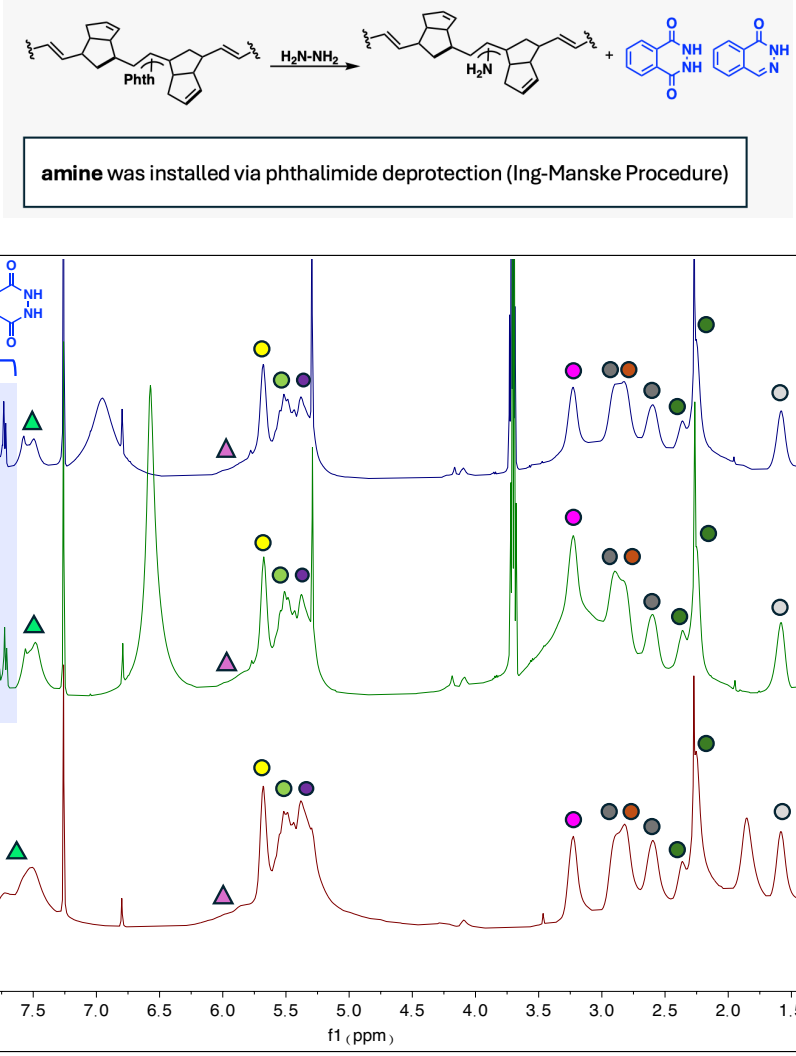

Supplementary Fig. 10 Deprotection of phthalimide moieties. Ing-Manske procedure is used to deprotect phthalimide functionals to amine on the functionalized oligo-DCPD backbone. ^{1}H NMR spectra of deprotection process of the phthalimide functionals. The small molecule products from the deprotection matches with the reported refence molecules.[7,8]

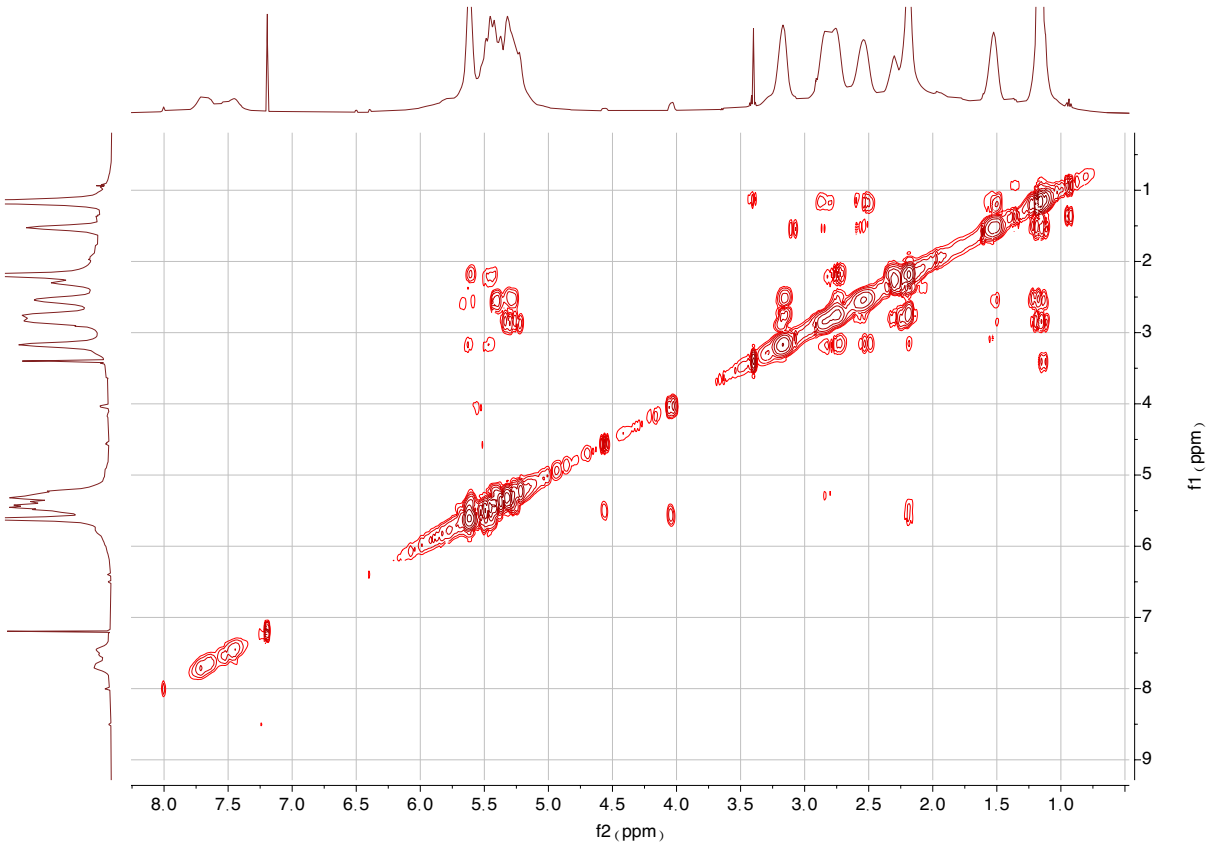

Supplementary Fig. 11 ^{1}H-^{1}H COSY spectrum of electro-functionalized deconstructed oligo-DCPD (1 g scale). Oligo-DCPD (1 g) was treated with 60 mol% NHPI, 1.5 equiv t-BuOOH (70 wt% in H_2O), 2 equiv pyridine in DCM at room temperature under 10 mA.

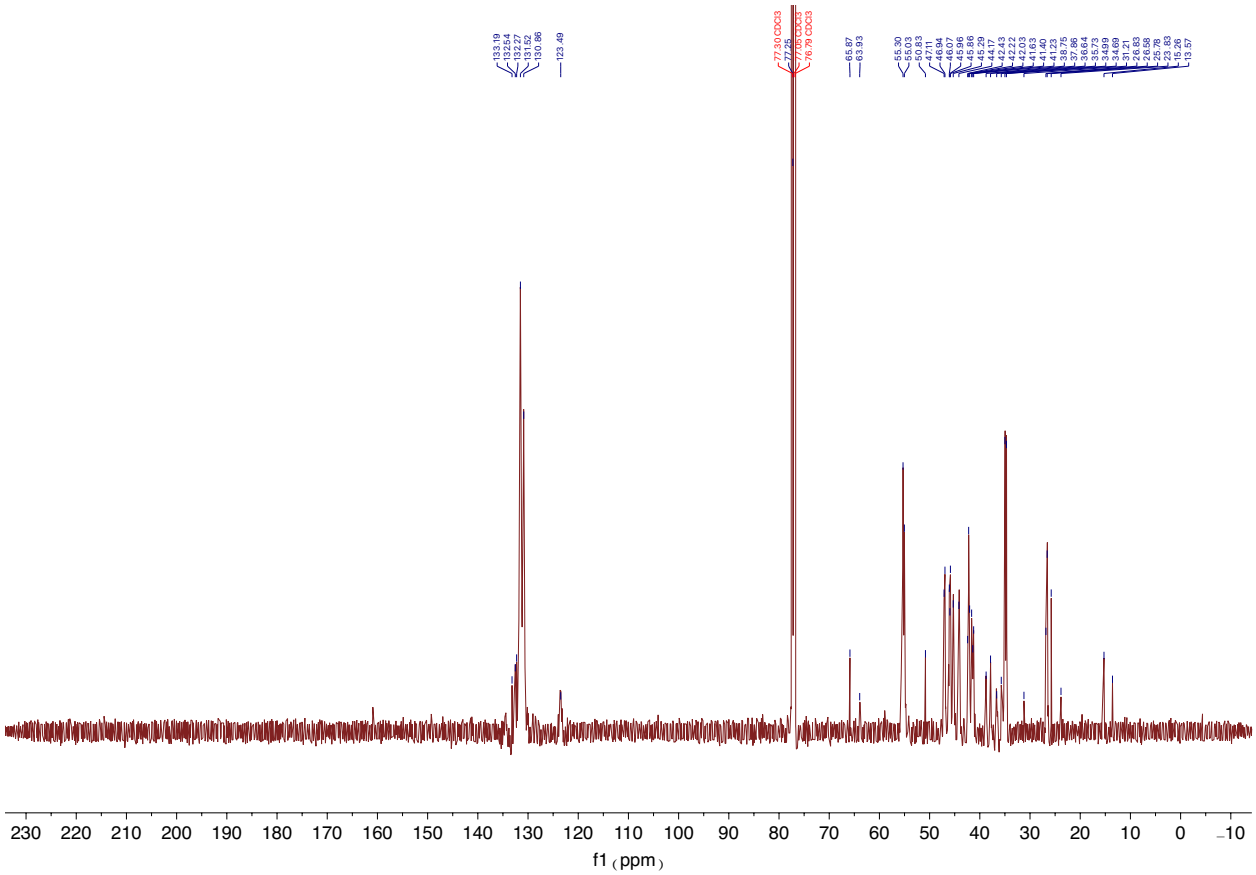

Supplementary Fig. 12 ^{13}C NMR spectrum of electro-functionalized deconstructed oligo-DCPD (1 g scale). Oligo-DCPD (1 g) was treated with 60 mol% NHPI, 1.5 equiv t-BuOOH (70 wt% in H_2O), 2 equiv pyridine in DCM at room temperature under 10 mA.

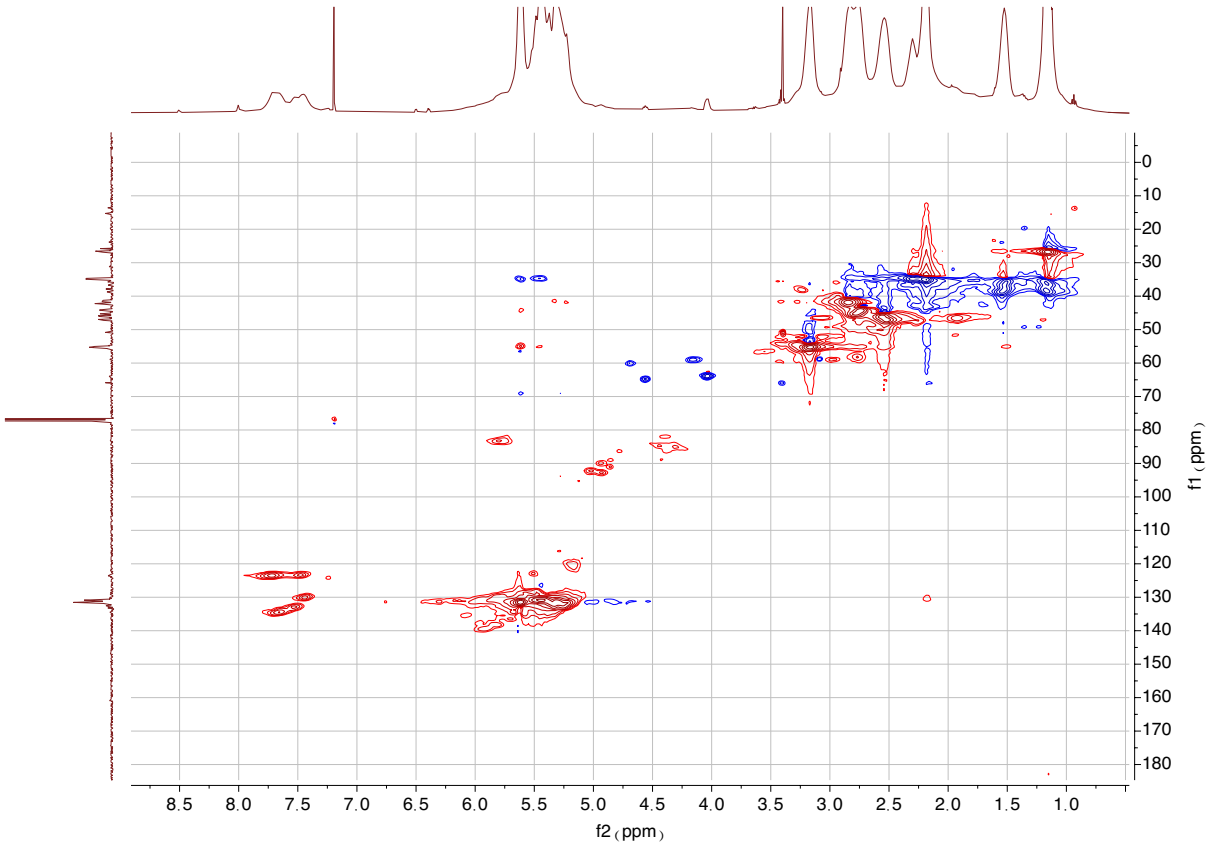

Supplementary Fig. 13 ^{1}H-^{13}C HSQC spectrum of electro-functionalized deconstructed oligo-DCPD (1 g scale). Oligo-DCPD (1 g) was treated with 60 mol% NHPI, 1.5 equiv t-BuOOH (70 wt% in H_2O), 2 equiv pyridine in DCM at room temperature under 10 mA.

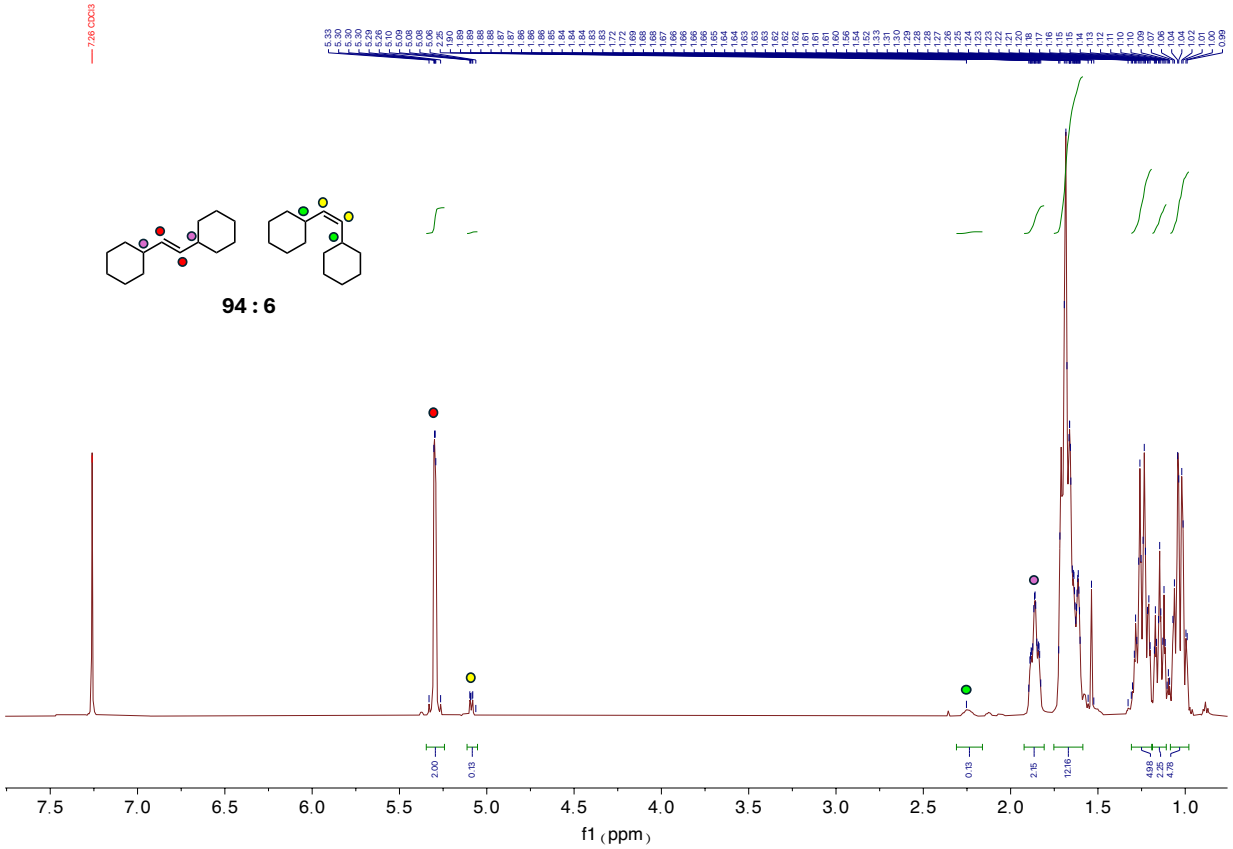

Supplementary Fig. 14 ^{1}H NMR spectrum of 1,2-dicyclohexylethylene. Spectral data are in accordance with those previously reported.[9]

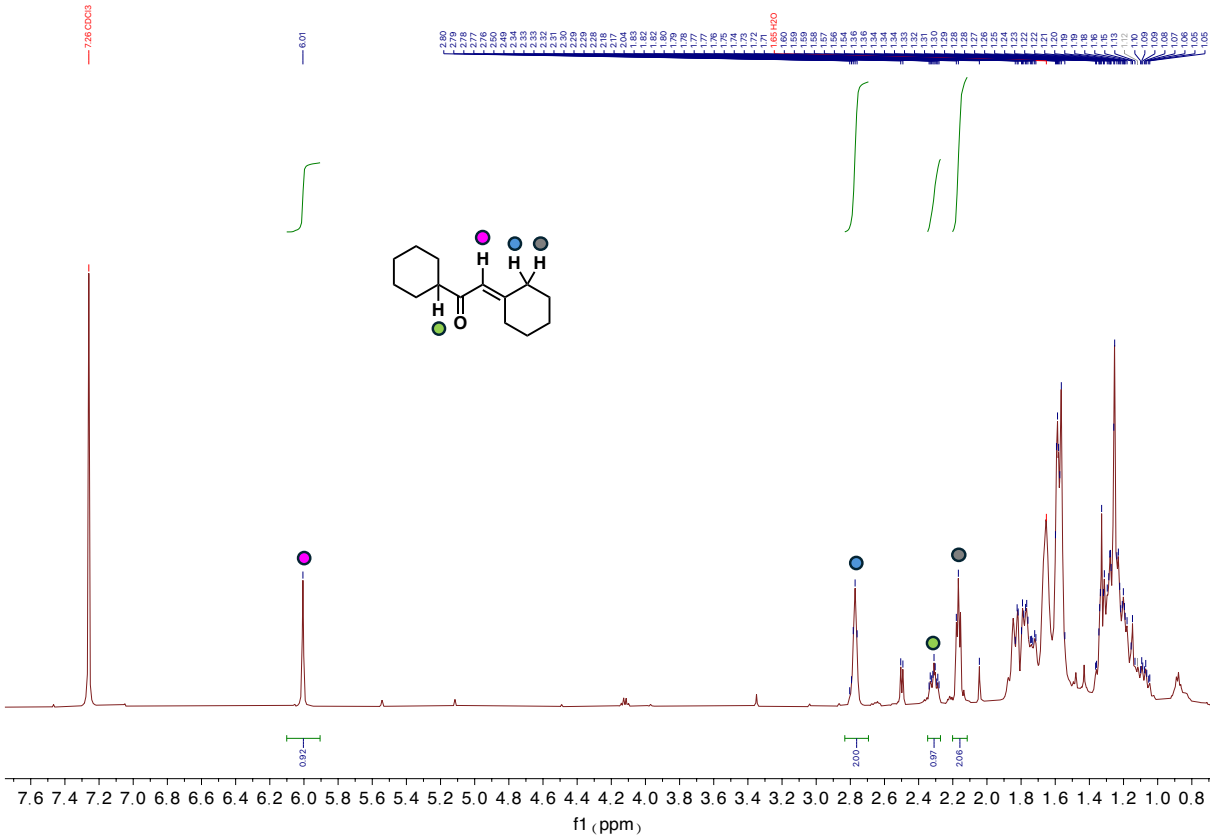

Supplementary Fig. 15 ^{1}H NMR spectrum of isolated ketone product of E-oxidation of 1,2-dicyclohexylethylene. Spectral data are in accordance with those previously reported.[10]

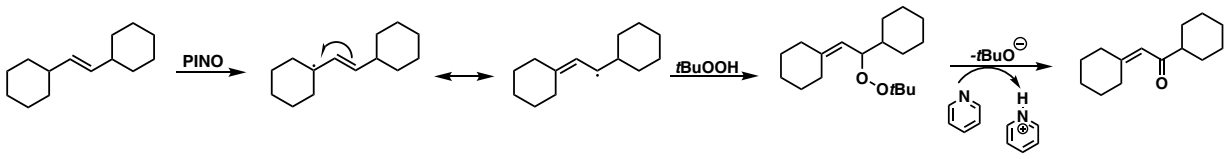

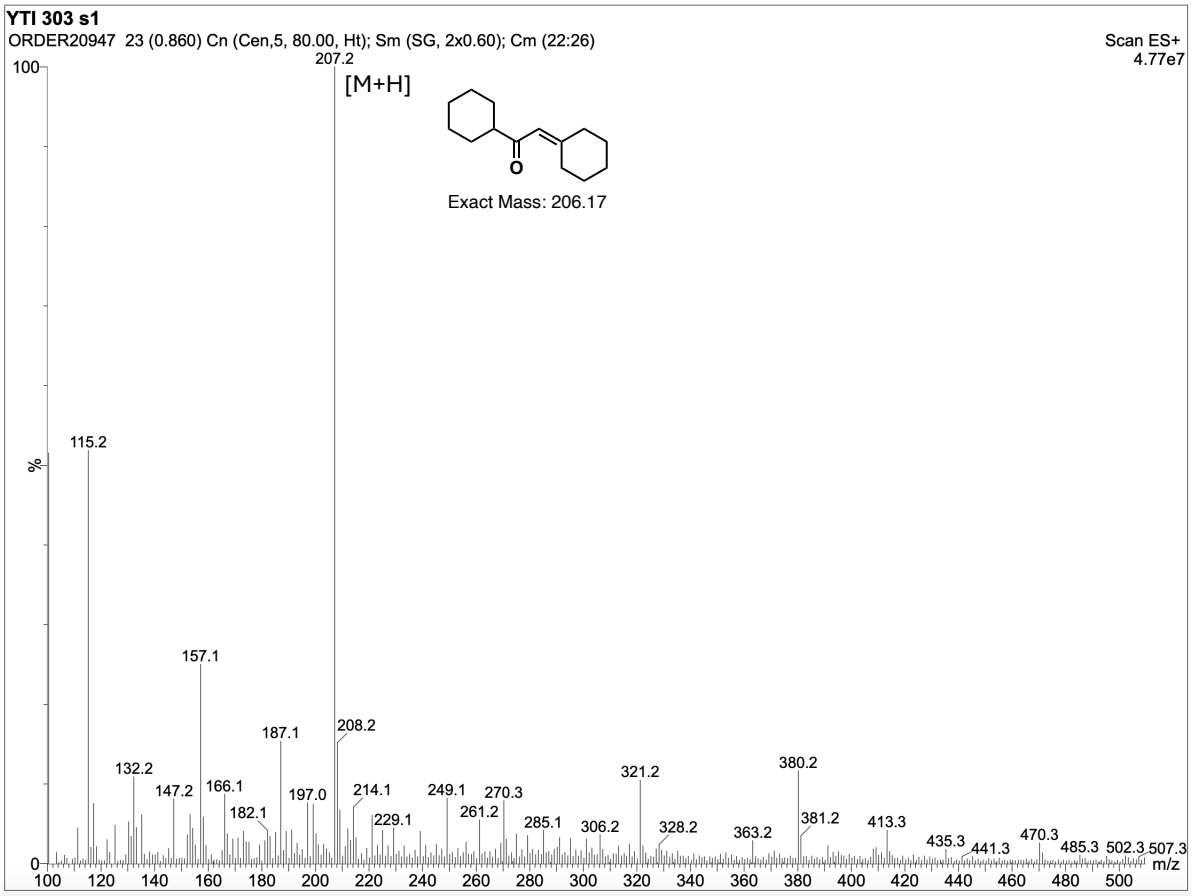

Supplementary Fig. 16 Mass spectrum (Low Resolution ESI) of the isolated ketone product of E-oxidation of 1,2-dicyclohexylethylene.

Product Distribution of Cyclohexene E-Oxidation at Different Screening Conditions

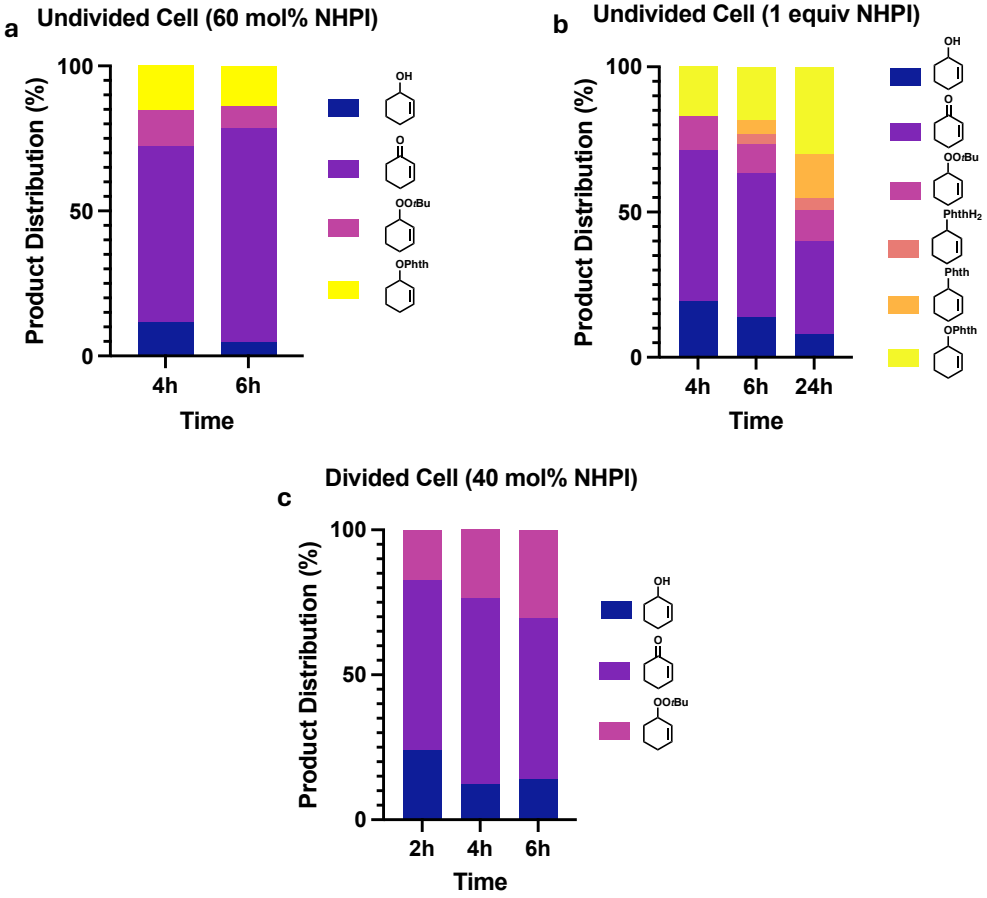

Supplementary Fig. 17 Product distribution of cyclohexene electro-oxidation under different electrochemical conditions. **a** 60 mol% of NHPI, 2 equiv of pyridine, 1 equiv of tBuOOH (70% aqueous solution), undivided cell, RVC-RVC. **b** 1 equiv of NHPI, 2 equiv of pyridine, 1 equiv of tBuOOH (70% aqueous solution), undivided cell, RVC-RVC. **c** 40 mol% of NHPI, 2 equiv of pyridine, 1 equiv of tBuOOH (70% aqueous solution), divided cell, RVC-RVC.

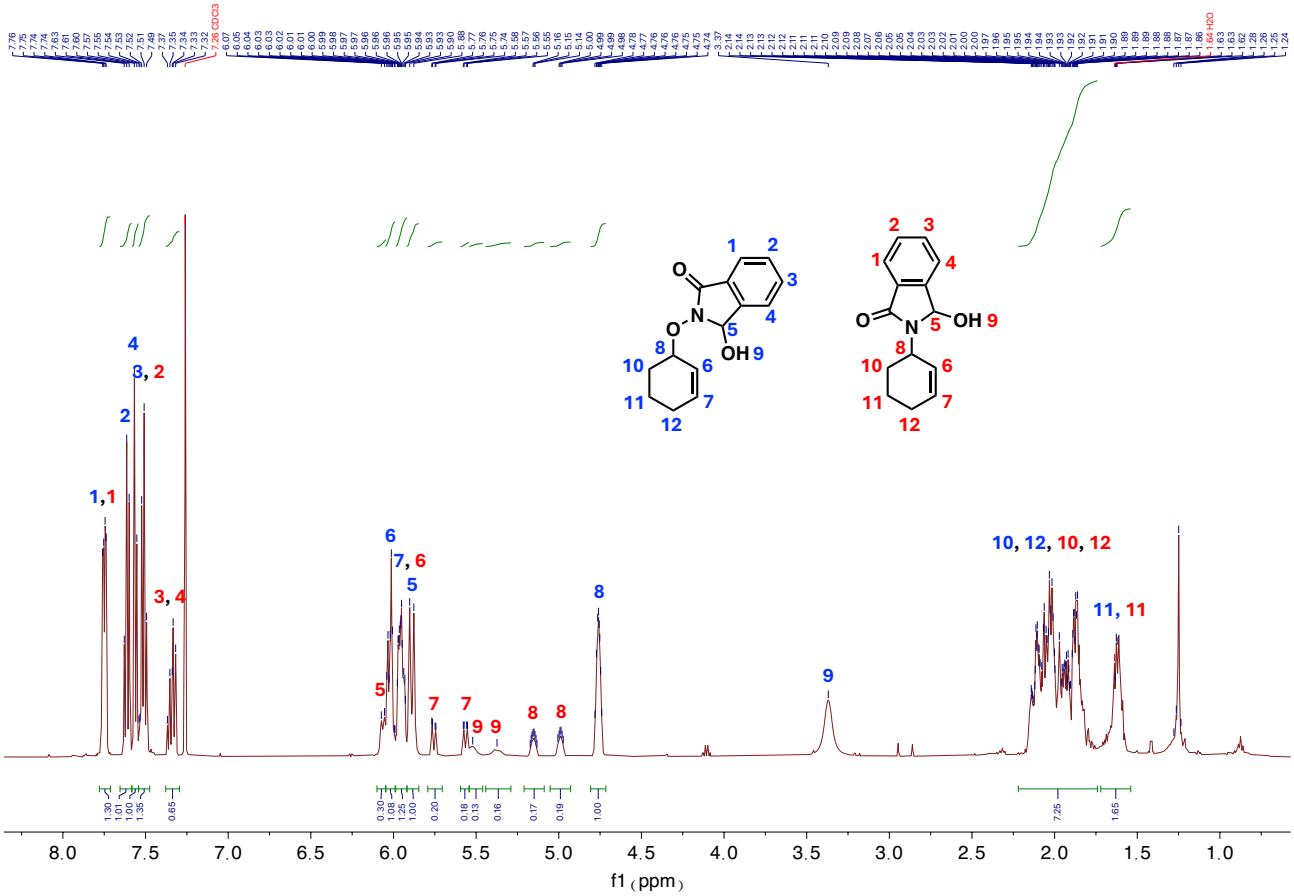

Supplementary Fig. 18 ^{1}H NMR spectrum of isolated phthalimide addition products of cyclohexene.

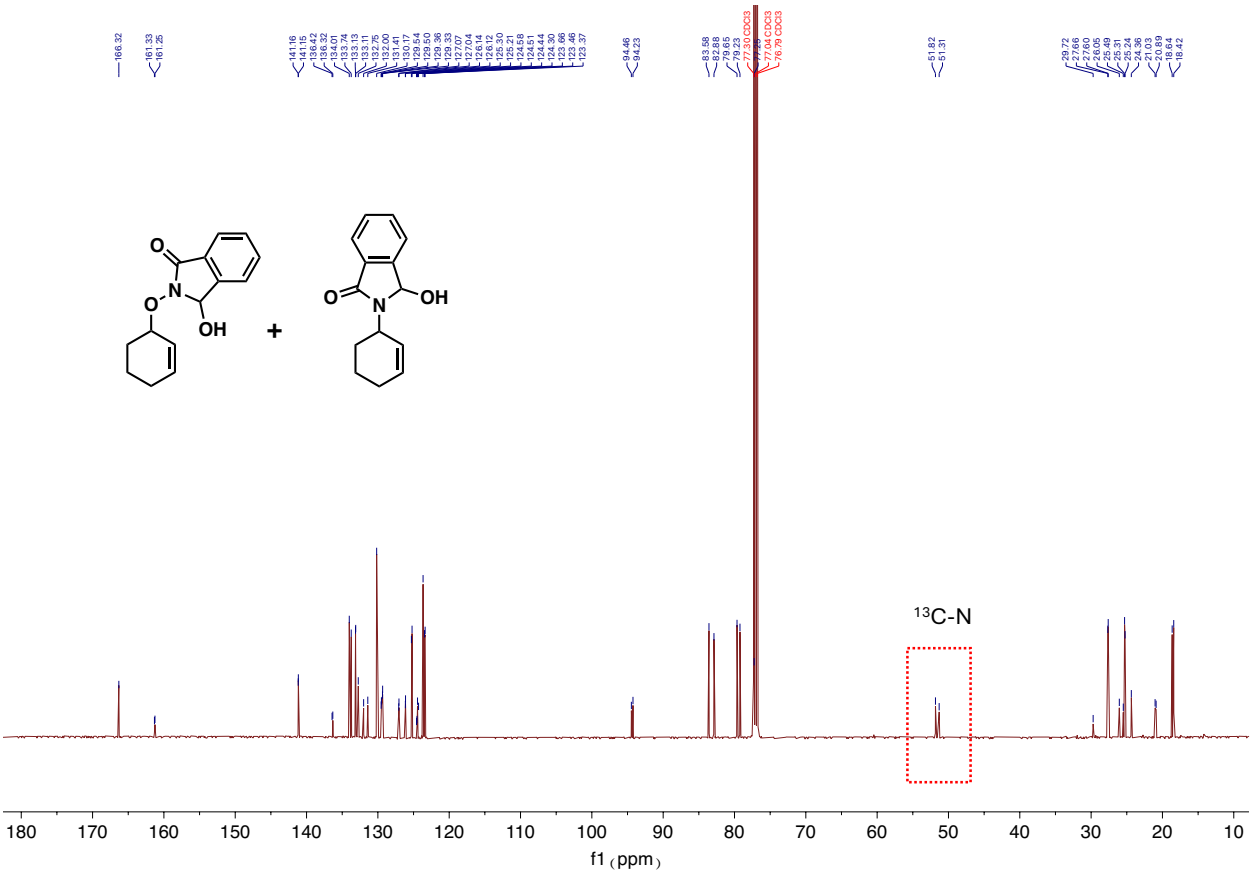

Supplementary Fig. 19 ^{13}C NMR spectrum of isolated phthalimide addition products of cyclohexene.

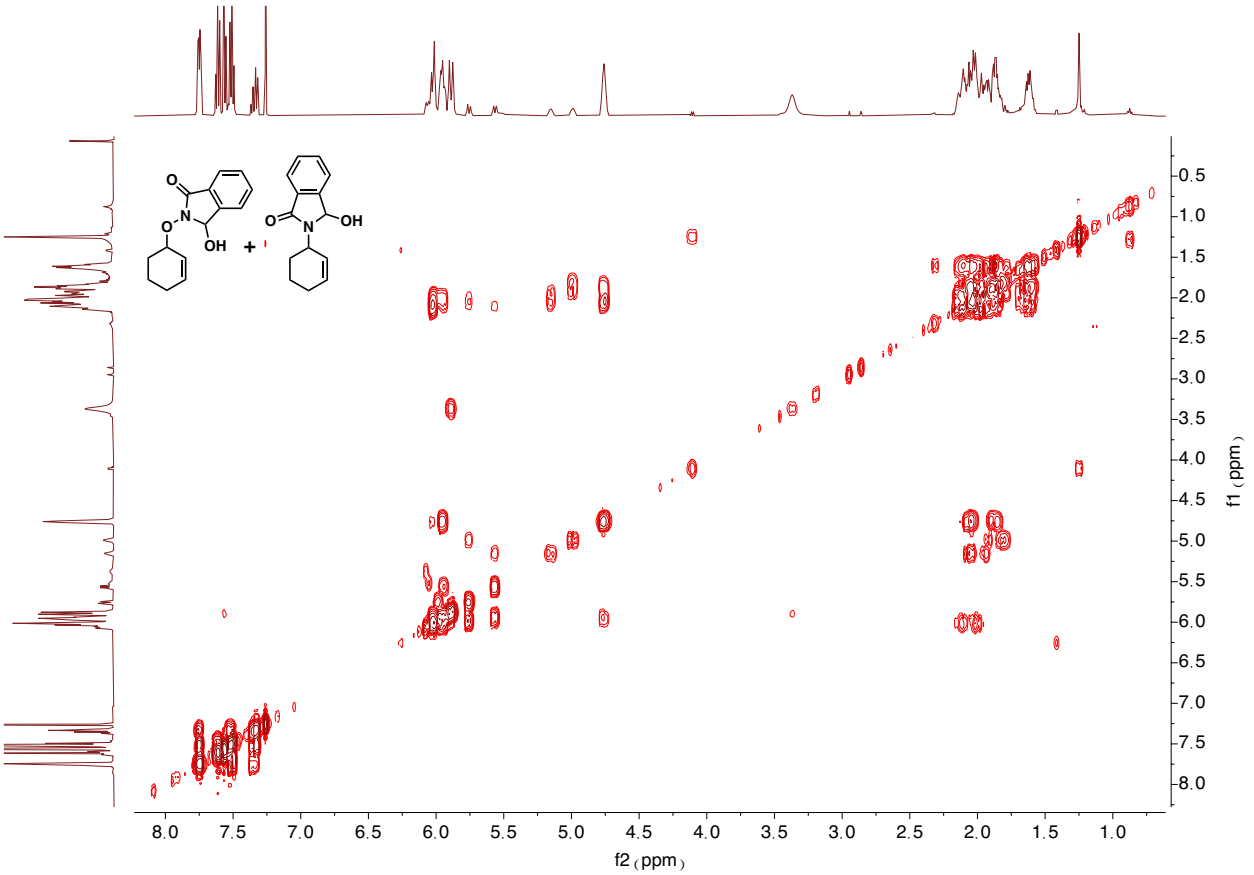

Supplementary Fig. 20 ^{1}H-^{1}H COSY spectrum of isolated phthalimide addition products of cyclohexene.

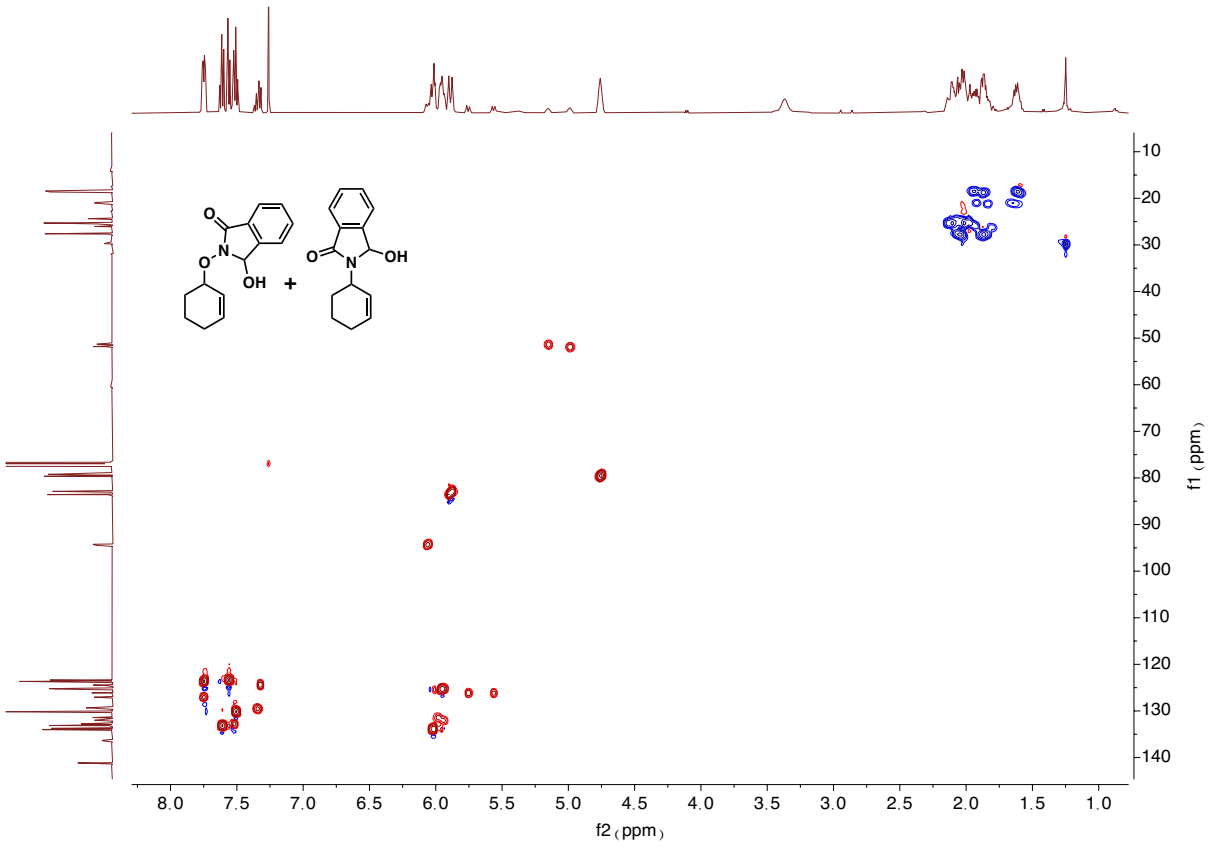

Supplementary Fig. 21 ^{1}H-^{13}C HSQC spectrum of isolated phthalimide addition products of cyclohexene.

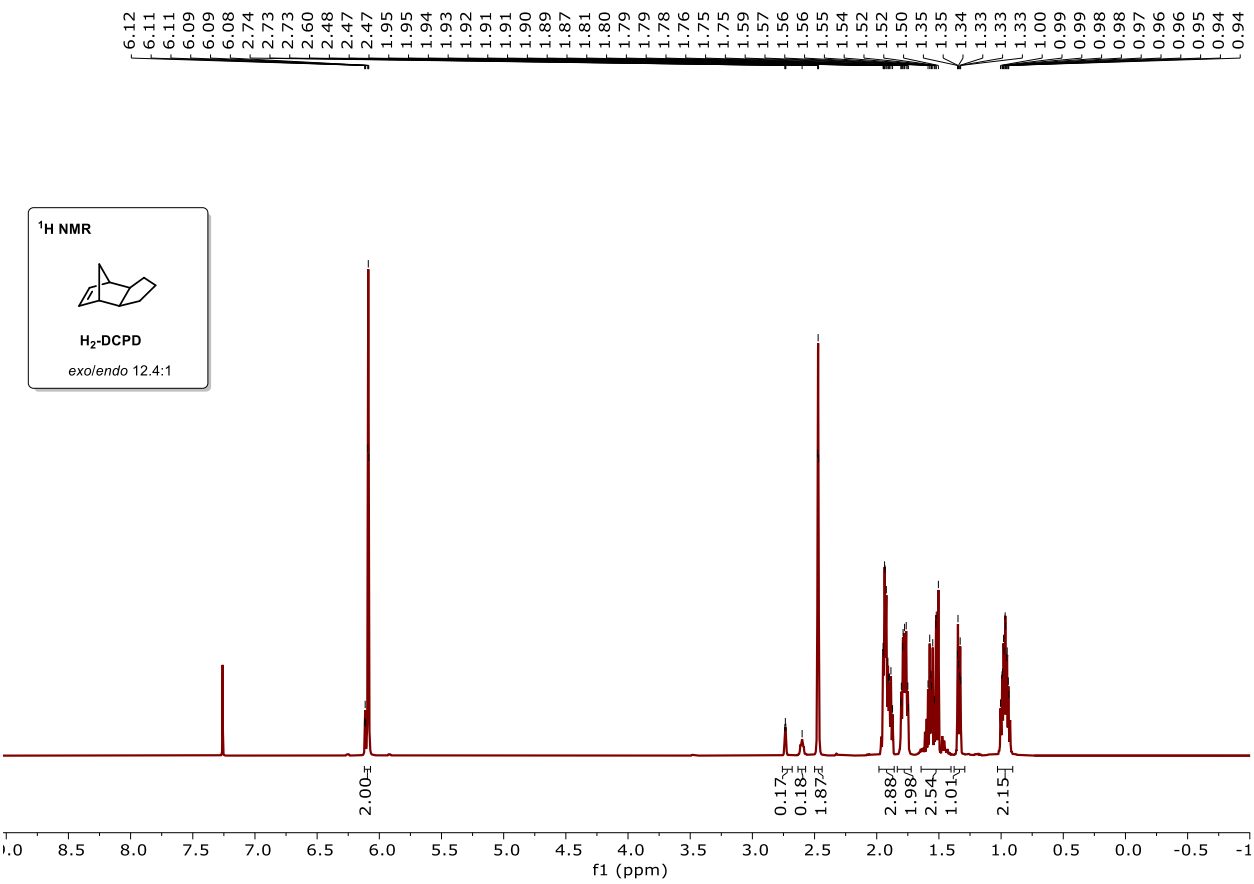

Supplementary Fig. 22 ^{1}H NMR spectrum of exo-H_2DCPD monomer. Spectral data are in accordance with those previously reported.[2] Contained 7% of endo-H_2DCPD isomer.

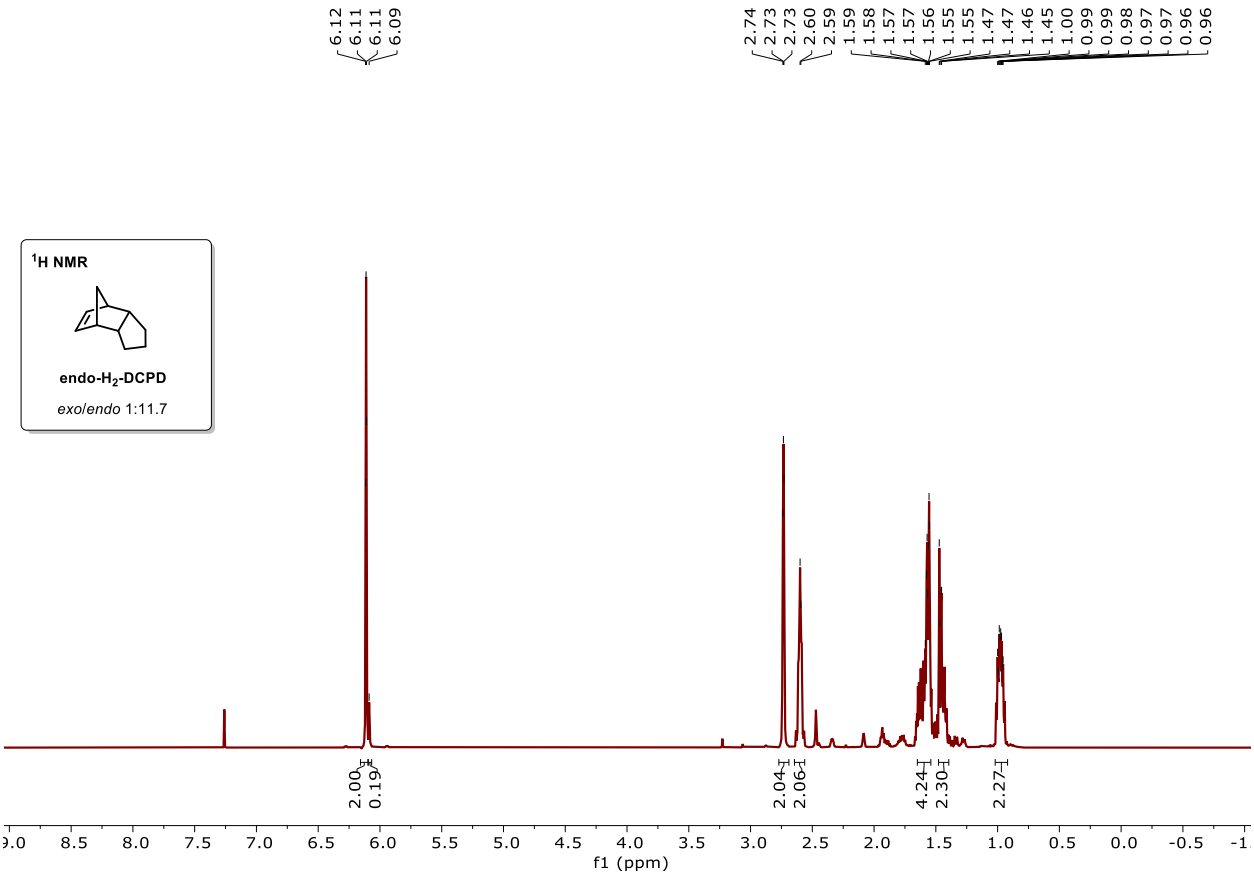

Supplementary Fig. 23 ^{1}H NMR spectrum of endo-H_2DCPD monomer. Contained 8% of exo-H_2DCPD isomer.

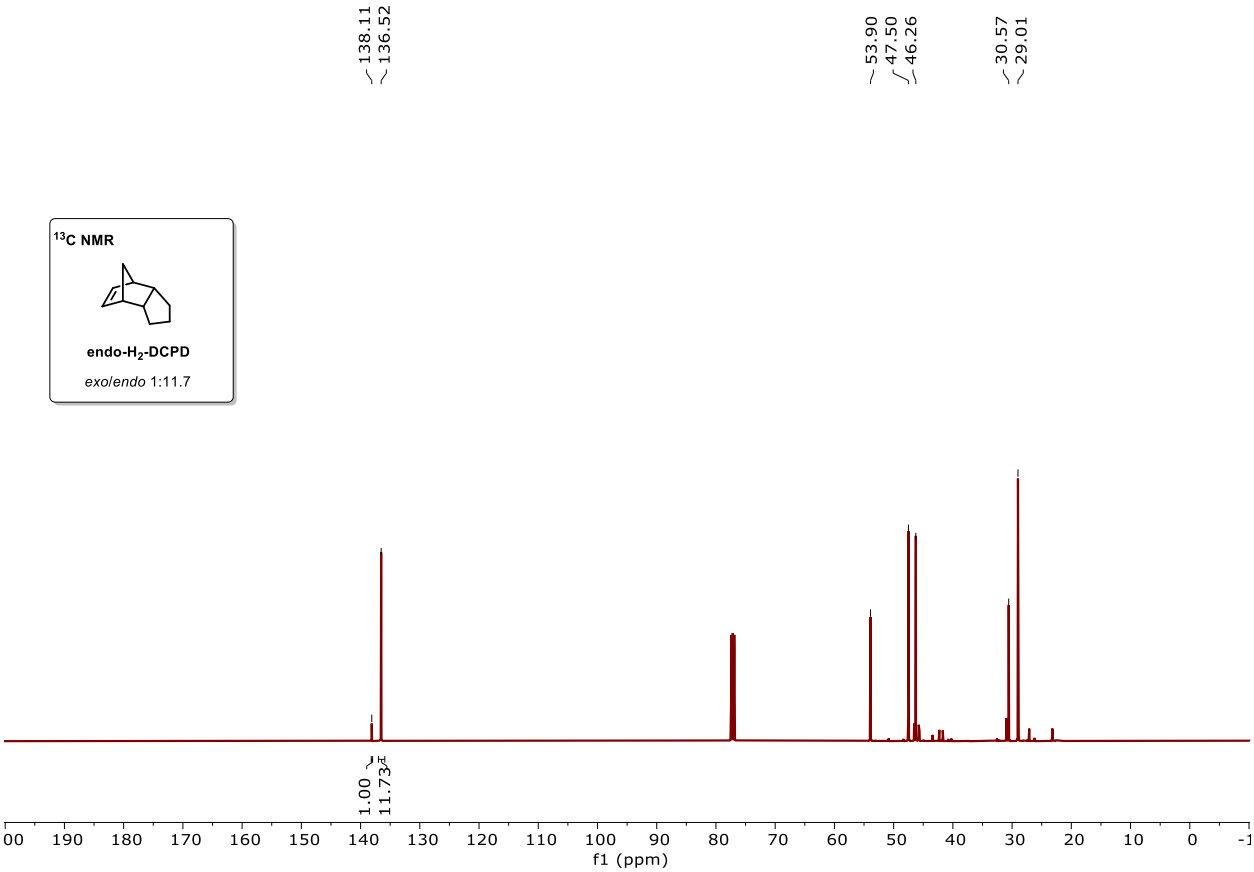

Supplementary Fig. 24 ^{13}C NMR spectrum of endo-H_2DCPD monomer. Contained 8% of exo-H_2DCPD isomer.

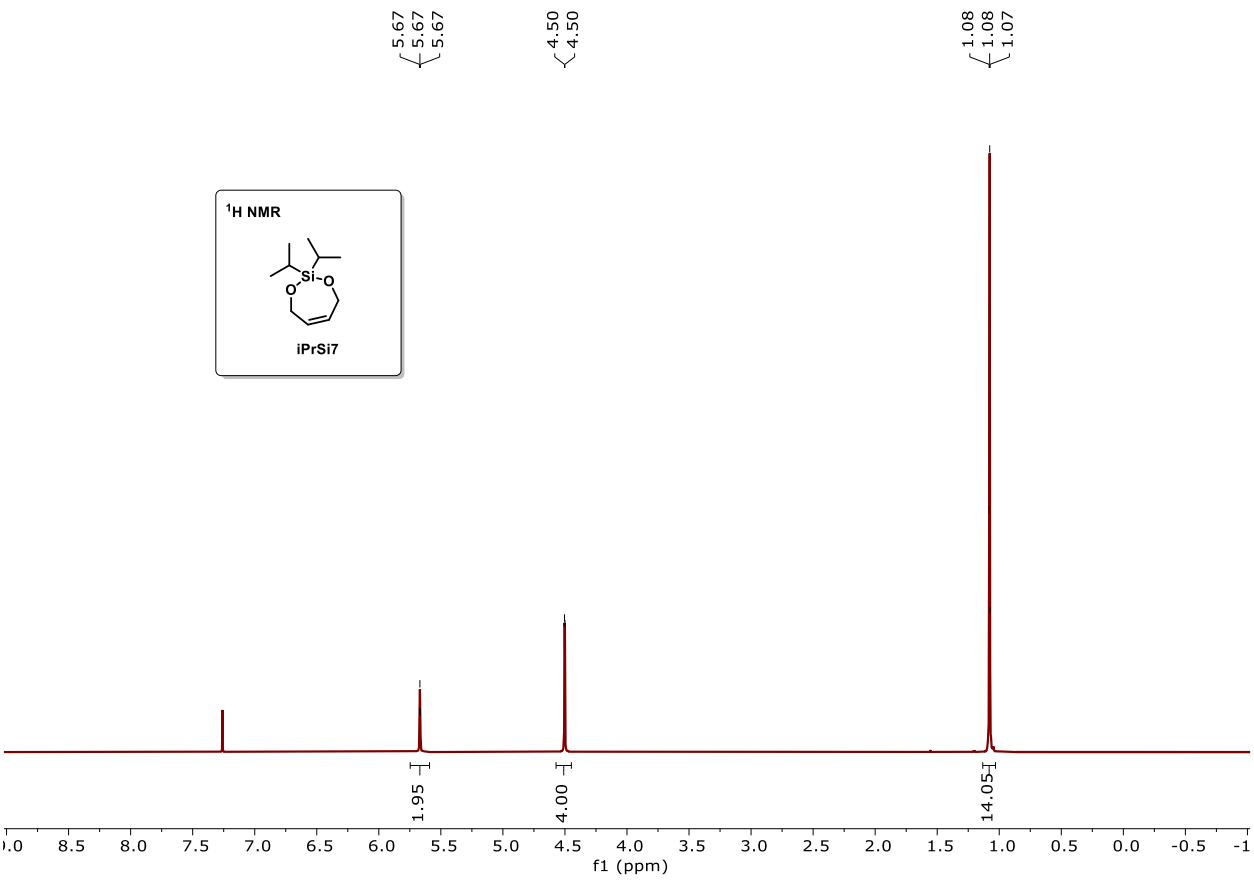

Supplementary Fig. 25 ^{1}H NMR spectrum of iPrSi7 cleavable comonomer. Spectral data are in accordance with those previously reported.[4]

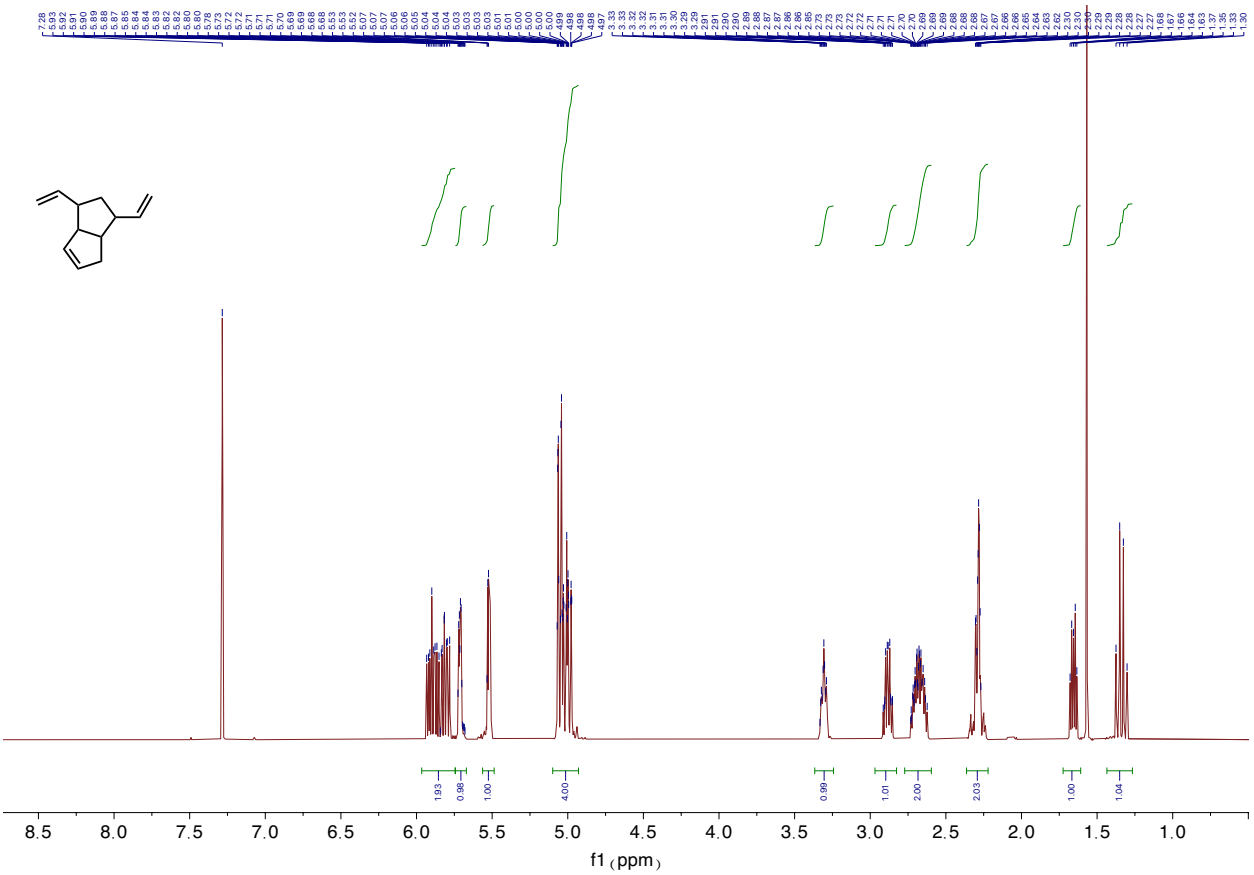

Supplementary Fig. 26 ^{1}H NMR spectrum of pDCPD monomer model.

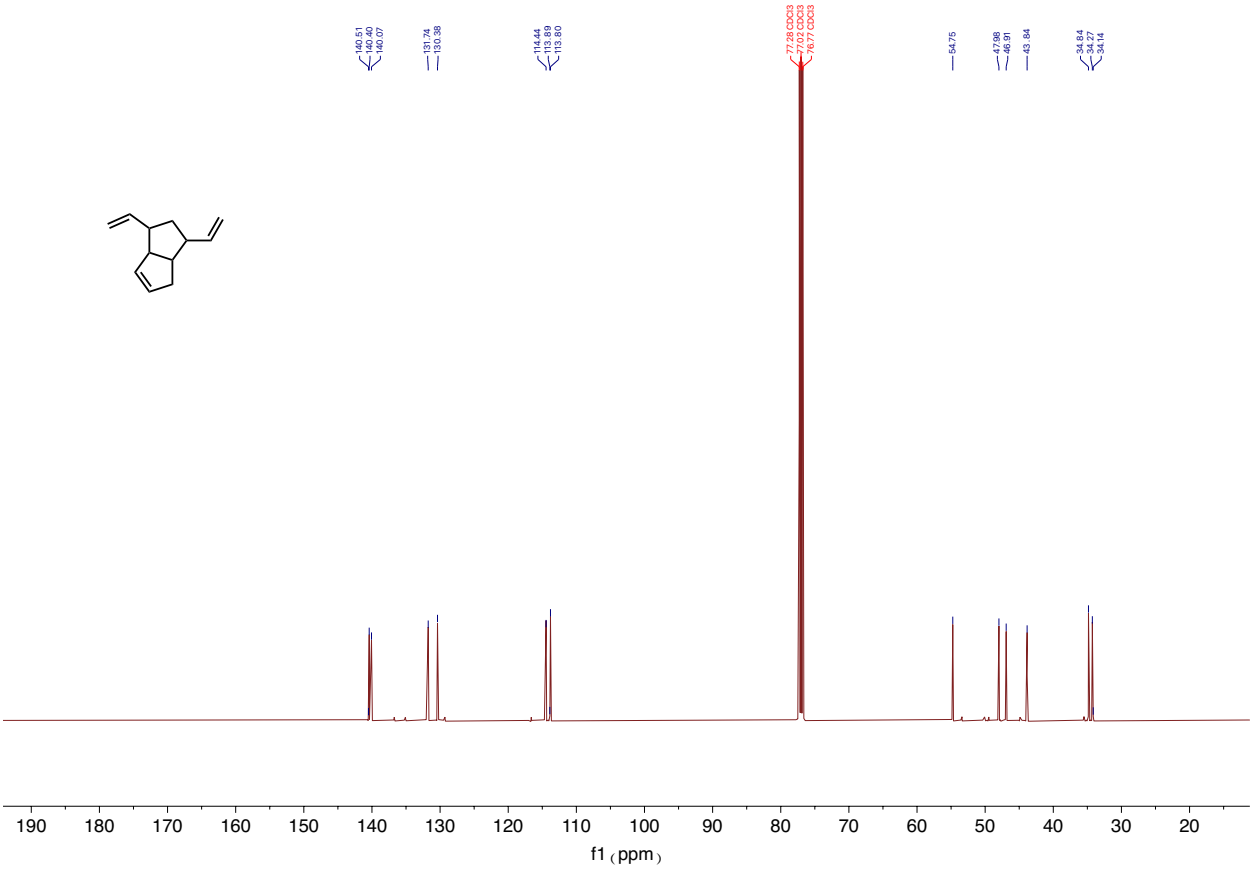

Supplementary Fig. 27 ^{13}C NMR spectrum of pDCPD monomer model.

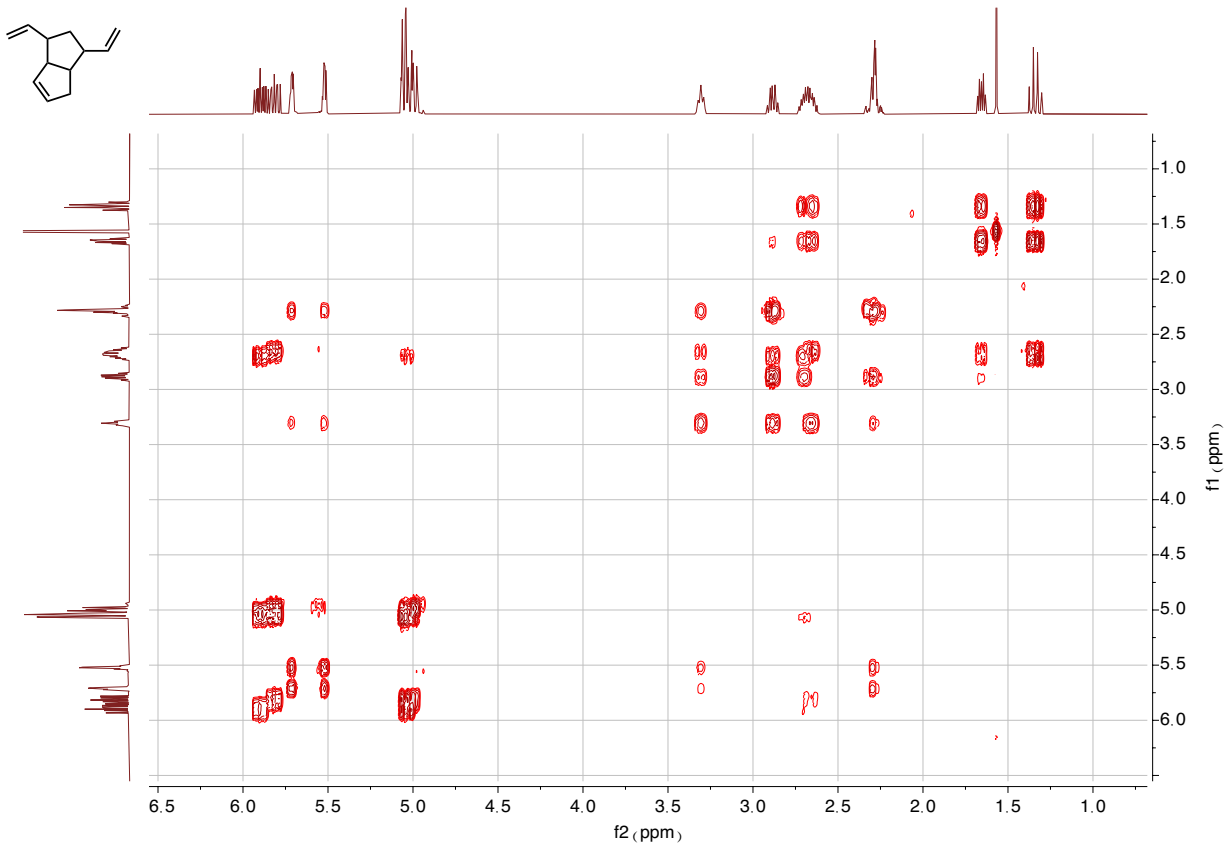

Supplementary Fig. 28 ^{1}H-^{1}H COSY spectrum of pDCPD monomer model.

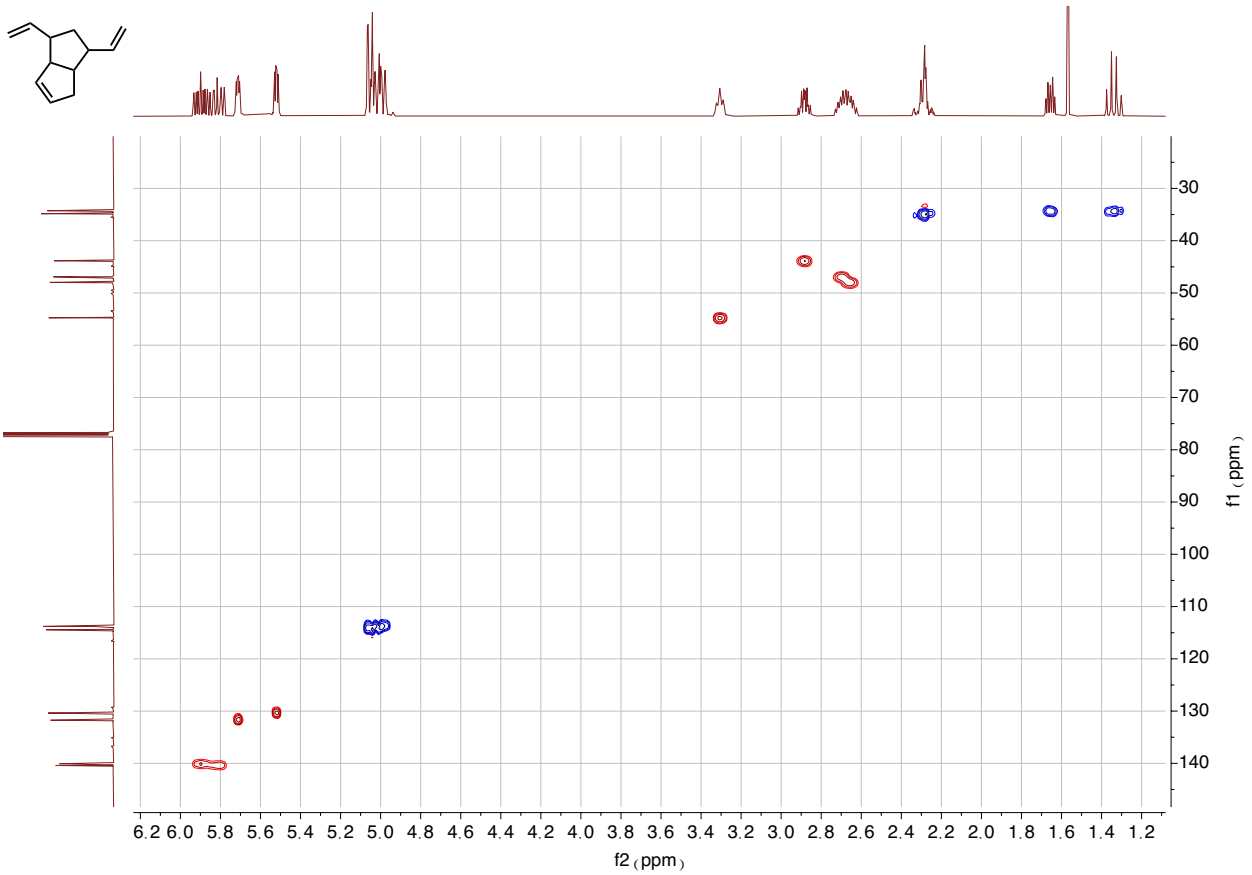

Supplementary Fig. 29 ^{1}H-^{13}C HSQC spectrum of pDCPD monomer model.

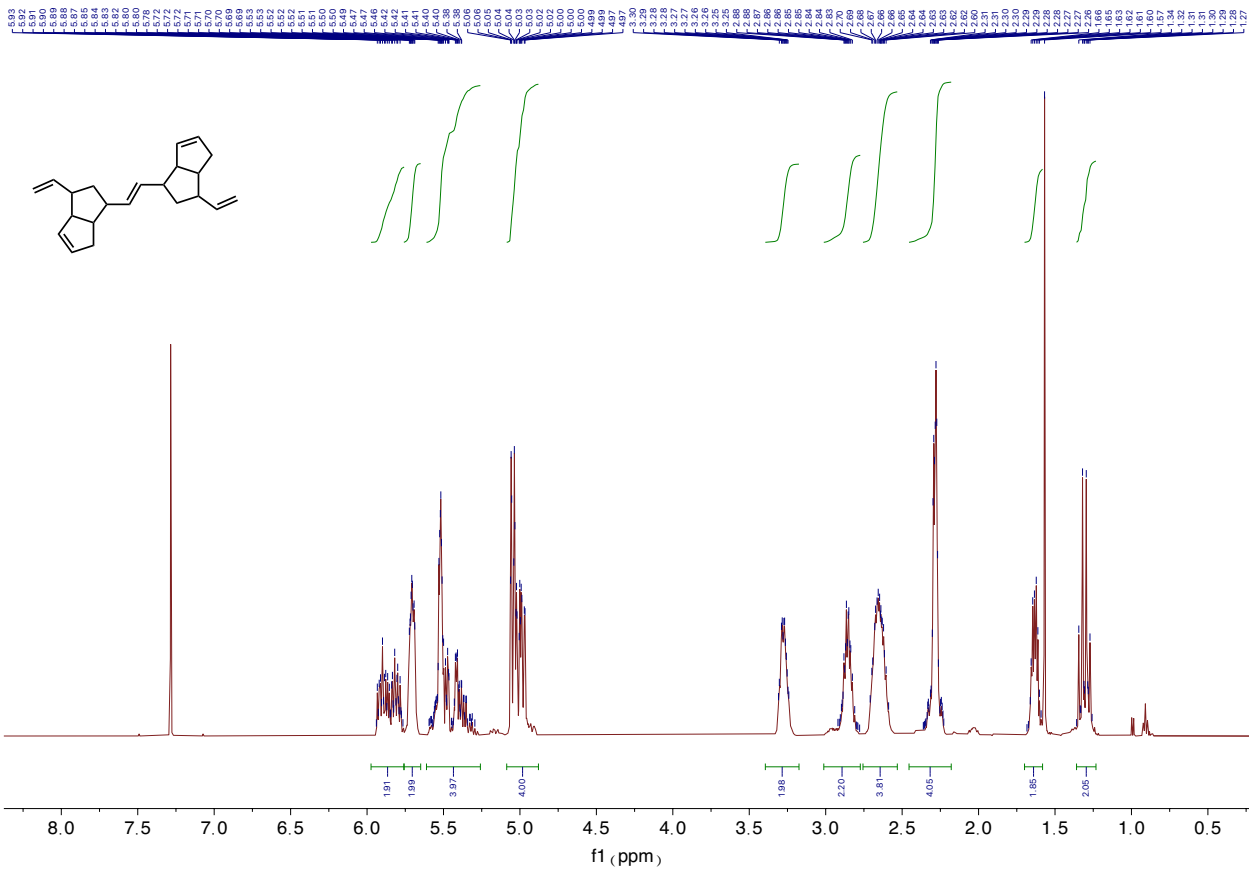

Supplementary Fig. 30 ^{1}H NMR spectrum of pDCPD dimer model.

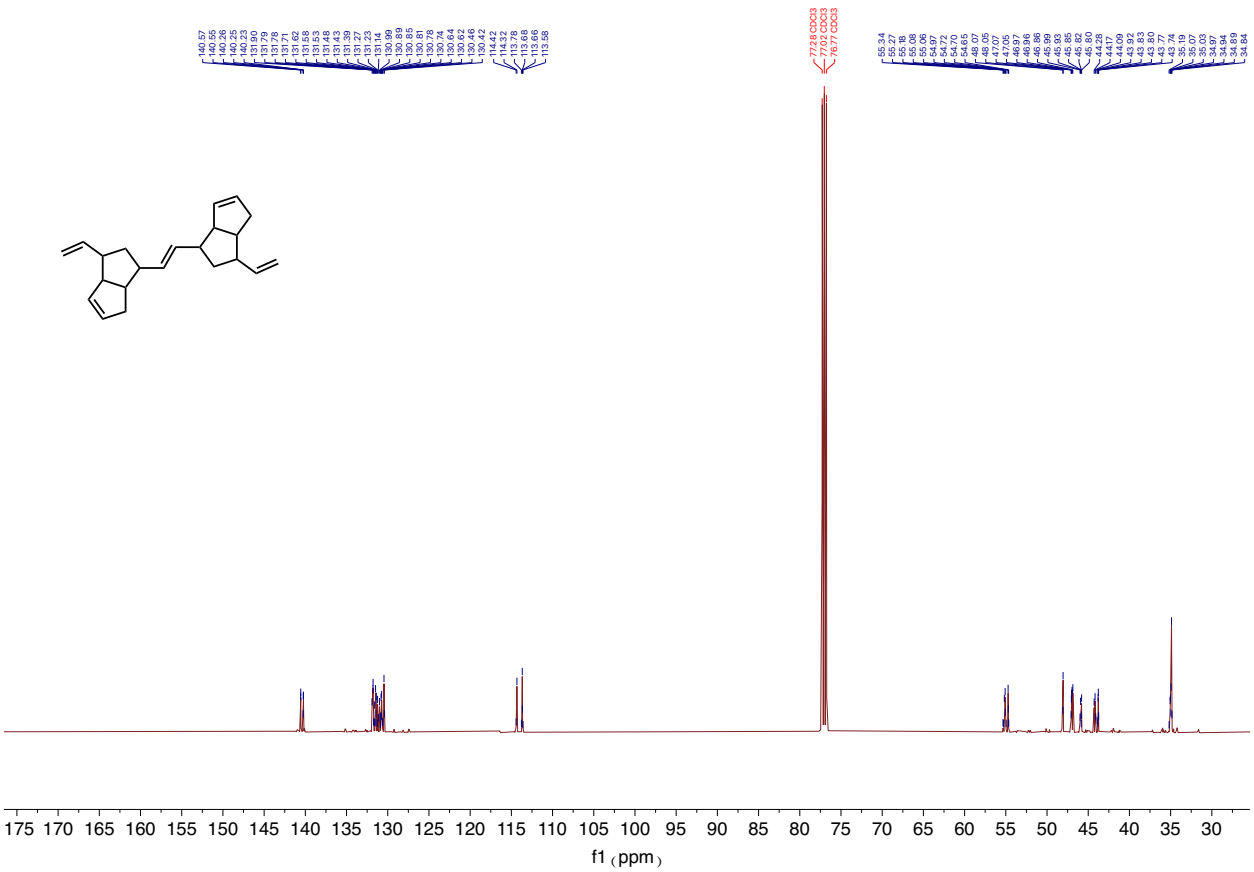

Supplementary Fig. 31 ^{13}C NMR spectrum of pDCPD dimer model.

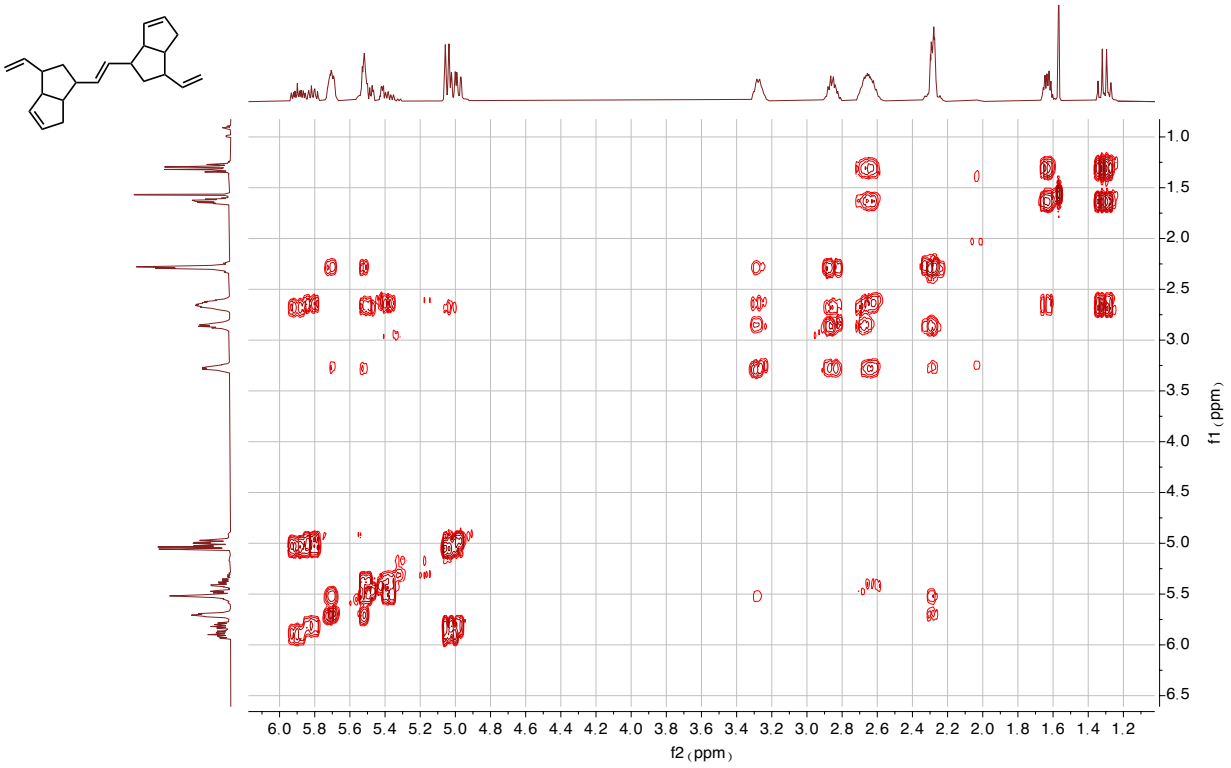

Supplementary Fig. 32 ^{1}H-^{1}H COSY spectrum of pDCPD dimer model.

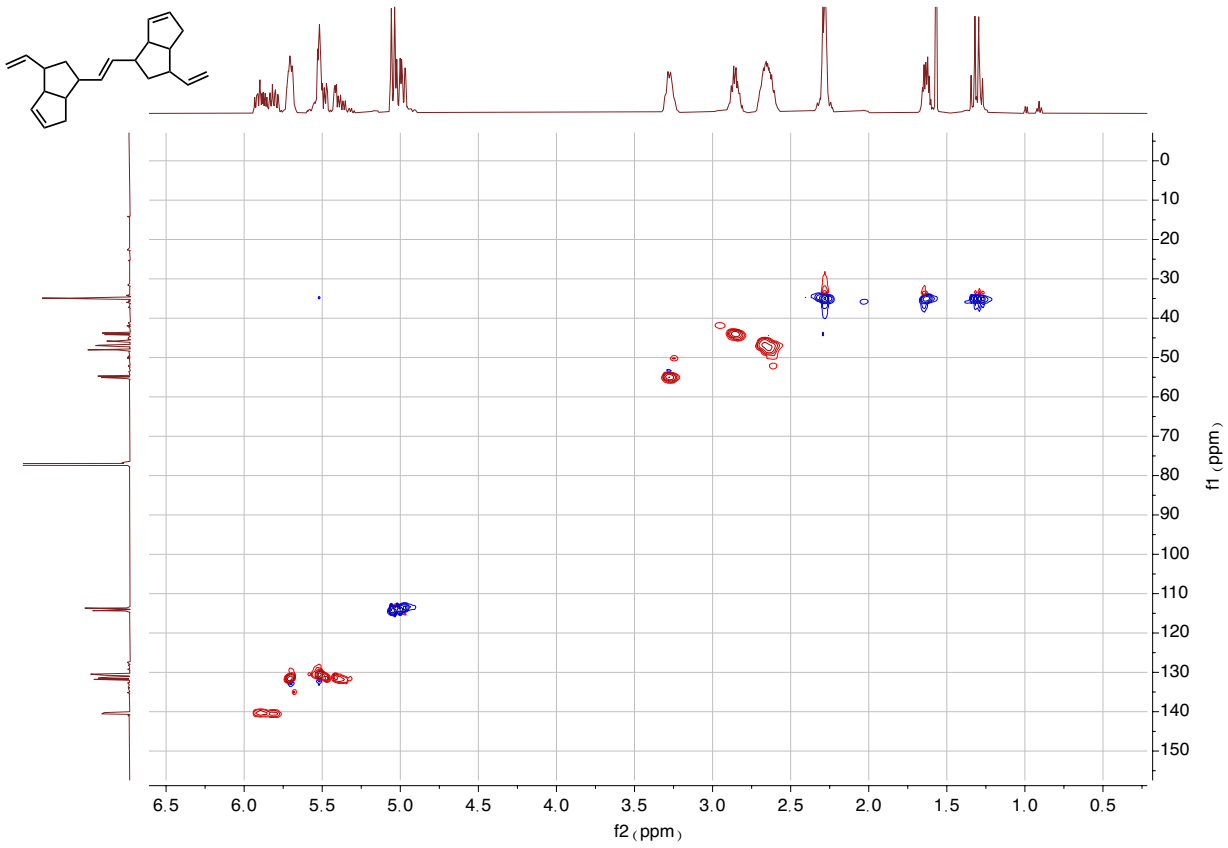

Supplementary Fig. 33 ^{1}H-^{13}C HSQC spectrum of pDCPD dimer model.

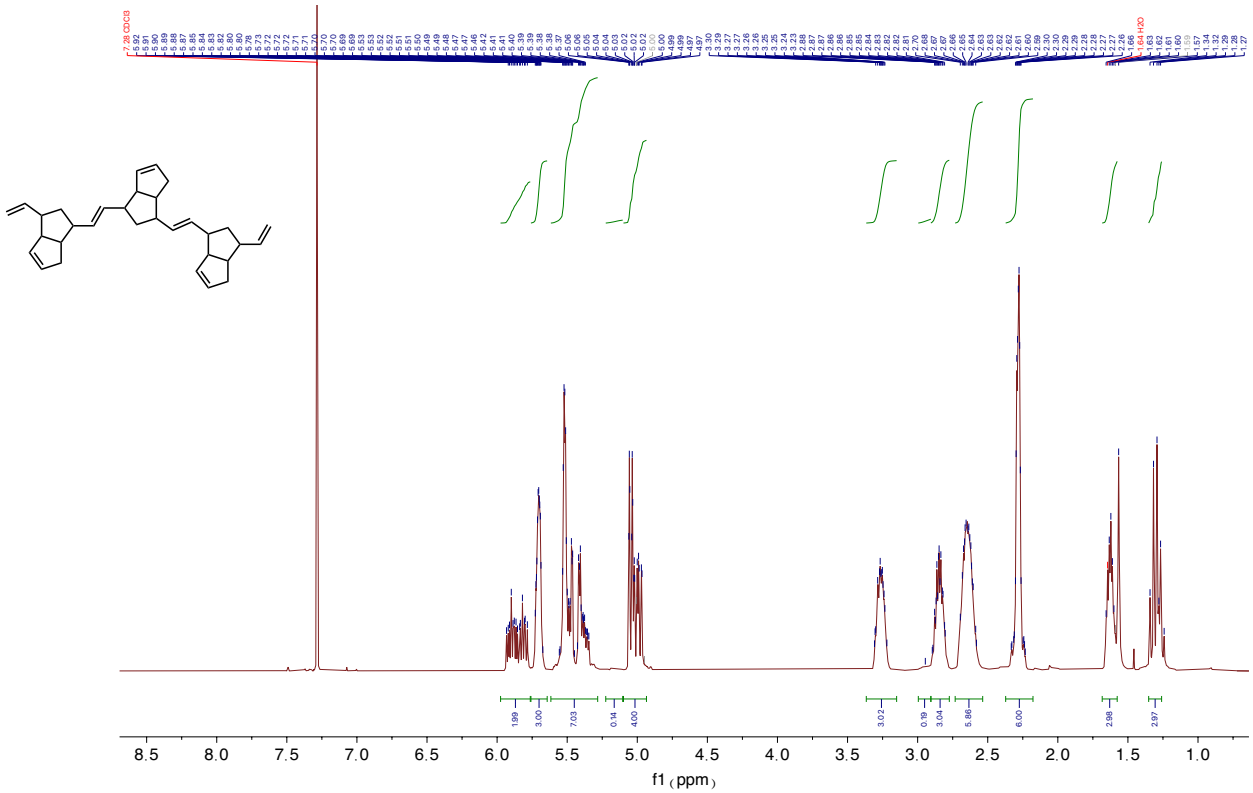

Supplementary Fig. 34 ^{1}H NMR spectrum of pDCPD trimer model.

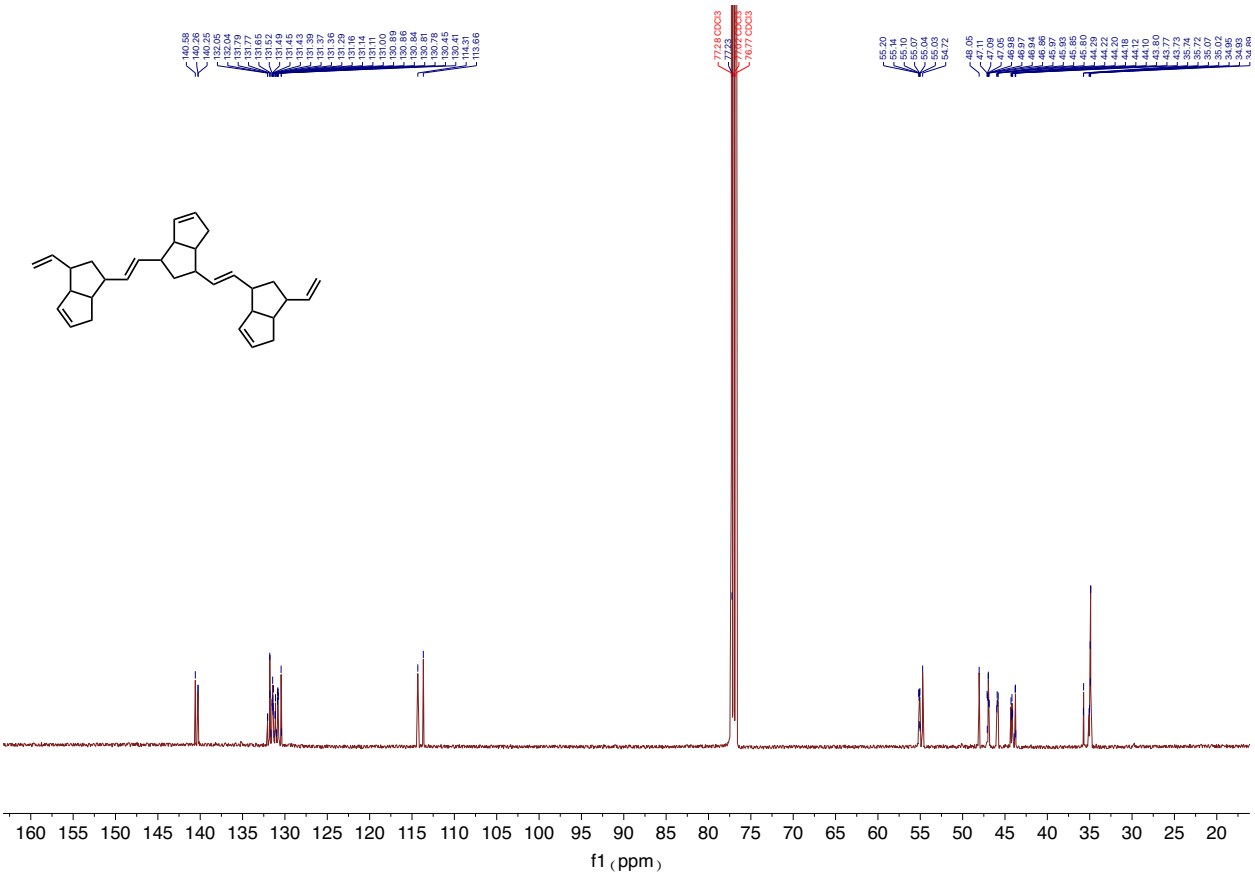

Supplementary Fig. 35 ^{1}C NMR spectrum of pDCPD trimer model.

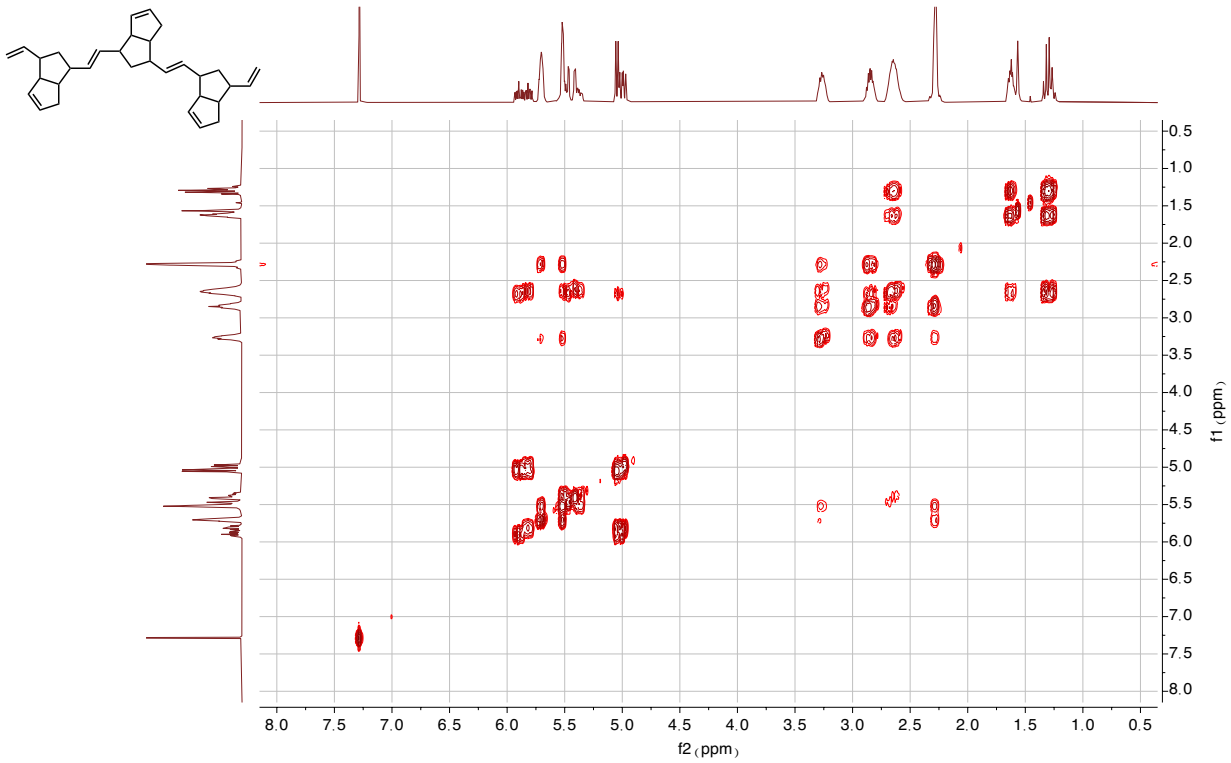

Supplementary Fig. 36 ^{1}H-^{1}H COSY spectrum of pDCPD trimer model.

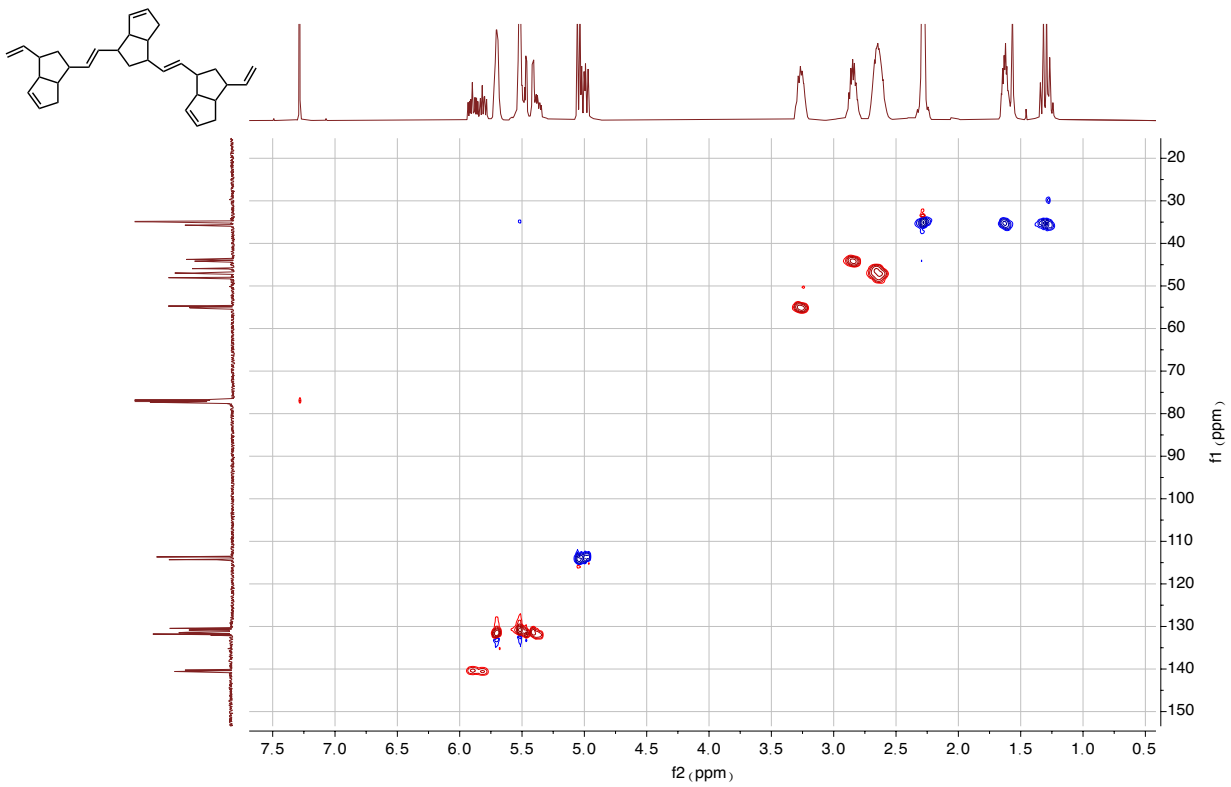

Supplementary Fig. 37 ^{1}H-^{13}C HSQC spectrum of pDCPD trimer model.

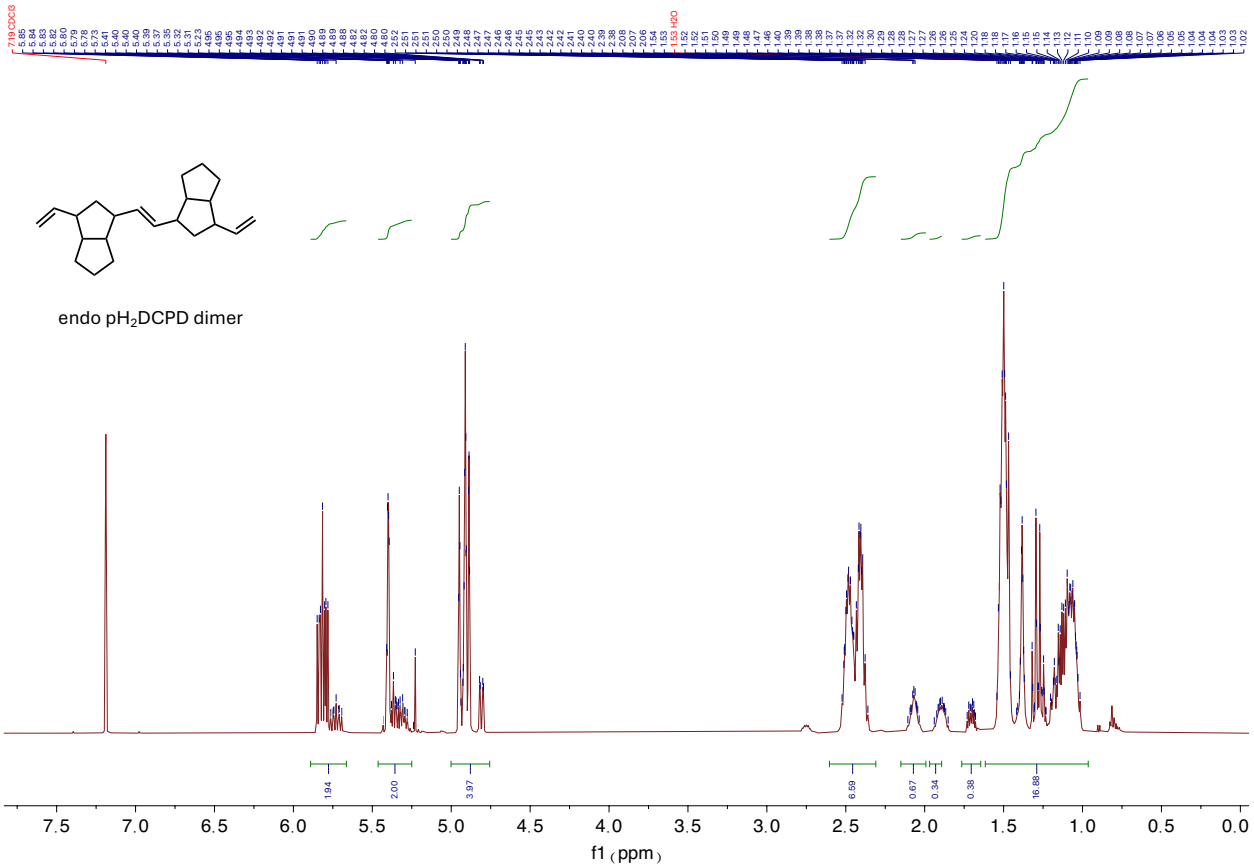

Supplementary Fig. 38 ^{1}H NMR spectrum of endo-pH$_2$DCPD dimer model. Spectrum contain stereo- isomers.

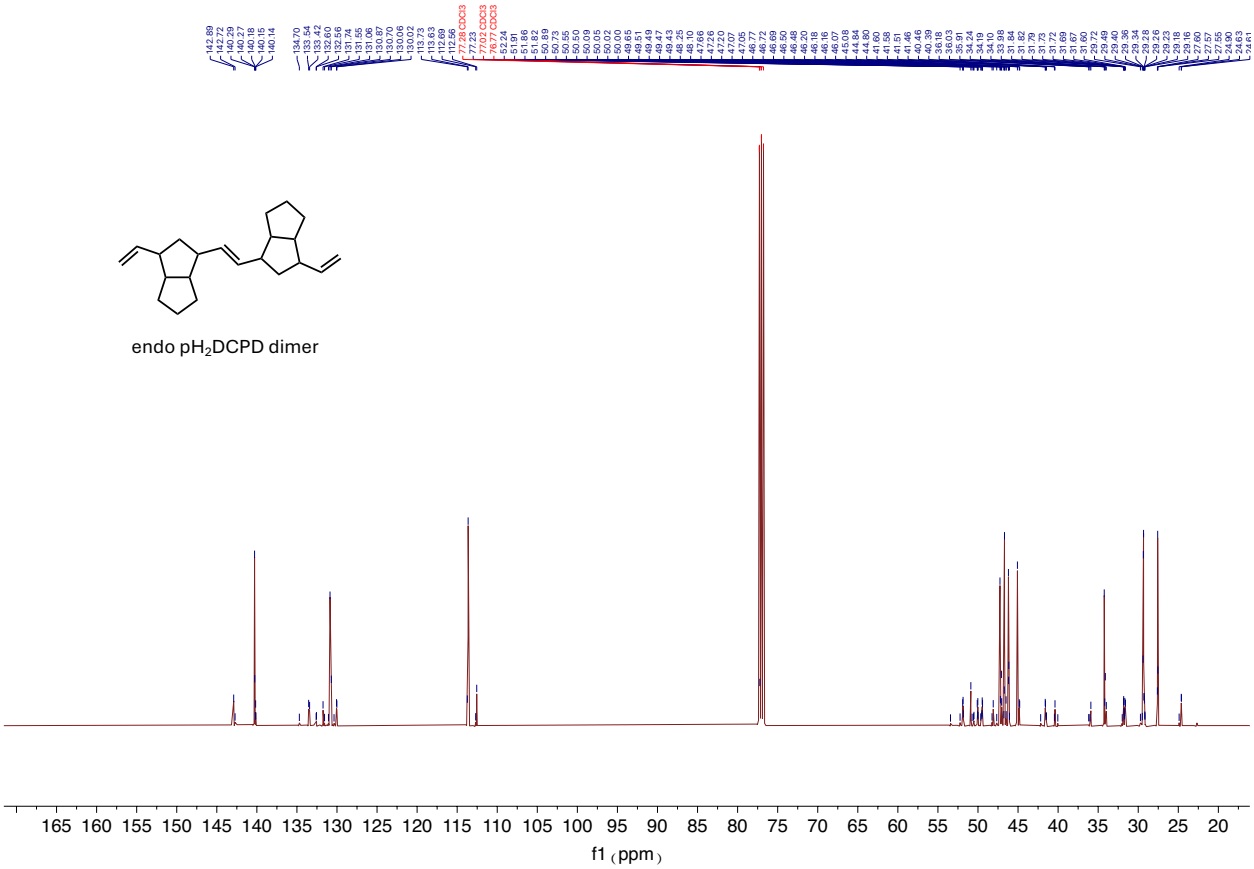

Supplementary Fig. 39 ^{13}C NMR spectrum of endo-pH$_2$DCPD dimer model. Spectrum contain stereo- isomers.

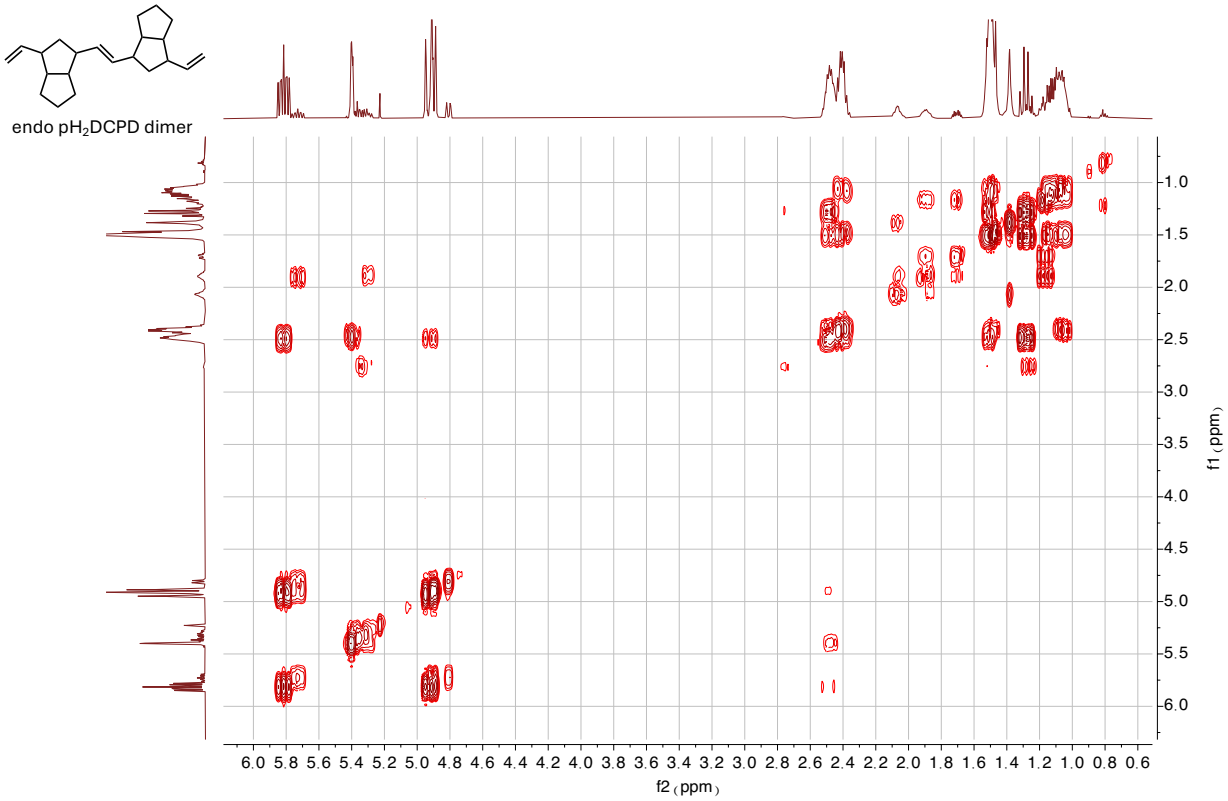

Supplementary Fig. 40 ^{1}H-^{1}H COSY spectrum of endo-pH$_2$DCPD dimer model. Spectrum contain stereo- isomers.

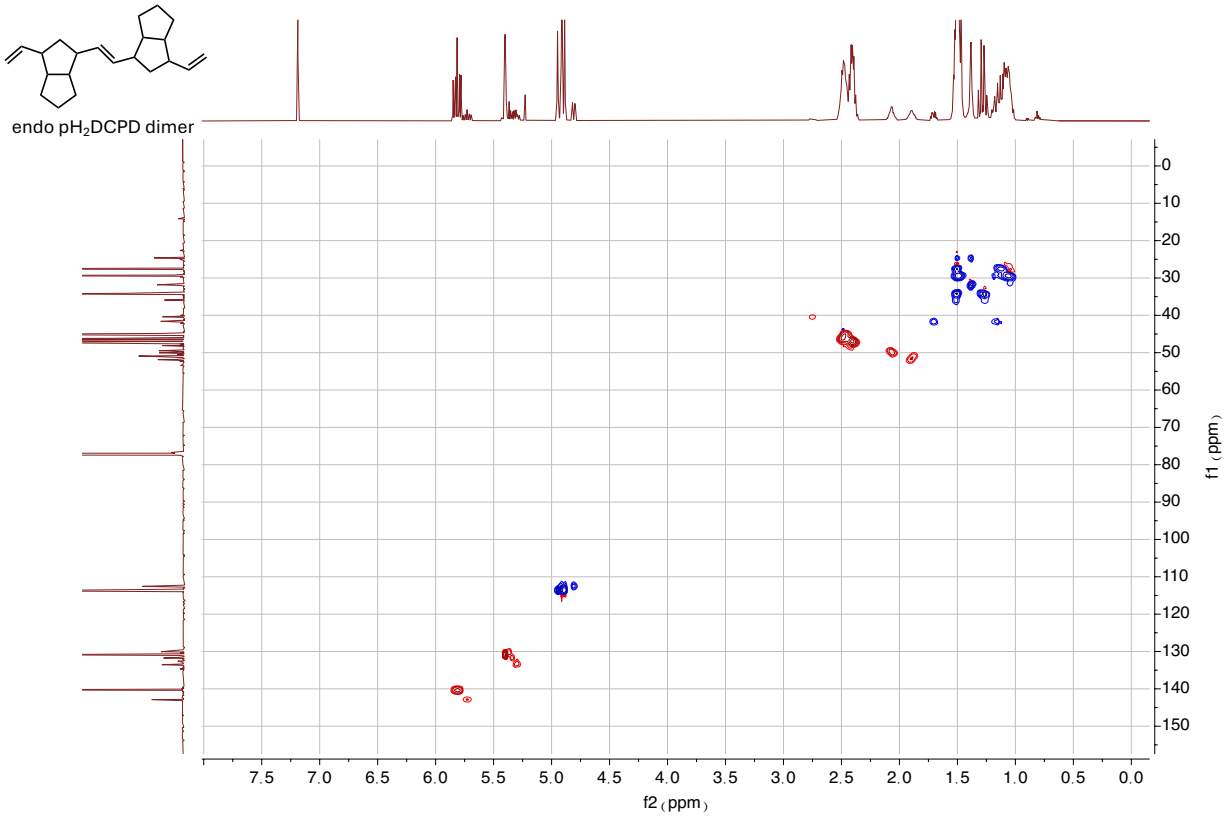

Supplementary Fig. 41 ^{1}H-^{13}C HSQC spectrum of endo-pH_2DCPD dimer model. Spectrum contain stereo- isomers.

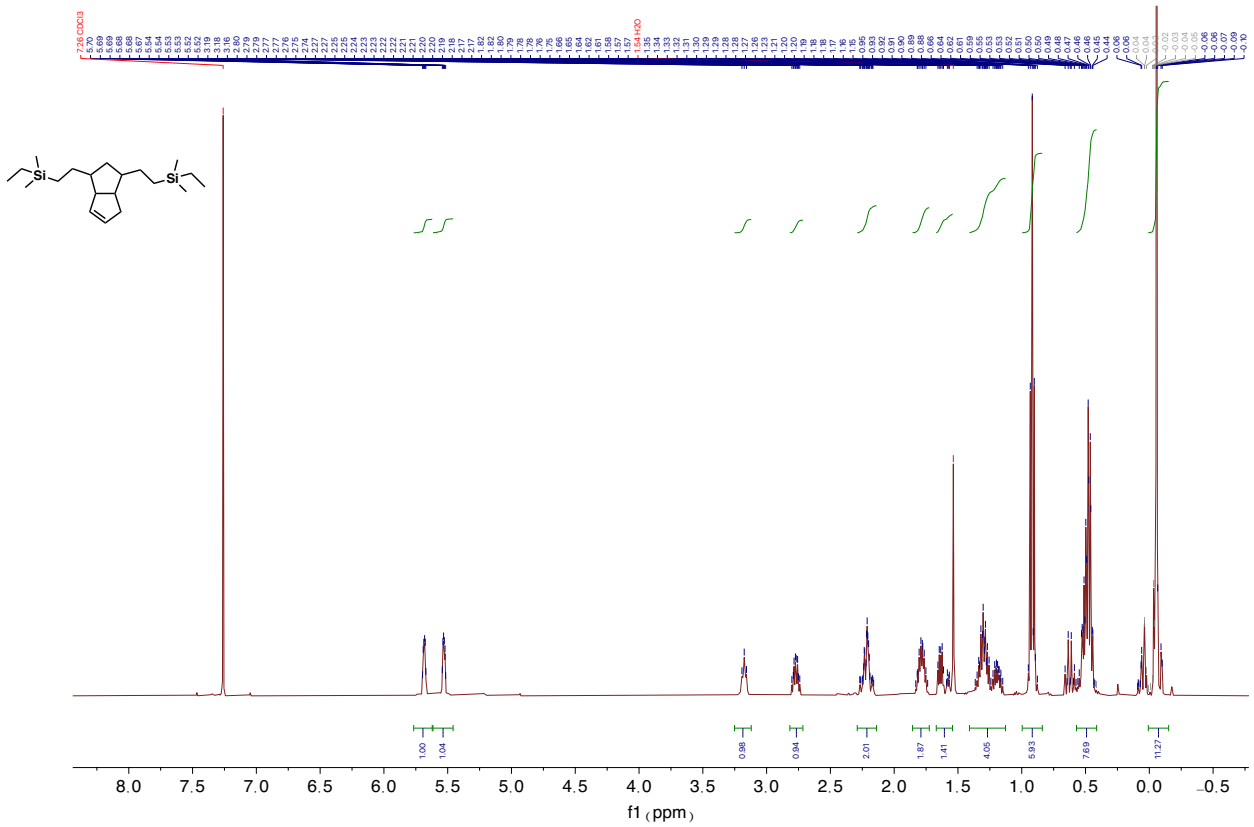

Supplementary Fig. 42 ^{1}H NMR spectrum of silane-reduced pDCPD monomer. Spectrum contain stereo- isomers.

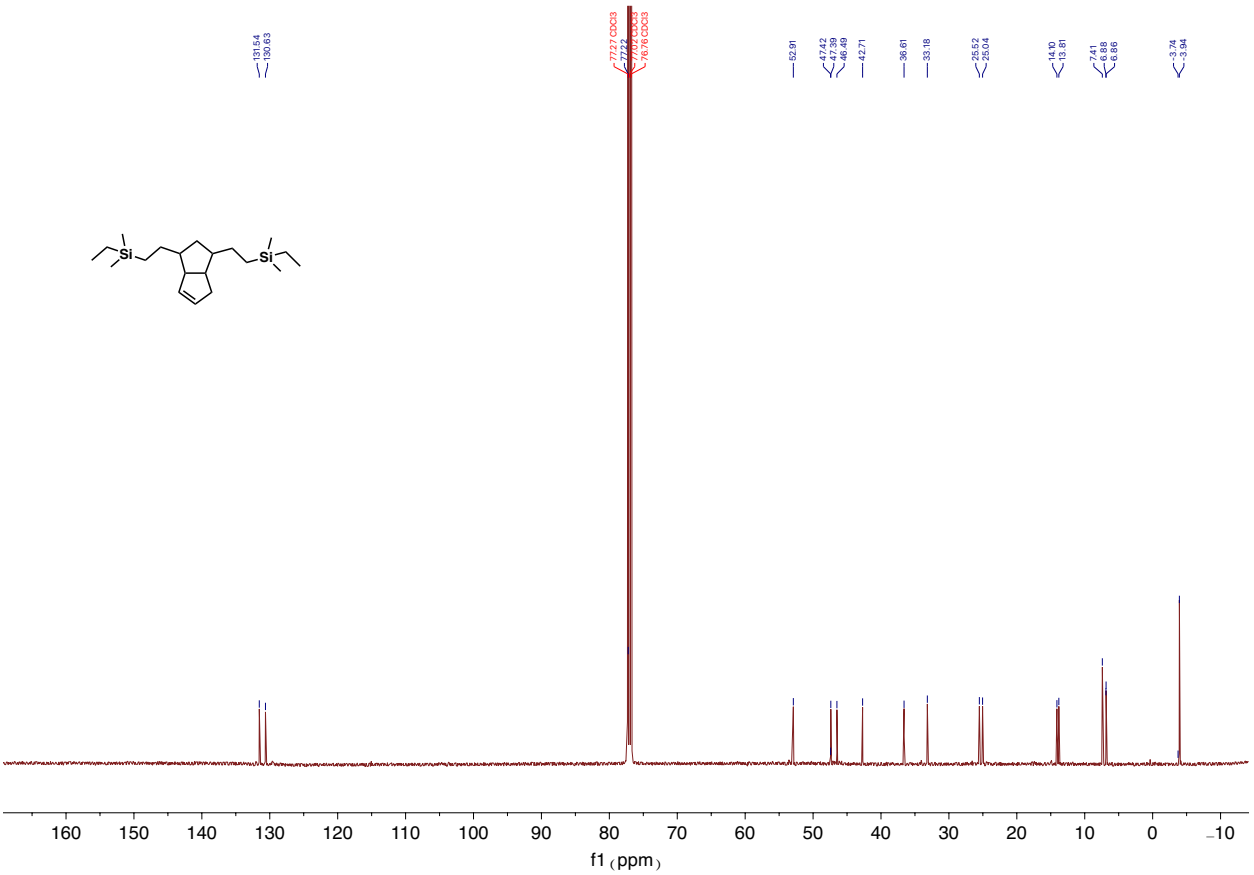

Supplementary Fig. 43 ^{13}C NMR spectrum of silane-reduced pDCPD monomer. Spectrum contain stereo- isomers.

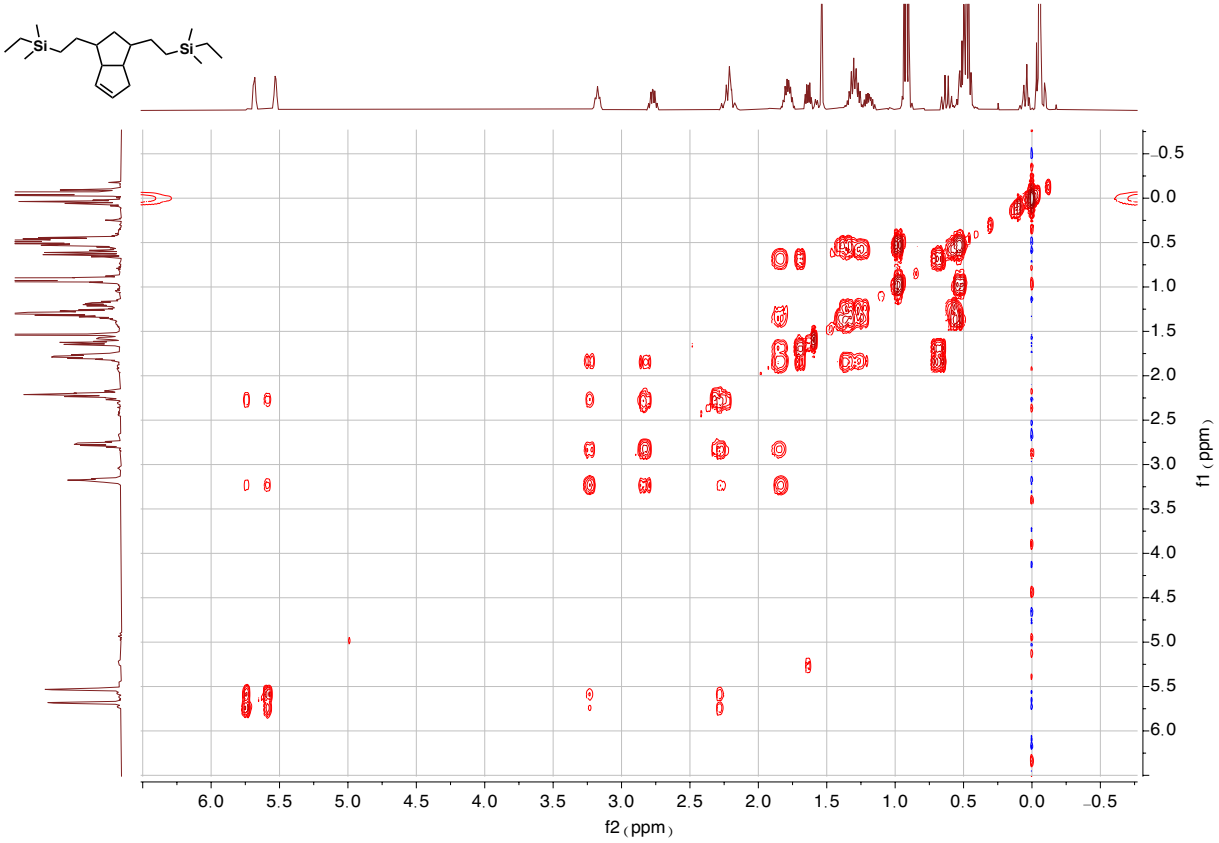

Supplementary Fig. 44 ^{1}H-^{1}H COSY spectrum of silane-reduced pDCPD monomer. Spectrum contain stereo- isomers.

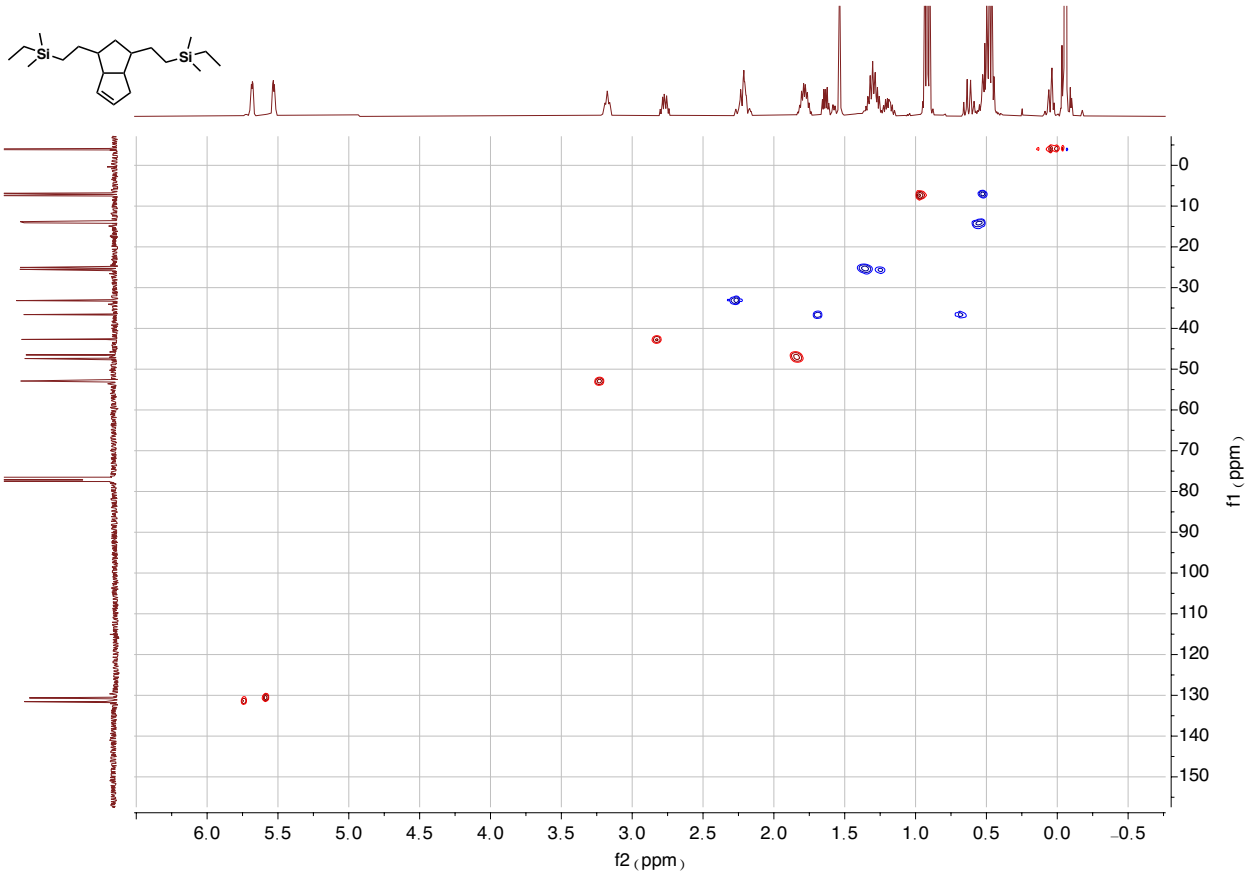

Supplementary Fig. 45 ^{1}H-^{13}C HSQC spectrum of silane-reduced pDCPD monomer. Spectrum contain stereo- isomers.

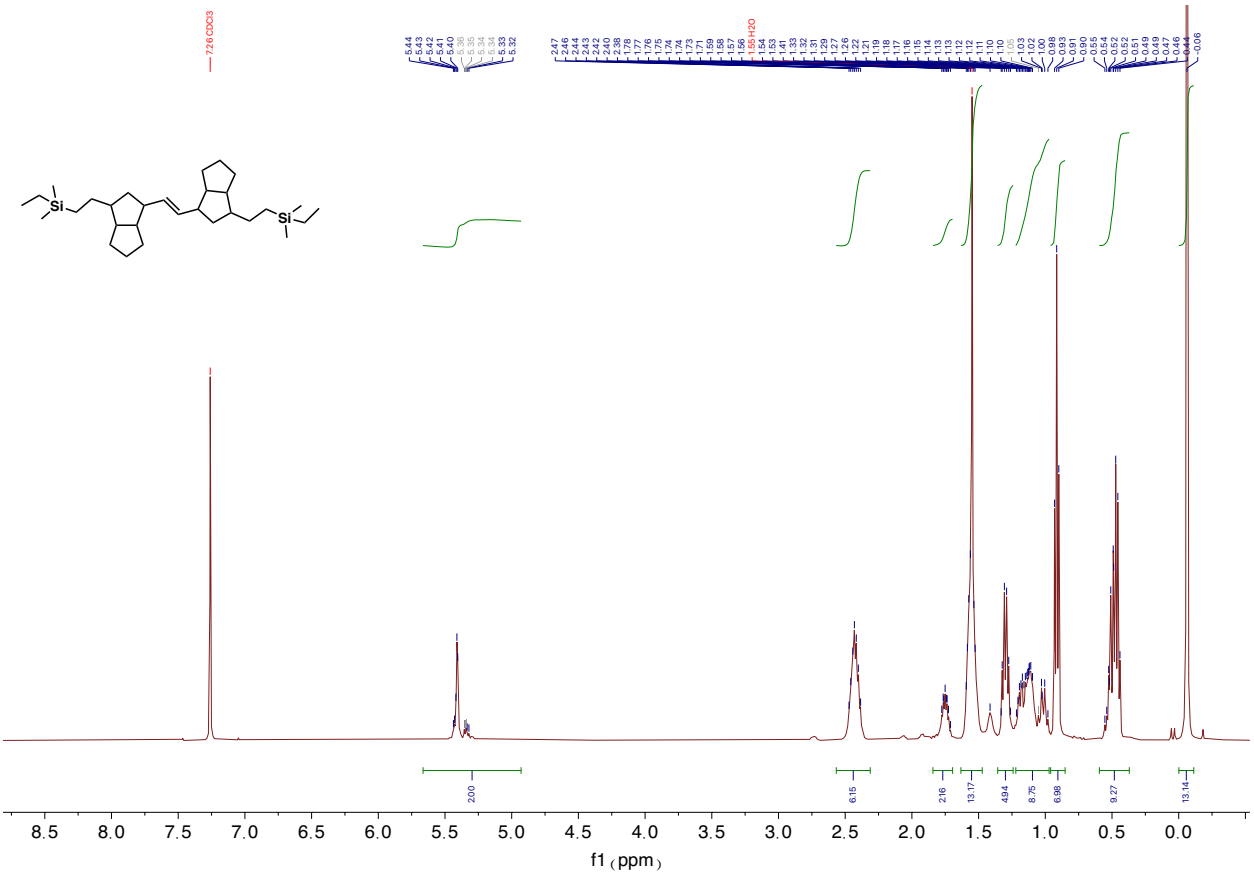

Supplementary Fig. 46 ^{1}H NMR spectrum of silane-reduced endo-pDCPD dimer. Spectrum contain various stereo- isomers.

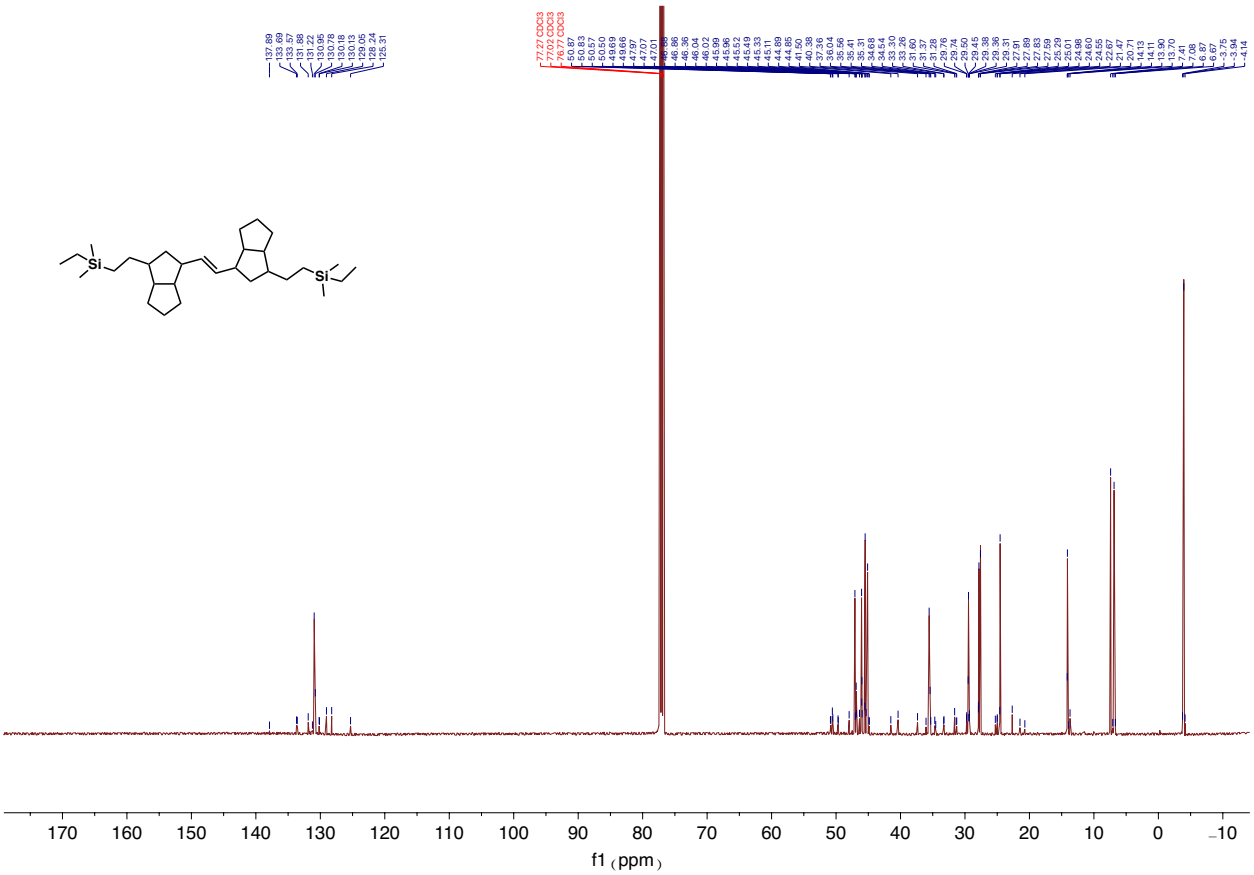

Supplementary Fig. 47 ^{13}C NMR spectrum of silane-reduced endo-pDCPD dimer. Spectrum contain various stereo- isomers.

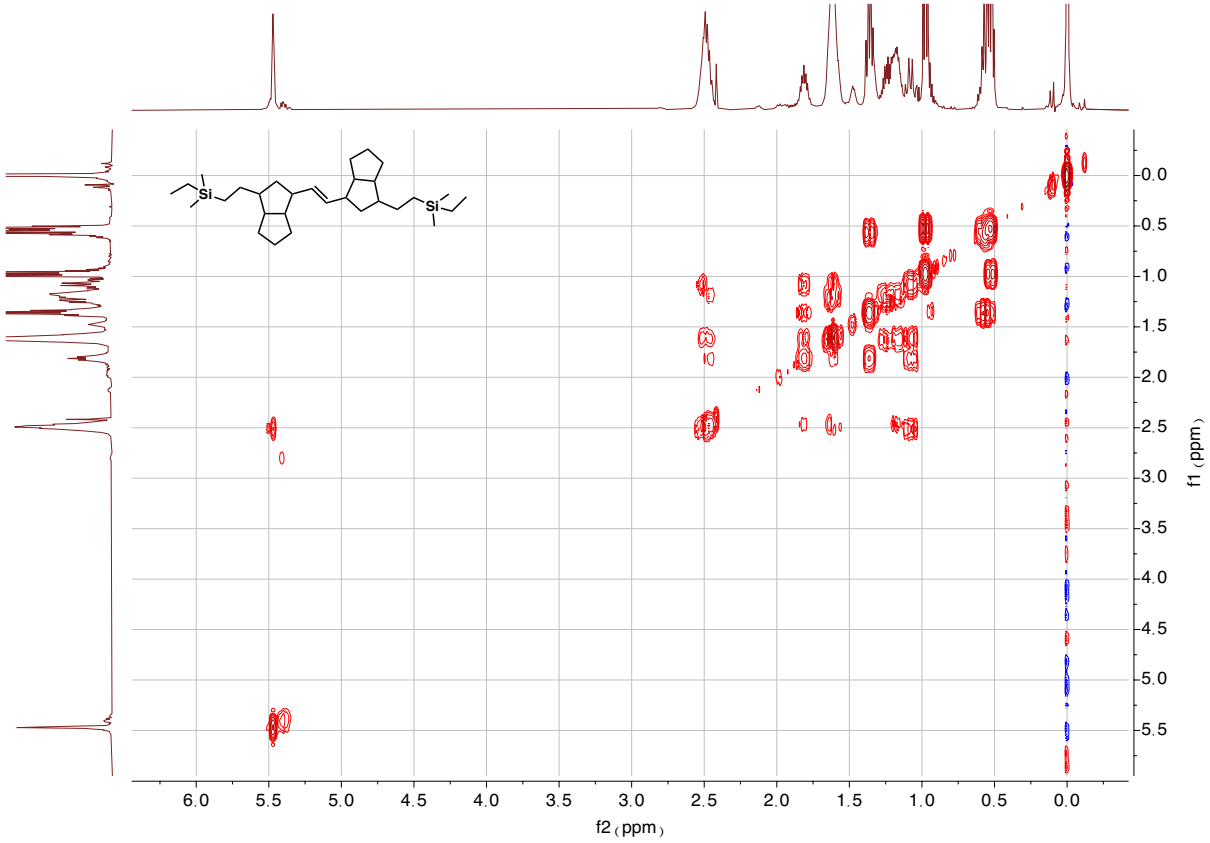

Supplementary Fig. 48 ^{1}H-^{1}H COSY spectrum of silane-reduced endo-pDCPD dimer. Spectrum contain stereoisomers.

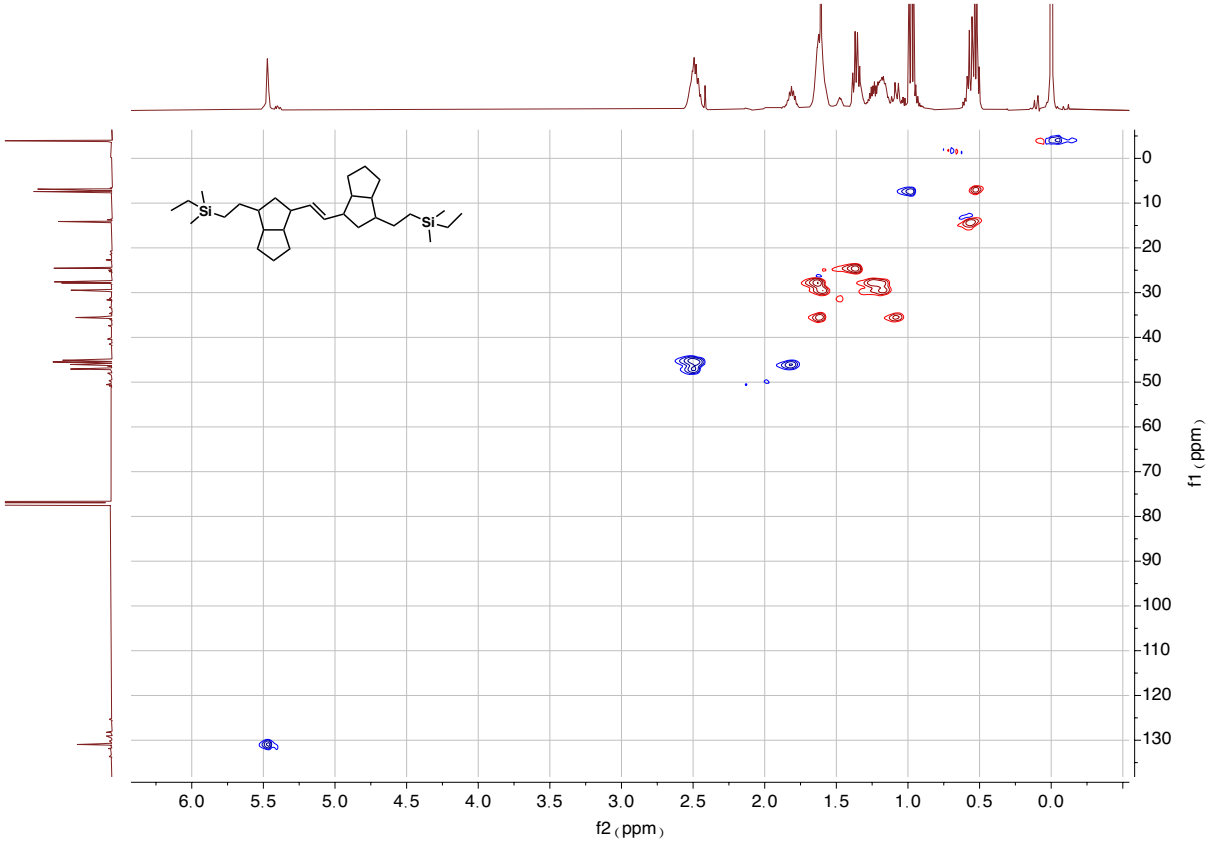

Supplementary Fig. 49 ^{1}H-^{1}C HSQC spectrum of silane-reduced endo-pDCPD dimer. Spectrum contain stereoisomers.

NMR Spectra of pDCPD Oligomers

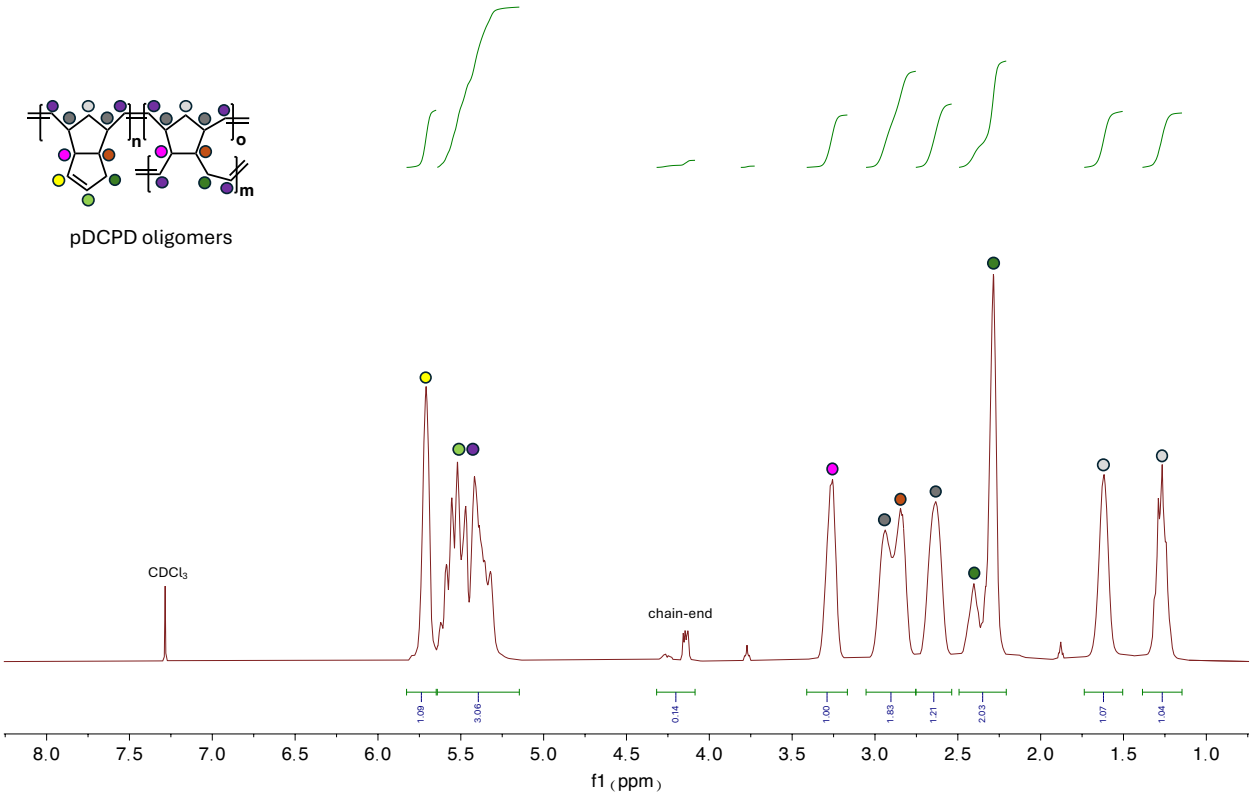

Supplementary Fig. 50 ^{1}H NMR spectrum of deconstructed pDCPD oligomers.

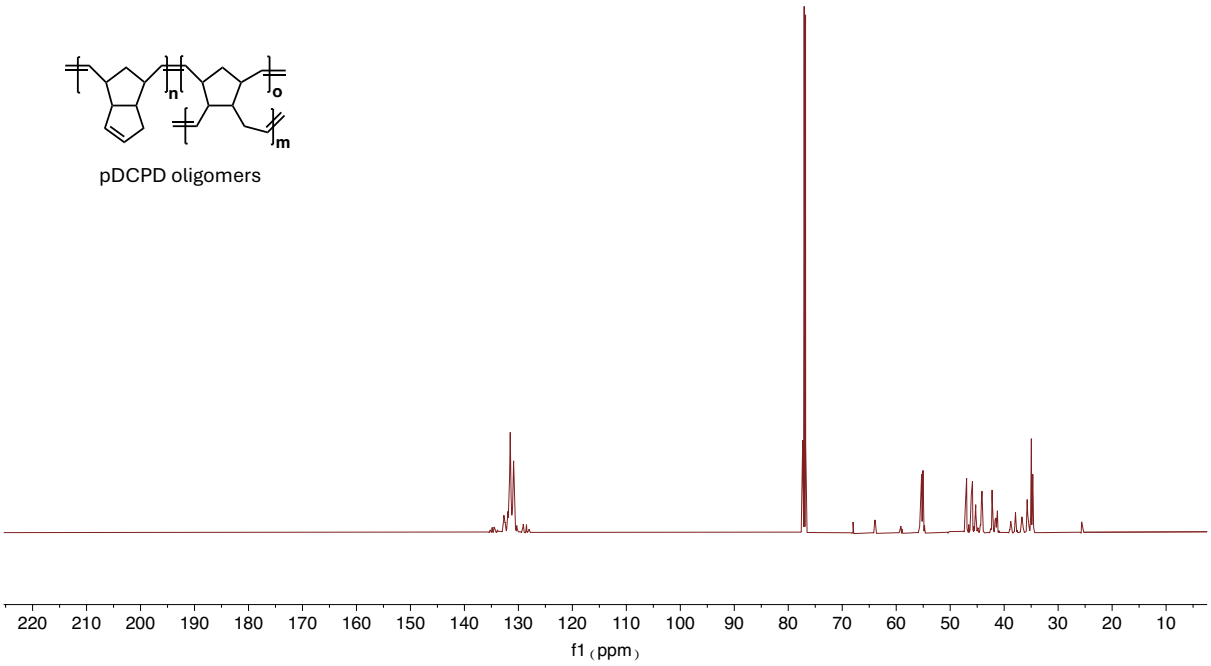

Supplementary Fig. 51 ^{13}C NMR spectrum of deconstructed pDCPD oligomers.

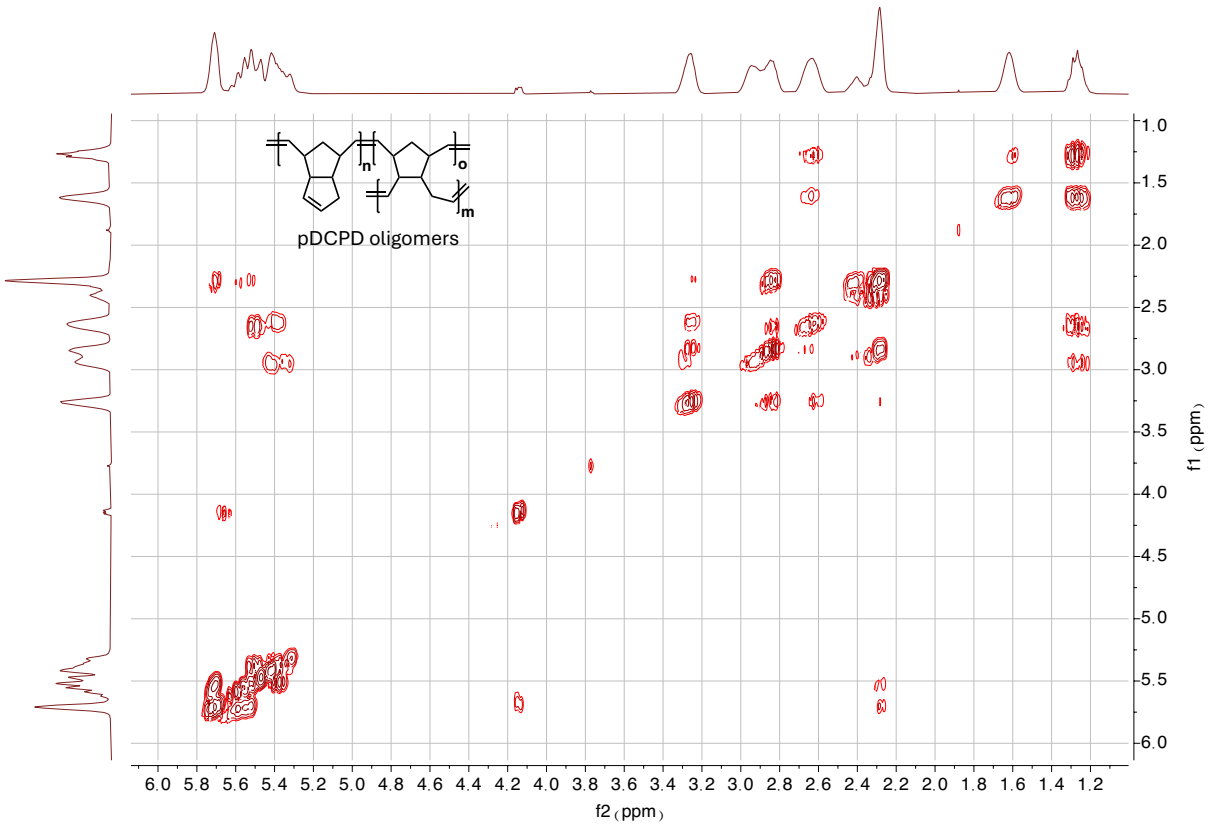

Supplementary Fig. 52 ^{1}H-^{1}H COSY spectrum of deconstructed pDCPD oligomers.

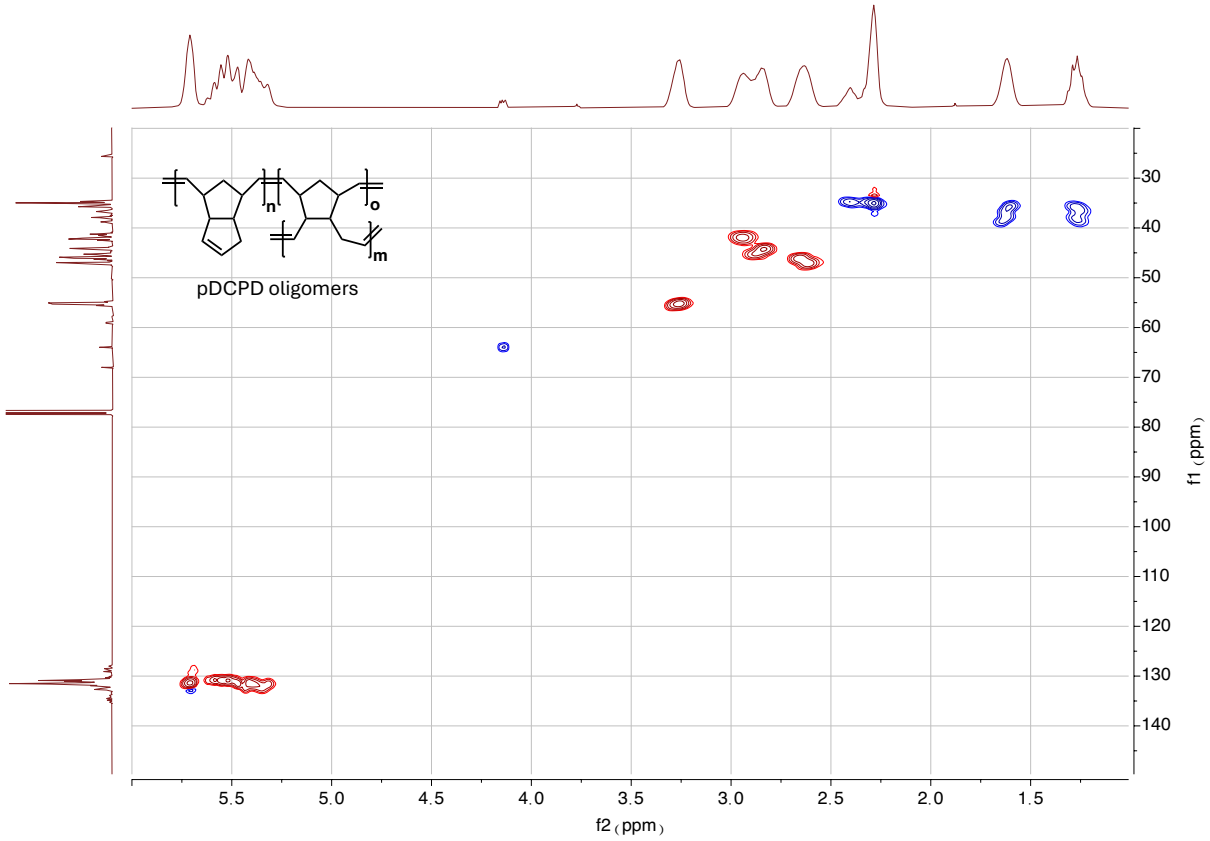

Supplementary Fig. 53 ^{1}H-^{13}C HSQC spectrum of deconstructed pDCPD oligomers.

NMR Spectra of pH$_2$DCPD Oligomers

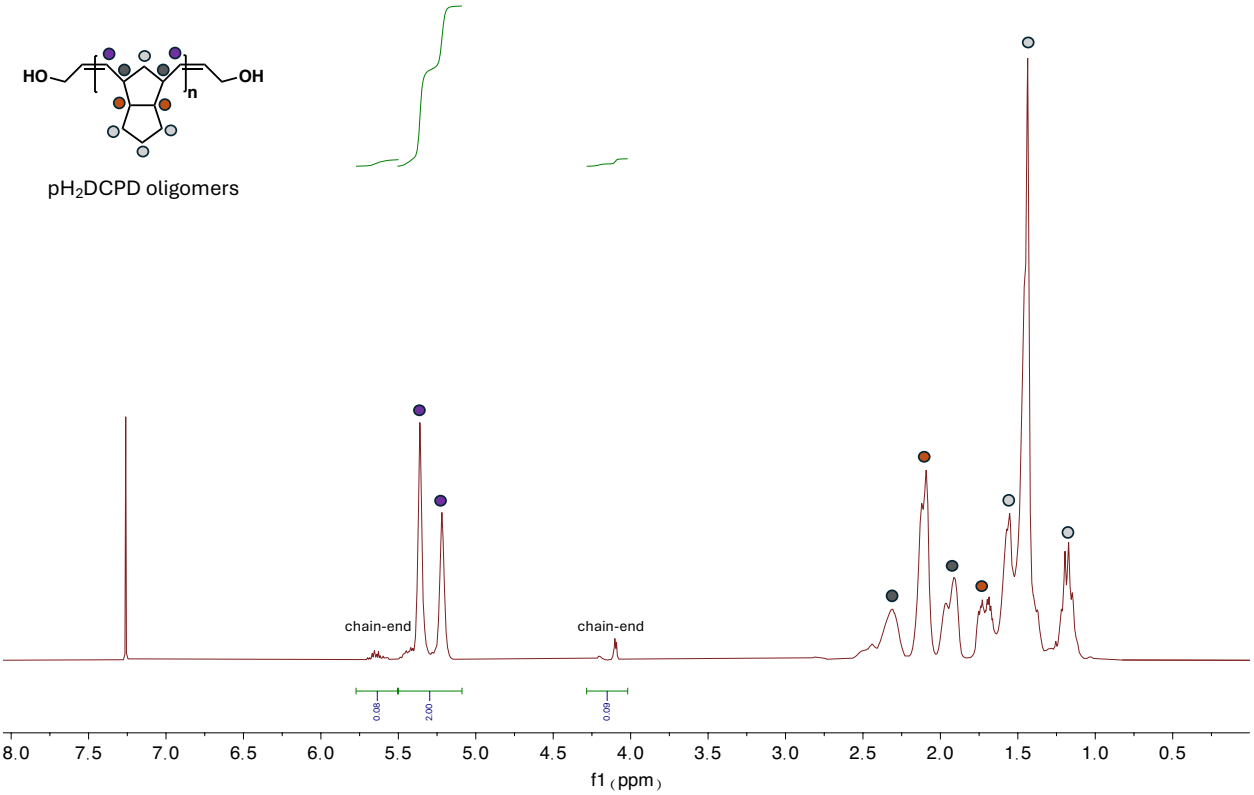

Supplementary Fig. 54 ^{1}H NMR spectrum of deconstructed pH$_2$DCPD oligomers. Linear polymer backbone. Prepared from exo-H$_2$DCPD monomer via frontal ring-opening polymerization.

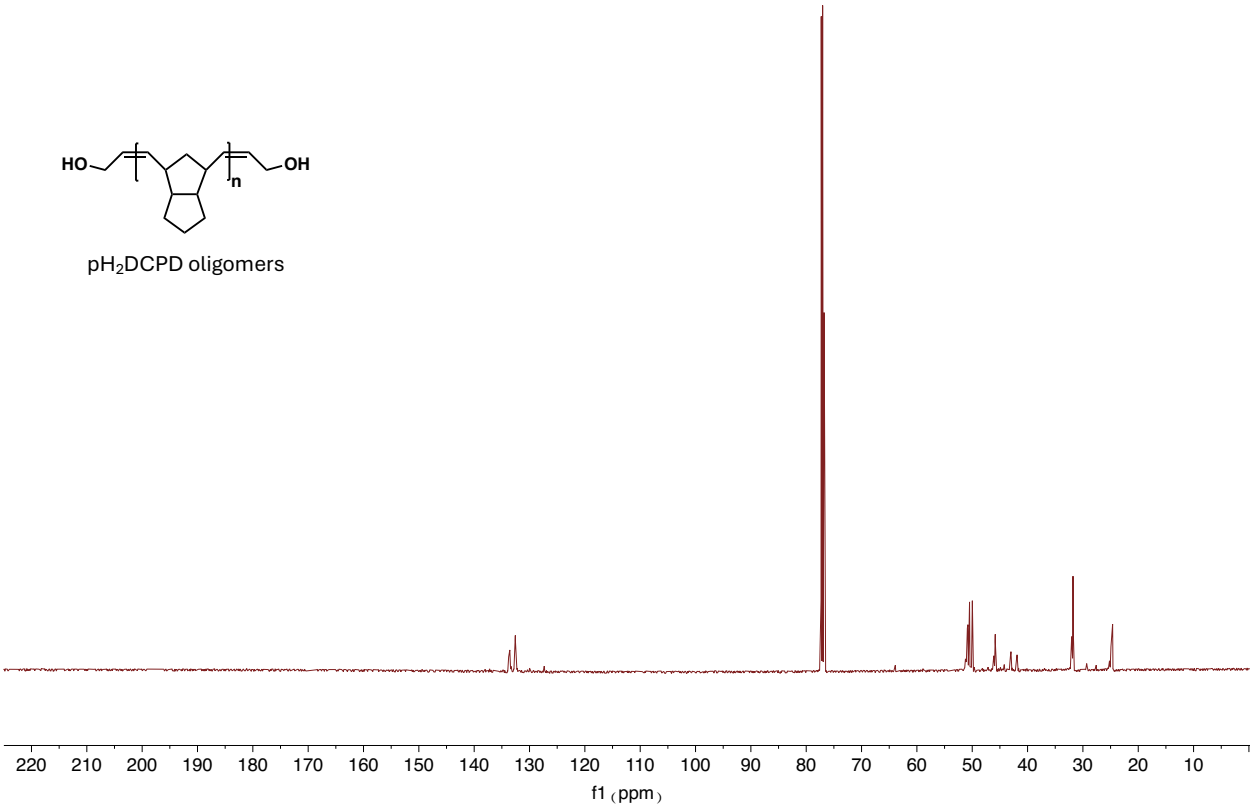

Supplementary Fig. 55 ^{13}C NMR spectrum of deconstructed pH_2DCPD oligomers.

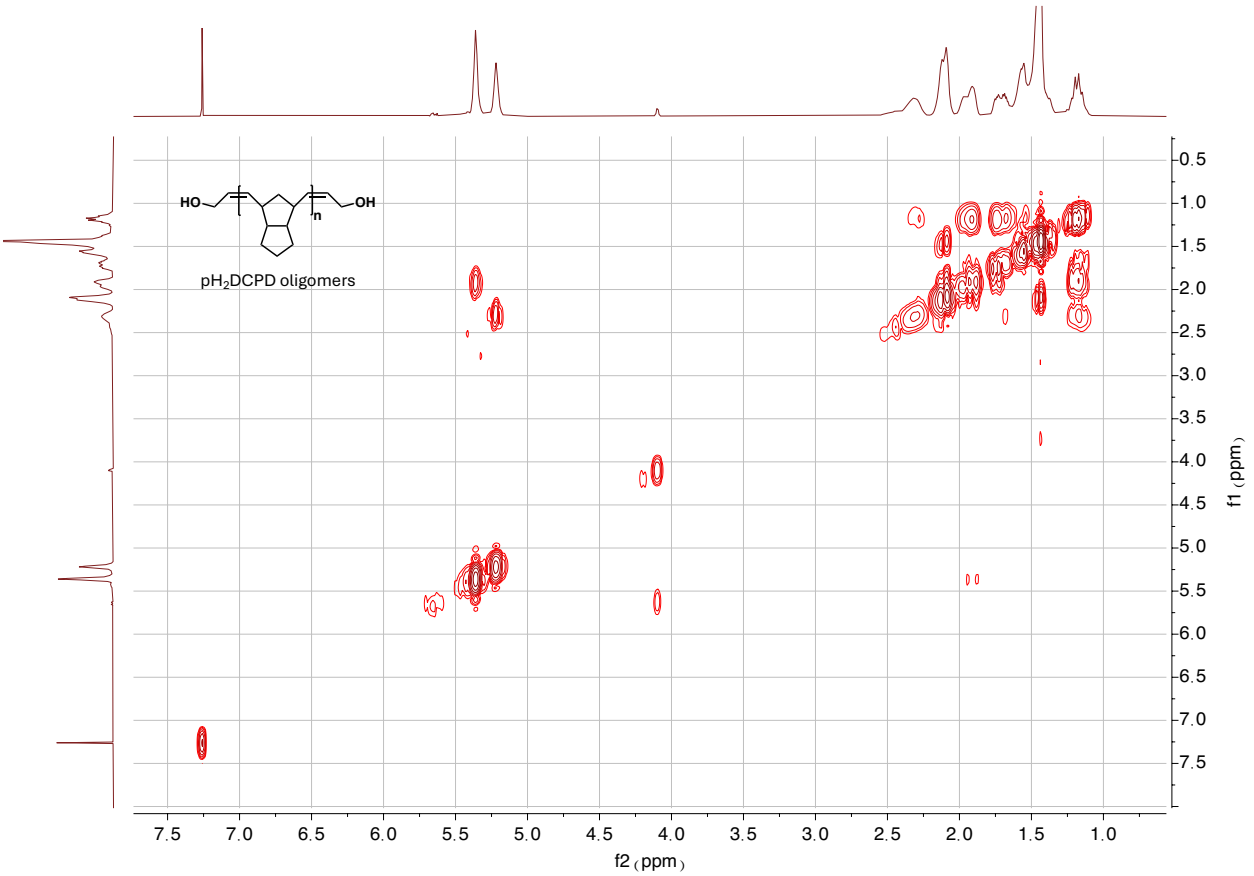

Supplementary Fig. 56 ^{1}H-^{1}H COSY spectrum of deconstructed pH_2DCPD oligomers.

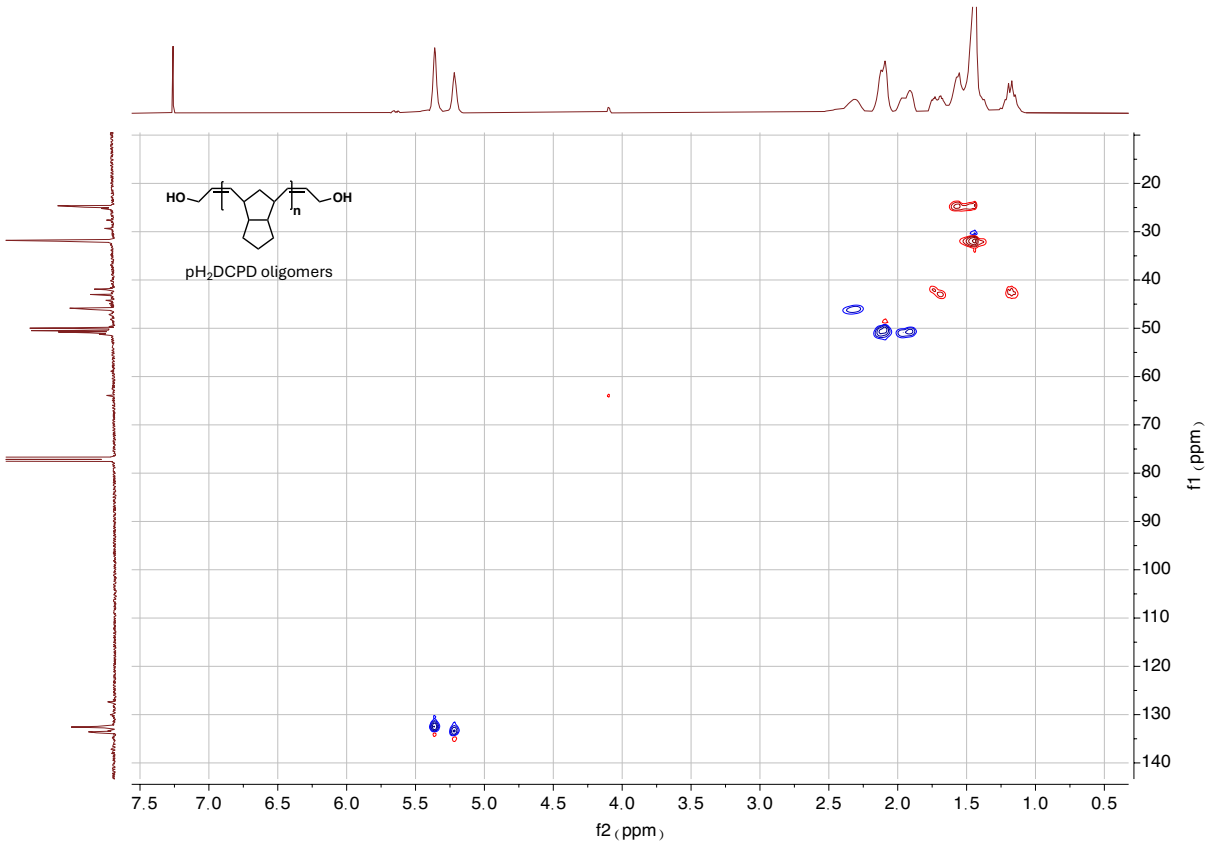

Supplementary Fig. 57 ^{1}H-^{13}C HSQC spectrum of deconstructed pH_2DCPD oligomers.

NMR Spectra of E-functionalization of Deconstructed pH$_2$DCPD Oligomers

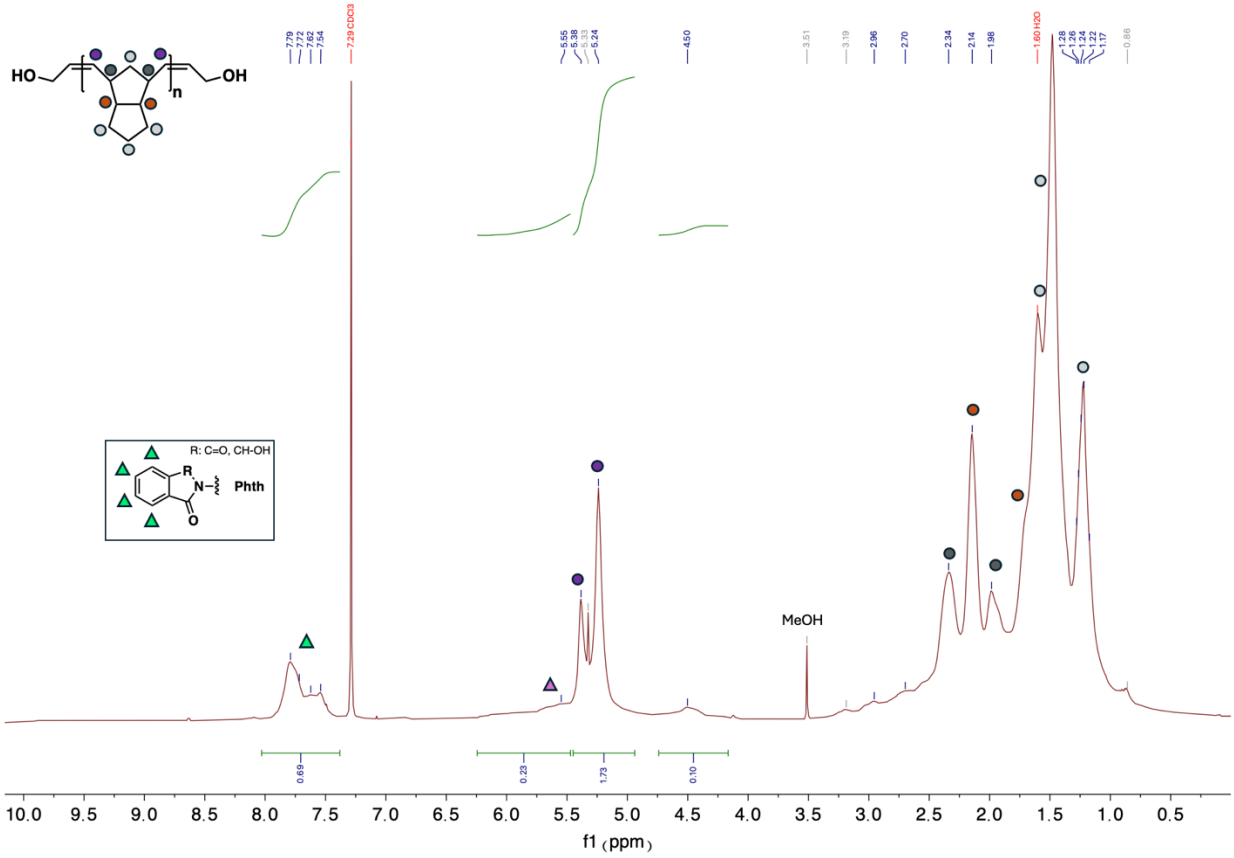

Supplementary Fig. 58 ^{1}H NMR spectrum of E-functionalized deconstructed pH$_2$DCPD oligomers.

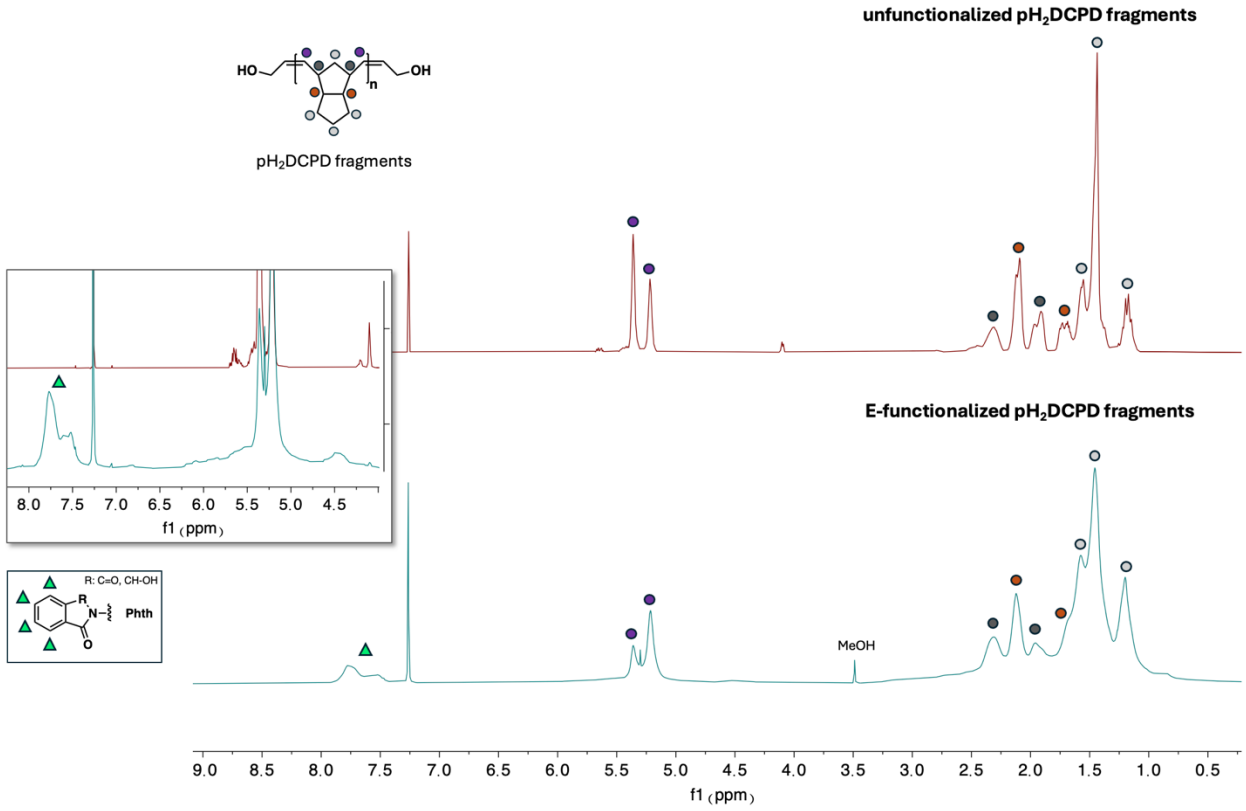

Supplementary Fig. 59 Stacked ^{1}H NMR spectra of E-functionalized deconstructed pH_2DCPD oligomers before and after functionalization.

Exploratory Data of E-functionalization of Polybutadiene

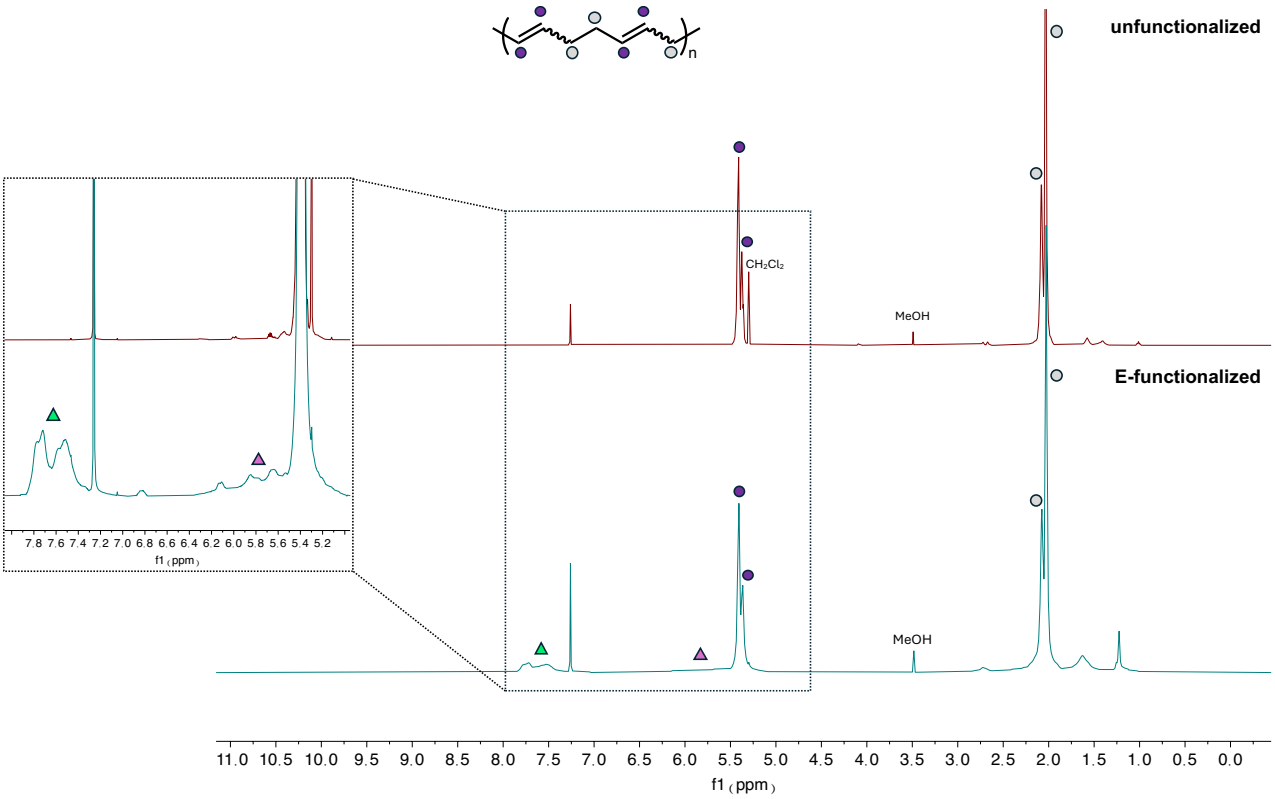

Supplementary Fig. 60 Stacked ^{1}H NMR spectra of polybutadiene before and after the electro-functionalization.

NMR Spectra of Direct Competitions

NHPI as Redox Mediator

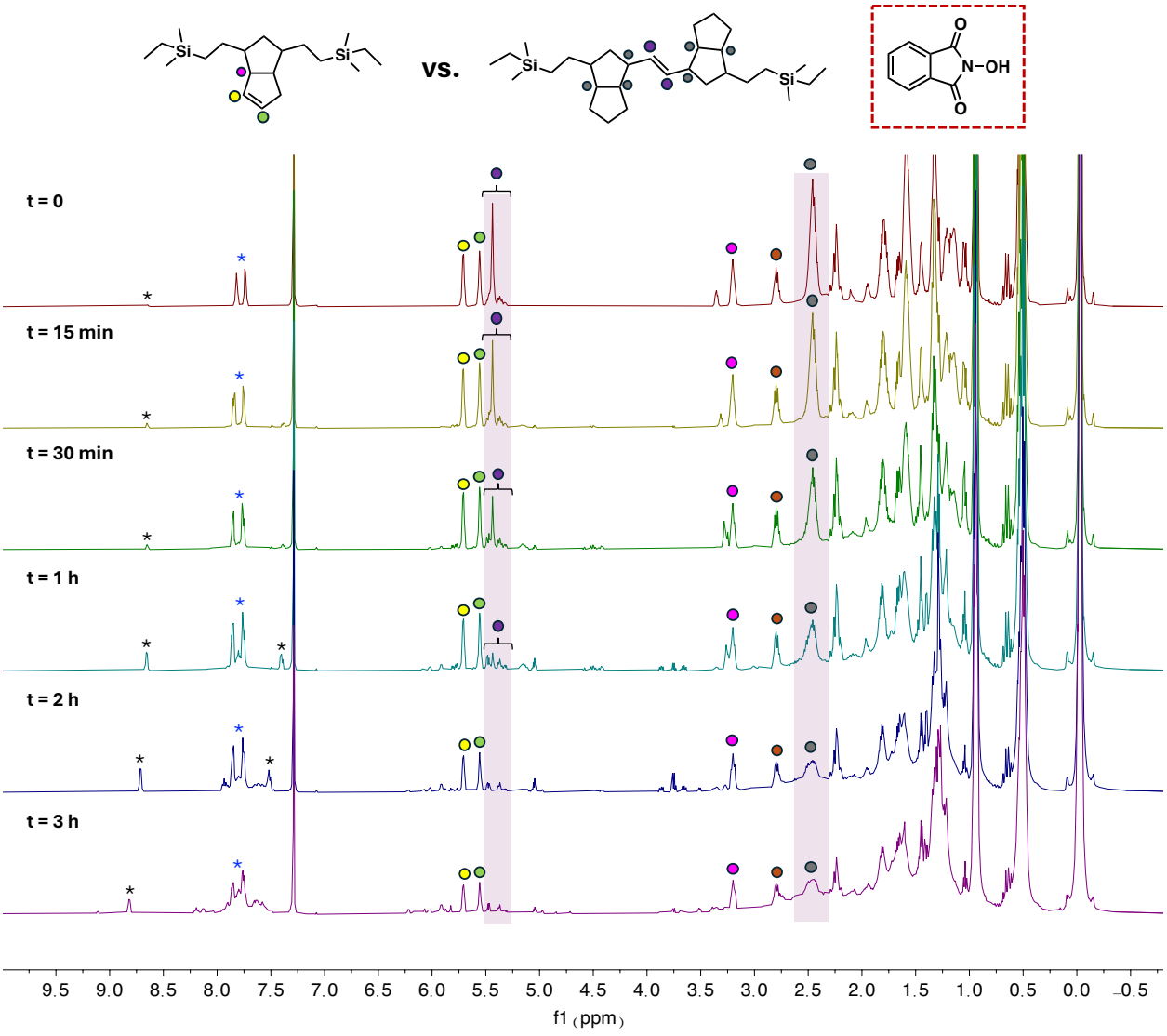

Supplementary Fig. 61 Reaction profile of direct competition study using 60 mol% NHPI. *Pyridine residue.

Substrate consumption was evaluated by comparing the integrals of residual alkene C–H peaks (yellow, green, and purple circles) to their initial values at t = 0, using the methyl silyl C–H peaks at ~0.0 ppm as the reference, as shown in **Figure 4f** of the main manuscript.

Cl_4NHPI as Redox Mediator

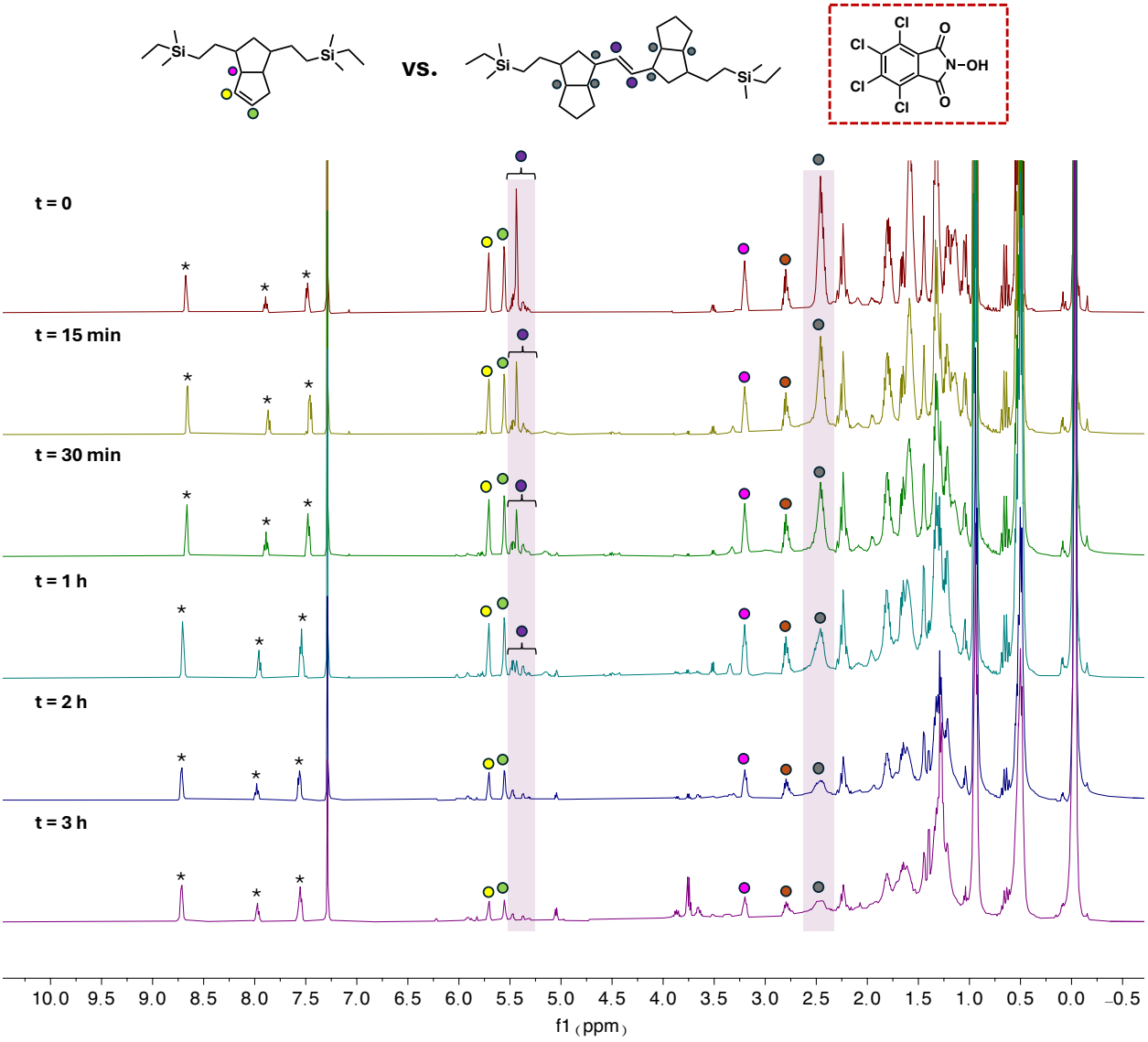

Supplementary Fig. 62 Reaction profile of direct competition study using 60 mol% Cl_4NHPI. *Pyridine residue.

Substrate consumption was evaluated by comparing the integrals of residual alkene C–H peaks (yellow, green, and purple circles) to their initial values at t = 0, using the methyl silyl C–H peaks at ~0.0 ppm as the reference, as shown in **Supplementary Fig. 66d**.

NHS as Redox Mediator

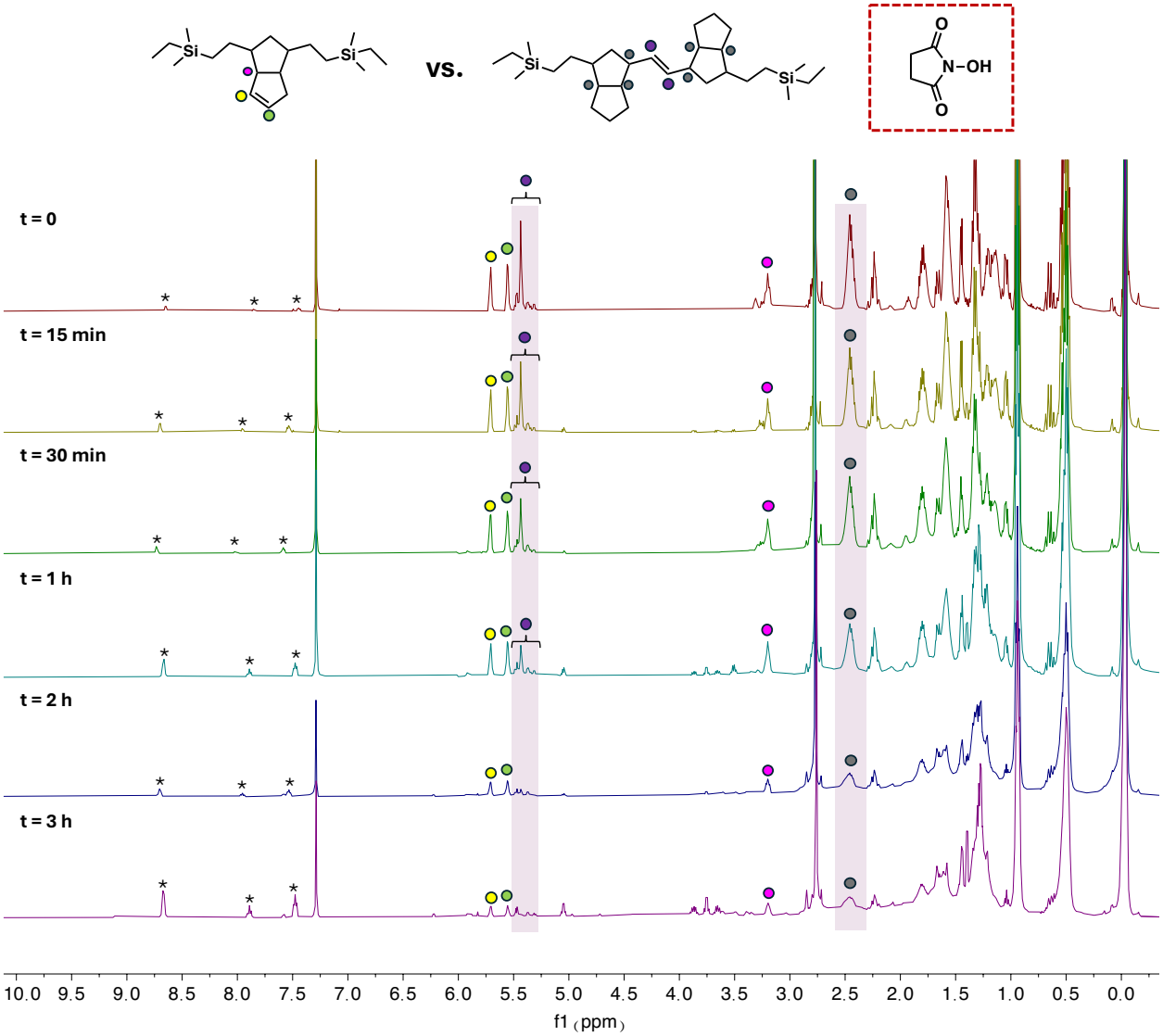

Supplementary Fig. 63 Reaction profile of direct competition study using 60 mol% NHS. *Pyridine residue.

Substrate consumption was evaluated by comparing the integrals of residual alkene C–H peaks (yellow, green, and purple circles) to their initial values at t = 0, using the methyl silyl C–H peaks at ~0.0 ppm as the reference, as shown in **Supplementary Fig. 66e**.

Example of the Calculation Procedure of the Functional Groups Percent Incorporations

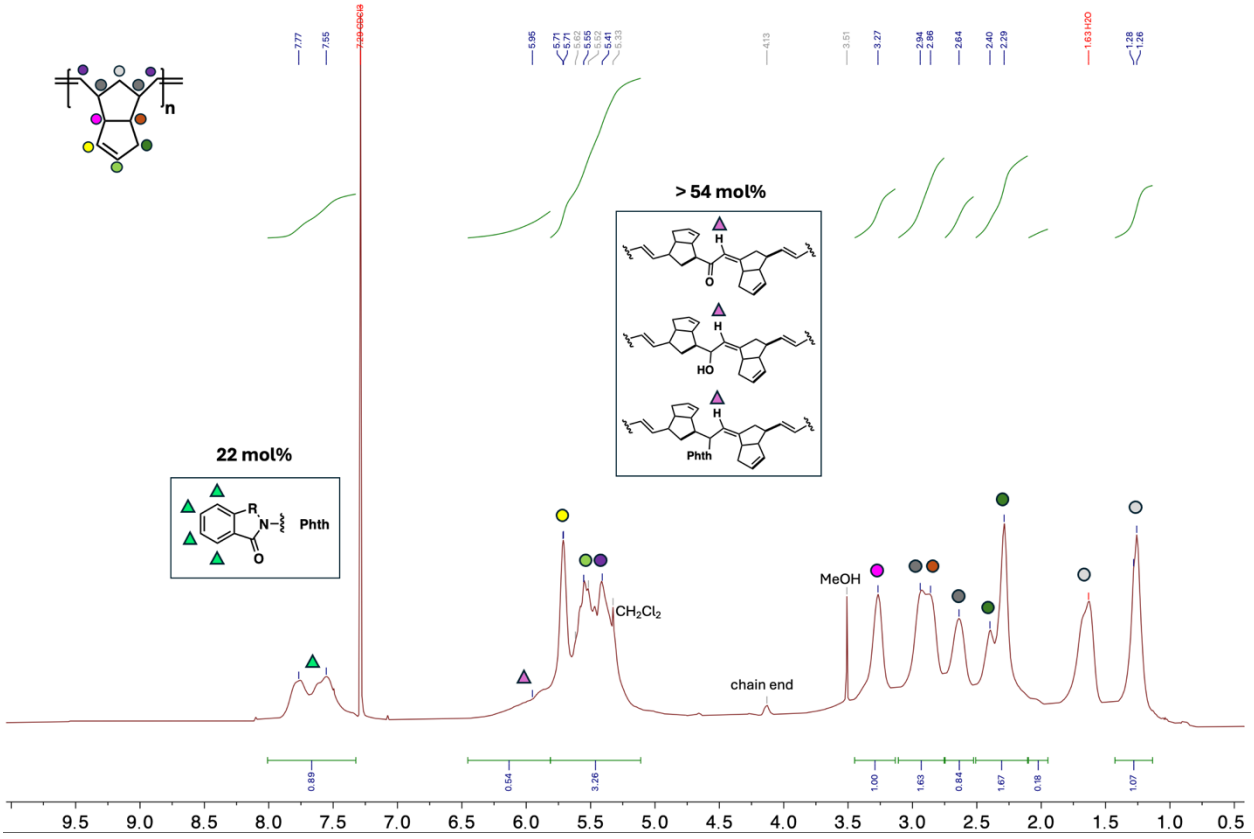

Supplementary Fig. 64 ^{1}H NMR spectrum of E-functionalized deconstructed pDCPD oligomers, reaction conditions: 100 mg of Oligo-DCPD, 60 mol% NHPI, 1 equiv *t*-BuOOH (70 wt% in H_2O), 2 equiv pyridine, DCM, rt, 10 mA, and t = 6h, trial I.

The percent conversion of the phthalimide (Phth) functional group was determined by referencing the integration of the proton peak at 3.24 ppm (indicated by a pink circle).

Supported by the ^{1}H NMR spectrum of dicyclohexylideneethanone, a representative α,β-unsaturated ketone derived from the main-chain bridge-alkene (3° allylic C-H) oxidation (Supplementary Fig. 15). In this spectrum, the β-alkene C-H appears as a characteristic peak at approximately 6.00 ppm, serving as a marker for this functional group. In the electro-oxidized oligo-DCPD, new peaks around 6.00 ppm were consistently observed in the ^{1}H NMR spectra of the functionalized polymers (pink triangle).

Note: Due to **significant peak overlap** in the alkene C-H region (5.0-6.5 ppm), the percent conversion of all bridge functional groups (pink triangle) were only partially integrated and reported as an estimated sum value, also referencing the integration of the proton peak at 3.24 ppm (pink circle).

Result Table of Varying the **Solvent and t-BuOOH** Concentration

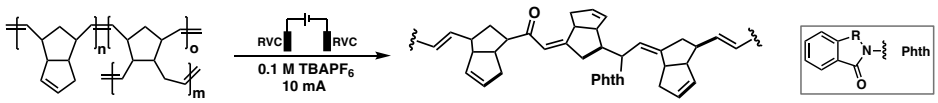

Entry	[NHPI]	[tBuOOH]	[Pyridine]	Solvent	Temperature	Time	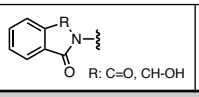 R: C=O, CH-OH	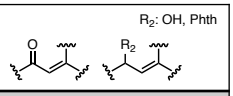 R_2: OH, Phth
1	20 mol%	1.5 equiv	2 equiv	CH_3CN:Benzene (1:1)	rt	2h	Crosslinked*	
2	20 mol%	1.5 equiv	2 equiv	CH_3CN:DCM (1:1)	rt	2h	Crosslinked*	
3	20 mol%	--	2 equiv	DCM	rt	2h	Crosslinked*	
4	20 mol%	1.5 equiv	2 equiv	DCM	rt	2h	6.5%	~ 21%
5	20 mol%	1 equiv	2 equiv	DCM	rt	2h	7.3%	~ 16%

Supplementary Table 1 Percent incorporation (calculation details see above page 74) of ketone, alcohol, and phthalimide functional groups with different solvents. *Insoluble solids were formed.

Result Table of Varying the Redox Mediator (NHPI) Concentration

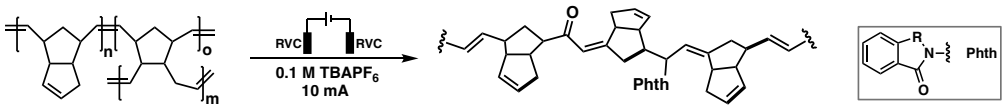

Entry	[NHPI]	[tBuOOH]	[Pyridine]	Solvent	Temperature	Time	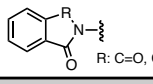 R: C=O, CH-OH	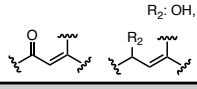 R_2: OH, Phth
1	20 mol%	1 equiv	2 equiv	DCM	rt	2h	7.3 %	~ 16%
						4h	12.5 %	~ 32%
						6h	17 %	~ 41%
2	40 mol%	1 equiv	2 equiv	DCM	rt	2h	7.5%	~ 19%
						4h	16.5%	~ 40%
						6h	23%	~ 59%
3	60 mol%	1 equiv	2 equiv	DCM	rt	2h	9%	~ 23%
						4h	17.8%	~ 39%
						6h	23.5%	~ 57%
4	1 equiv	1 equiv	2 equiv	DCM	rt	4h	22.3%	~ 50%
						6h*	32%	~ 66%
5	60 mol%	0.8 equiv	2 equiv	DCM	rt	2h	9.5%	~ 15%
						4h	19.5%	~ 39%
						6h	23.8%	~ 39%
6	60 mol%	0.6 equiv	2 equiv	DCM	rt	2h	9.3%	~ 25%
						4h	19.8%	~ 52%
						6h*	23.3%	~ 53 %

Supplementary Table 2 Percent incorporation (calculation details see page 74) of ketone, alcohol, and phthalimide functional groups at different catalyst loading. *Insoluble solids were formed.

Result Table of Varying the **Molecular Weight** of the Deconstructed Oligomers

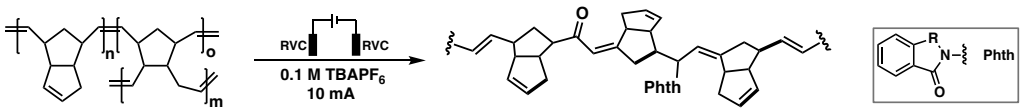

Entry	Oligomer Size (Mn)	[NHPI]	[tBuOOH]	Time	R: C=O, CH-OH	R_2: OH, Phth
1	8.7 kDa	60 mol%	1 equiv	2h	8.5%	~ 20%
				4h	13.8%	~ 38%
				6h*	27.8%	~ 58%
2	6.6 kDa	60 mol%	1 equiv	2h	9%	~ 23%
				4h	17.8%	~ 39%
				6h	23.5%	~ 57%
3	3.3 kDa	60 mol%	1 equiv	2h	10.3%	~ 20%
				4h	19.8%	~ 40%
				6h	26.3%	~ 60%

Supplementary Table 3 Percent incorporation (calculation details see page 74) of ketone, alcohol, and phthalimide functional groups when using deconstructed oligomers with different molecular weights. *Insoluble solids were formed.

Result Table of Varying the **Chain-End** of the Deconstructed Oligomers

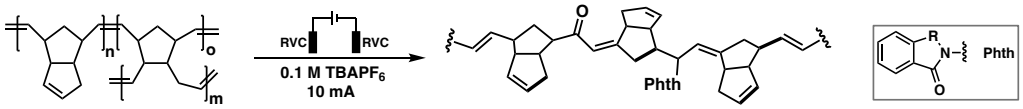

Entry	Oligomers	Comonomer Formulation	[NHPI]	[tBuOOH]	Time	R: C=O, CH-OH	R_2: OH, Phth
1	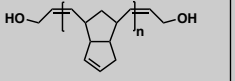	10 wt% iPrSi7	60 mol%	1 equiv	2h	9%	~ 23%
					4h	17.8%	~ 39%
					6h	23.5%	~ 57%
2	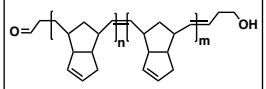	10 wt% DHF	60 mol%	1 equiv	2h	9%	~ 22%
					4h	19%	~ 34%
					6h	26%	~ 58%
3	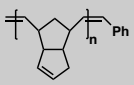	(10:1) Sytrene	60 mol%	1 equiv	2h	8.5%	~ 18%
					4h	16.8%	~ 29%
					6h	25.3%	~ 56%

Supplementary Table 4 Percent incorporation (calculation details see page 74) of ketone, alcohol, and phthalimide functional groups when using deconstructed oligomers with different chain-ends.

Result Table of Varying the **Redox Potential** of the Mediator (Different Catalyst)

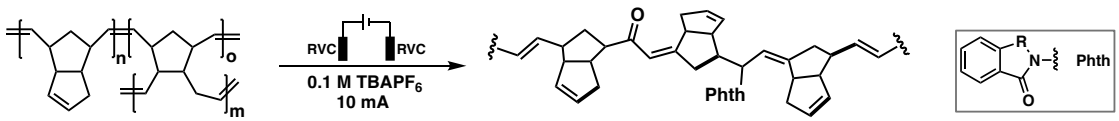

Entry	[Mediator]	[pyridine]	[tBuOOH]	Time	R: C=O, CH-OH	R_2: OH, Phth
1	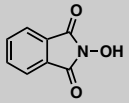	2 equiv	1 equiv	2h	9%	~ 23%
				4h	17.8%	~ 39%
				6h	23.5%	~ 57%
2	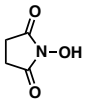	2 equiv	1 equiv	2h	NA	~ 19%
				4h	NA	~ 48%
				6h*	NA	~ 50%
3	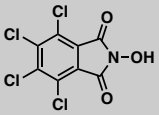	2 equiv	1 equiv	2h*	NA	~ 19%
				4h*	NA	insoluble
				6h*	NA	insoluble

Supplementary Table 5 Percent incorporation (calculation details see page 74) of ketone, alcohol, and phthalimide functional groups when using different redox mediators. *Insoluble solids were formed.

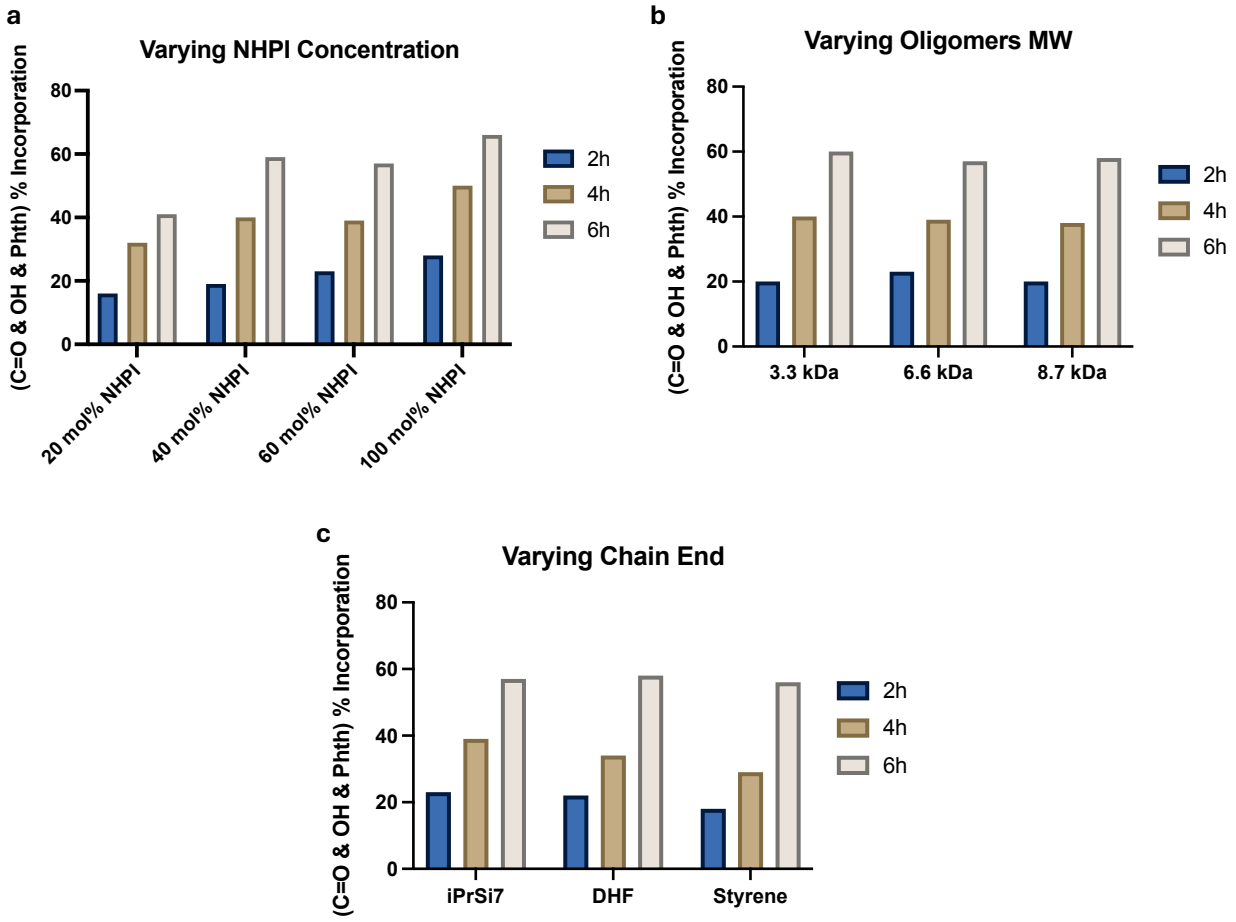

Supplementary Fig. 65 Degree of functionalization with different screening parameters. The molecular weights of oligo-DCPD were reported as M_n ranging from 3.3 to 8.7 kDa.

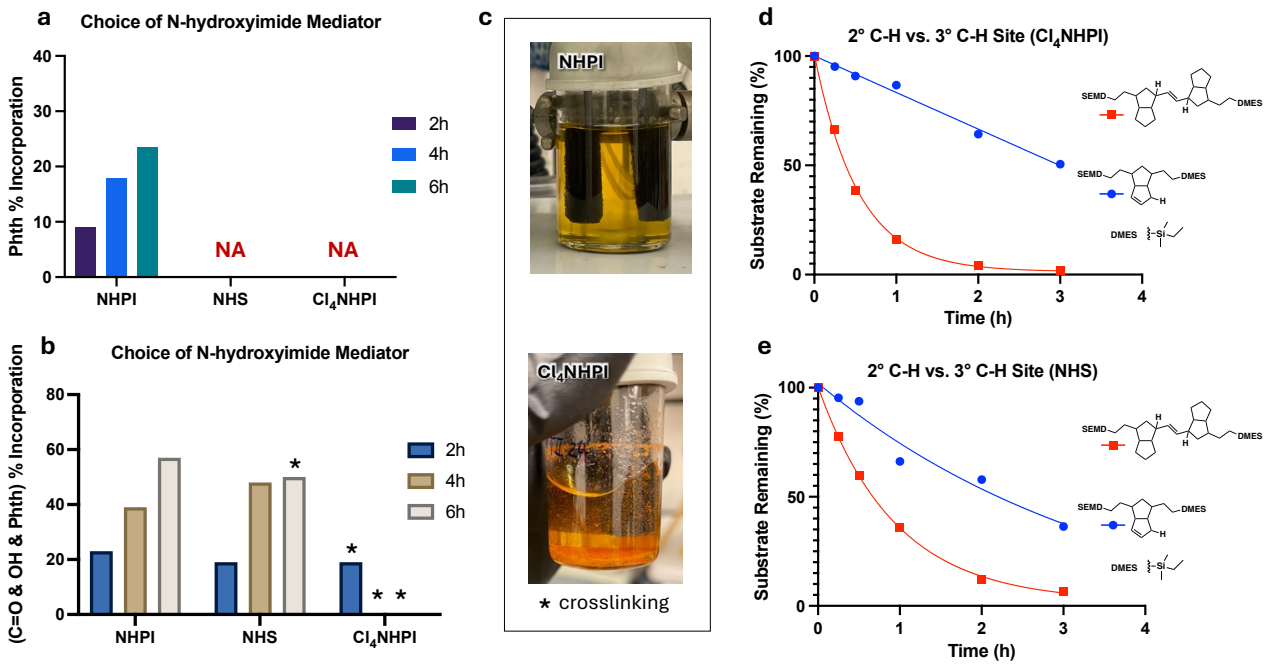

Supplementary Fig. 66 Degree of functionalization using different redox mediators and the extended competition data for the chemoselectivity.

Supplementary Fig. 66a shows that due to the absence of phthalimide aromatic C-Hs, the percent incorporation of N-alkoxy groups is undetectable for both N-hydroxysuccinimide (NHS) and N-hydroxytetrachlorophthalimide (Cl_4NHPI). Supplementary Fig. 66b reveals that the oxidation profile of NHS closely resembles that of the parent NHPI at the 2-hour and 4-hour time points. However, after 6 hours of extended electrolysis, insoluble solids began to form. In contrast, Cl_4NHPI generated insoluble material immediately upon reaction initiation (66b and 66c). Notably, NHPI, which has a lower redox potential and a more stable radical, proved to be the most effective and economical catalyst for C-H bond activation in oligo-DCPD.

Competition experiments between Cl_4NHPI and NHS reveal that NHS, which has a slightly higher redox potential, exhibits reduced selectivity for tertiary allylic C–H sites compared to NHPI and Cl_4NHPI.

NMR Spectra of E-functionalization of Deconstructed pDCPD Oligomers

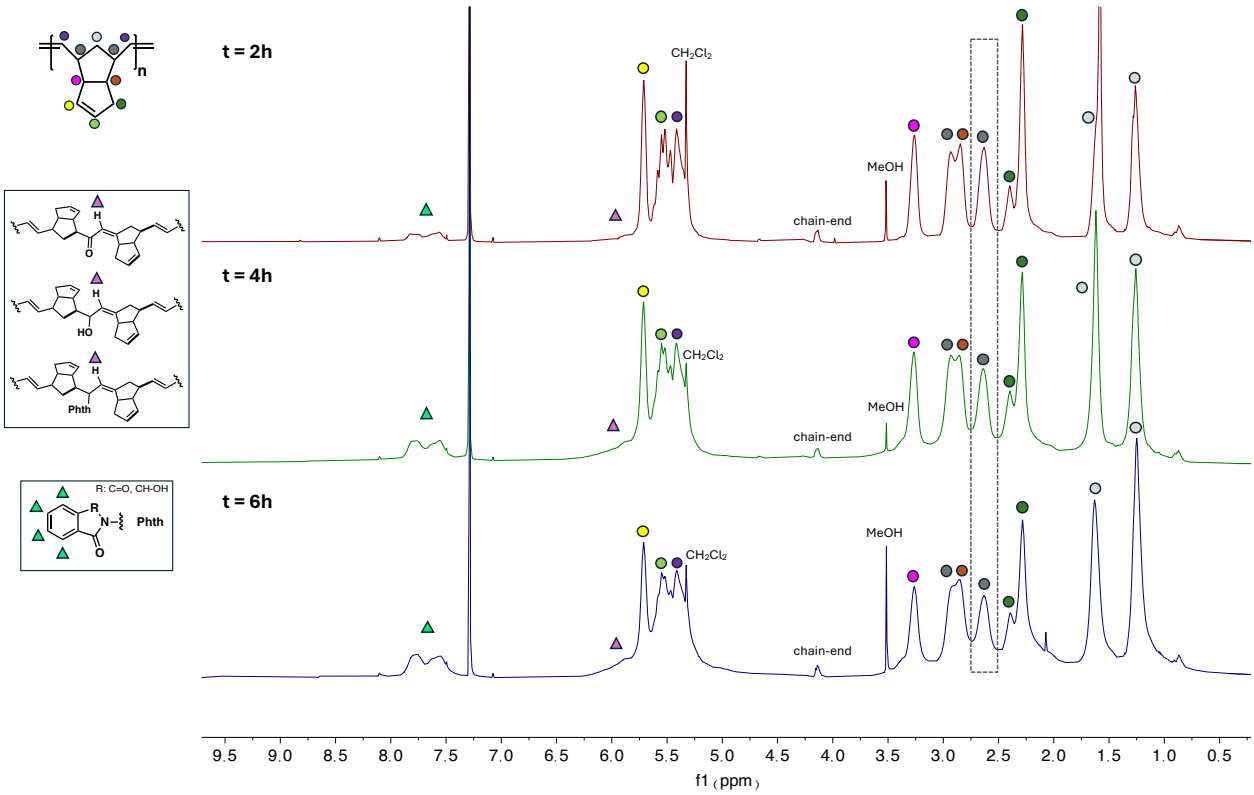

Supplementary Fig. 67 Stacked ^{1}H NMR spectra of E-functionalized deconstructed pDCPD oligomers at different reaction time point (after purification), for detailed reaction conditions, see Supplementary Table 1, Entry 5.

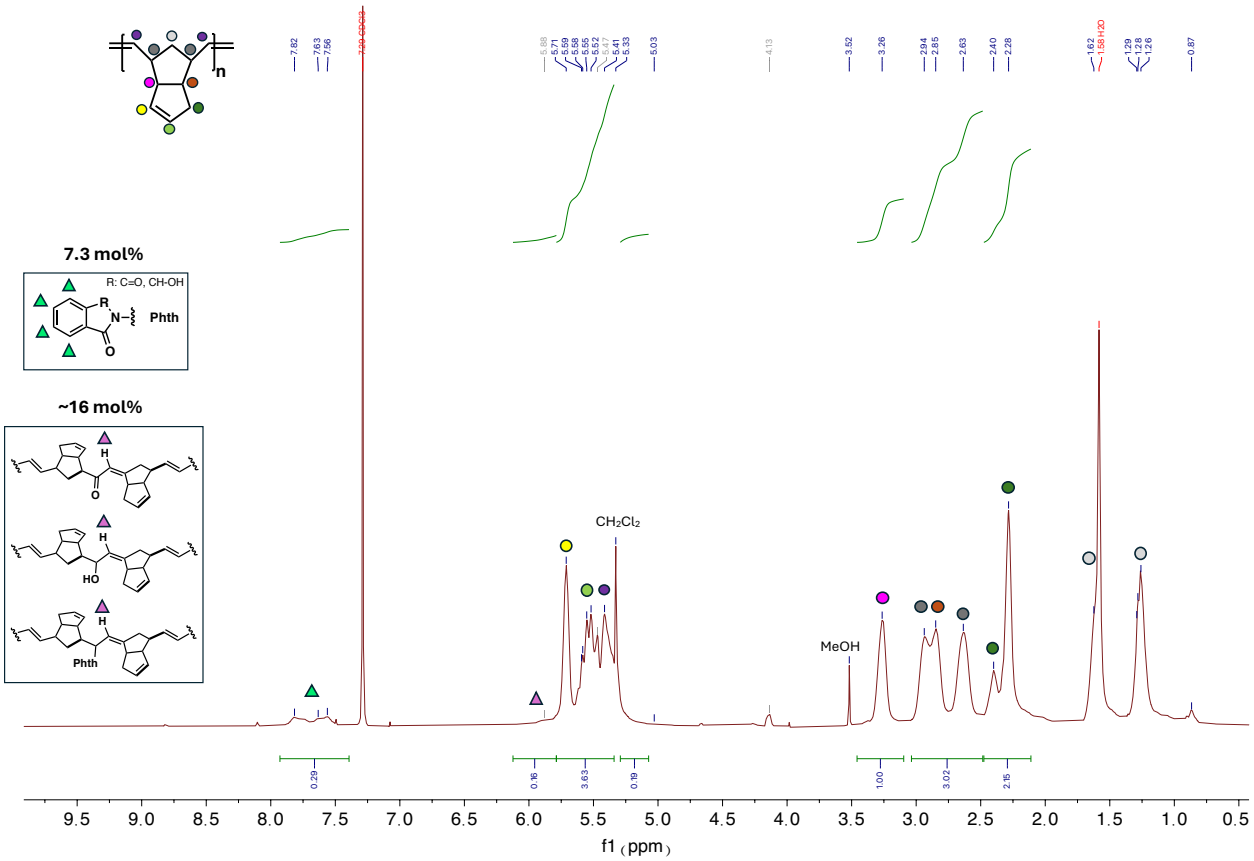

Supplementary Fig. 68 ^{1}H NMR spectrum of E-functionalized deconstructed pDCPD oligomers at t = 2h (after purification), for detailed reaction conditions, see Supplementary Table 1, Entry 5.

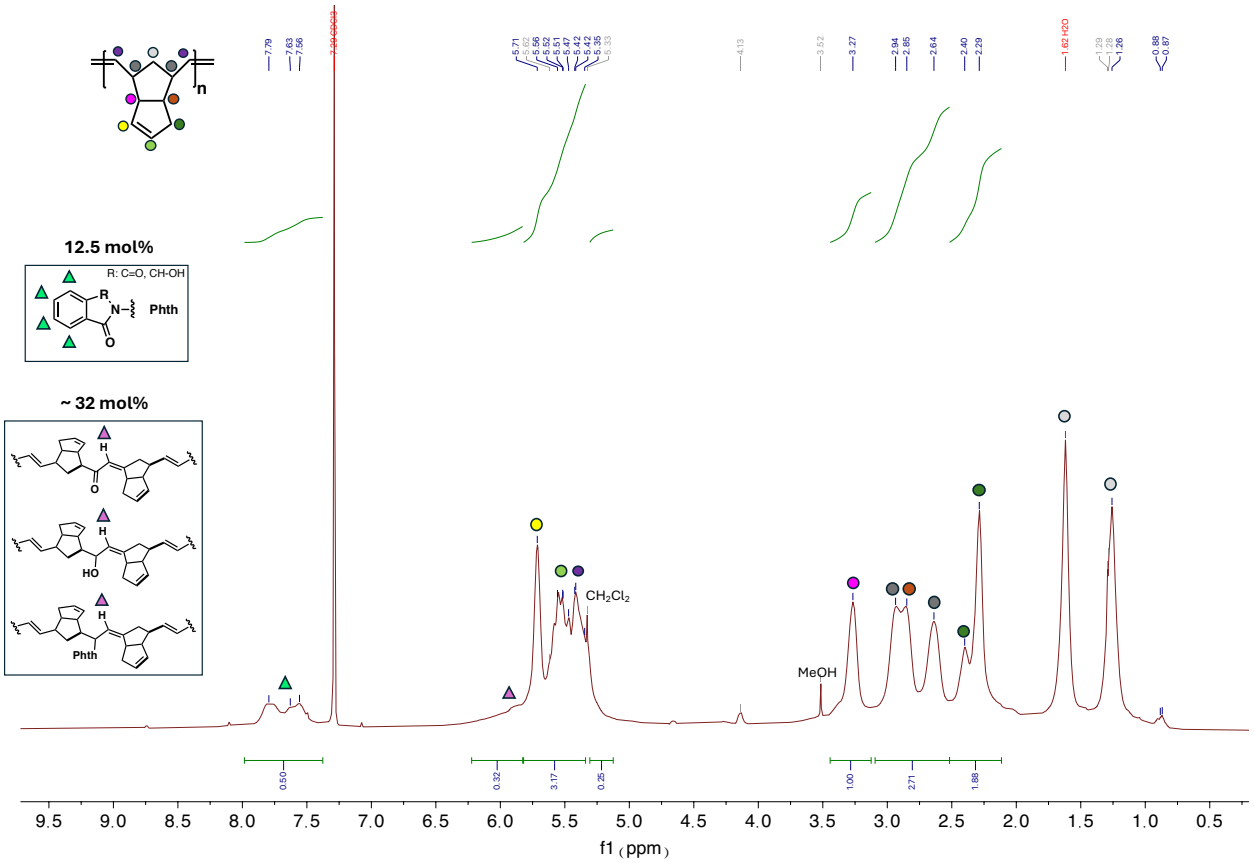

Supplementary Fig. 69 ^{1}H NMR spectrum of E-functionalized deconstructed pDCPD oligomers at t = 4h (after purification), for detailed reaction conditions, see Supplementary Table 1, Entry 5.

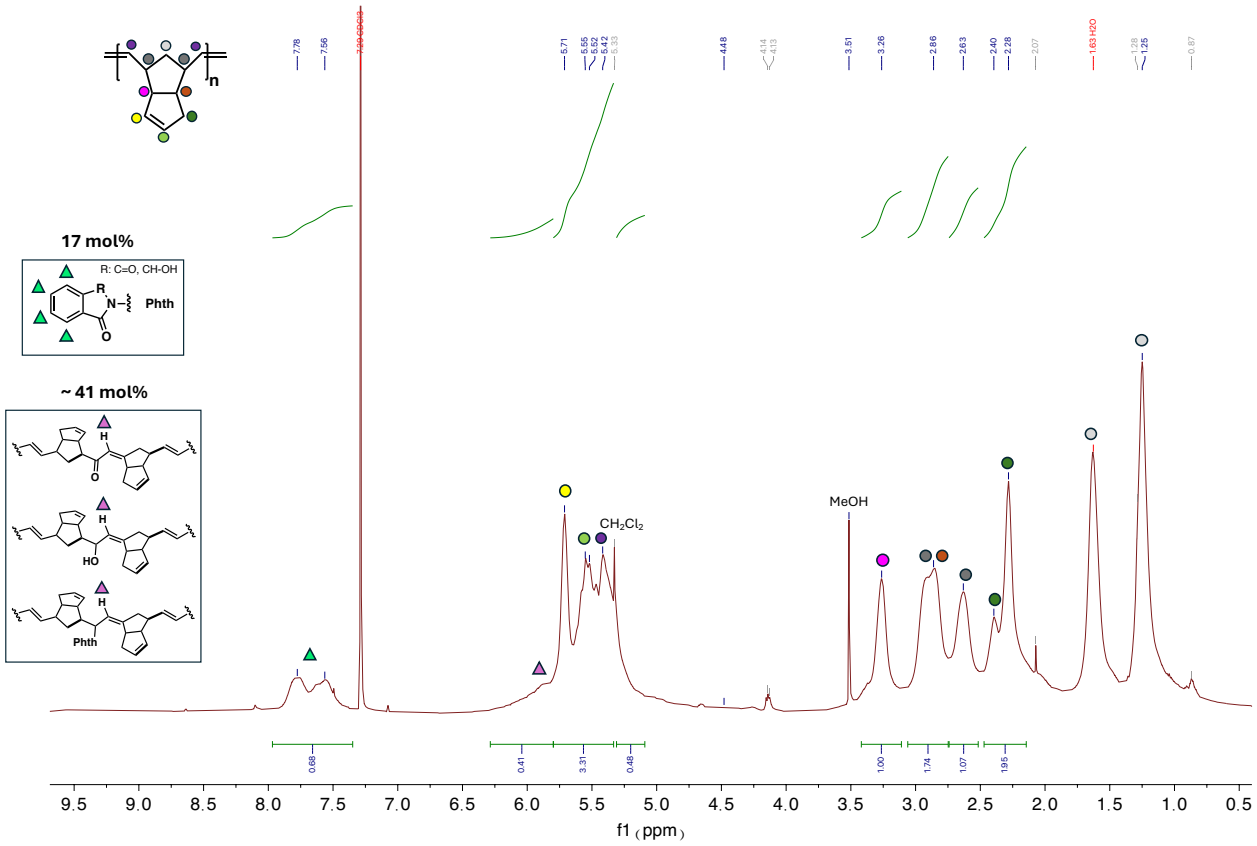

Supplementary Fig. 70 ^{1}H NMR spectrum of E-functionalized deconstructed pDCPD oligomers at t = 6h (after purification), for detailed reaction conditions, see Supplementary Table 2, Entry 1.

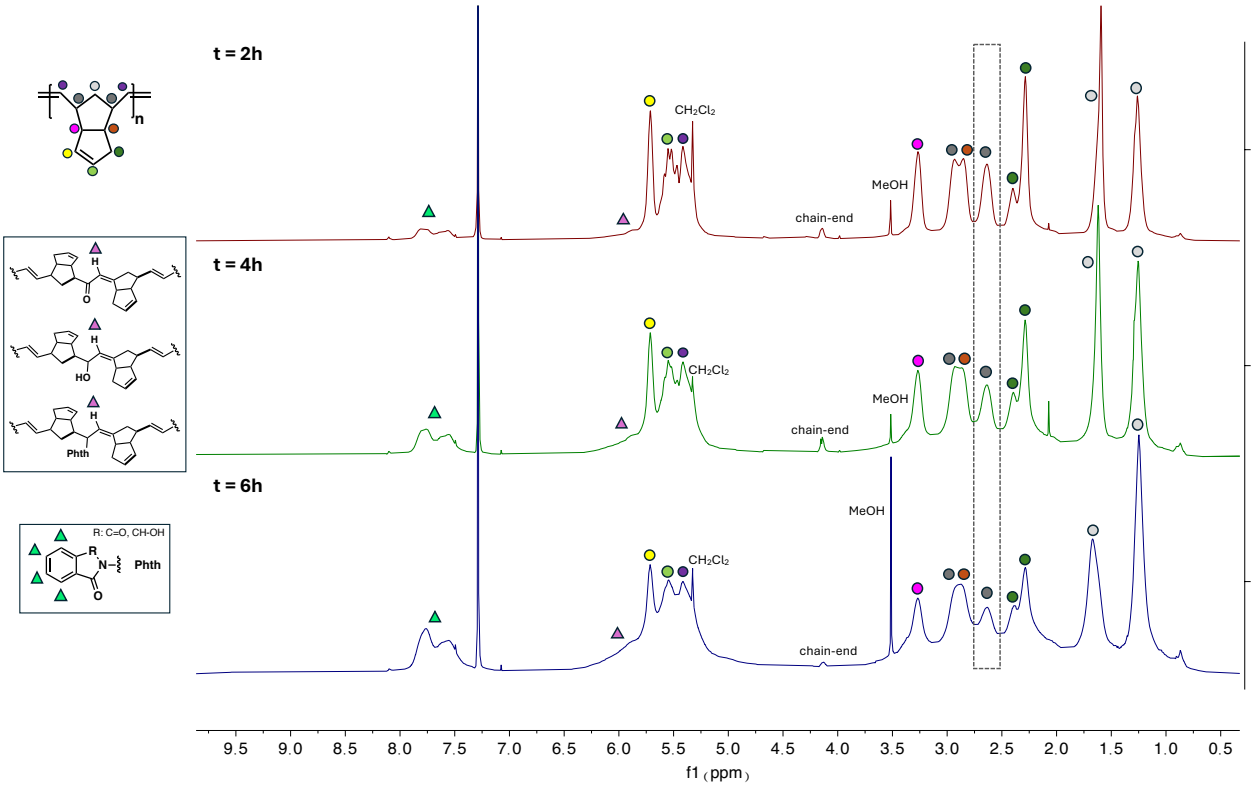

Supplementary Fig. 71 Stacked ^{1}H NMR spectra of E-functionalized deconstructed pDCPD oligomers at different reaction time point (after purification), for detailed reaction conditions, see Supplementary Table 2, Entry 2.

Supplementary Table 2 Entry 2, 2h

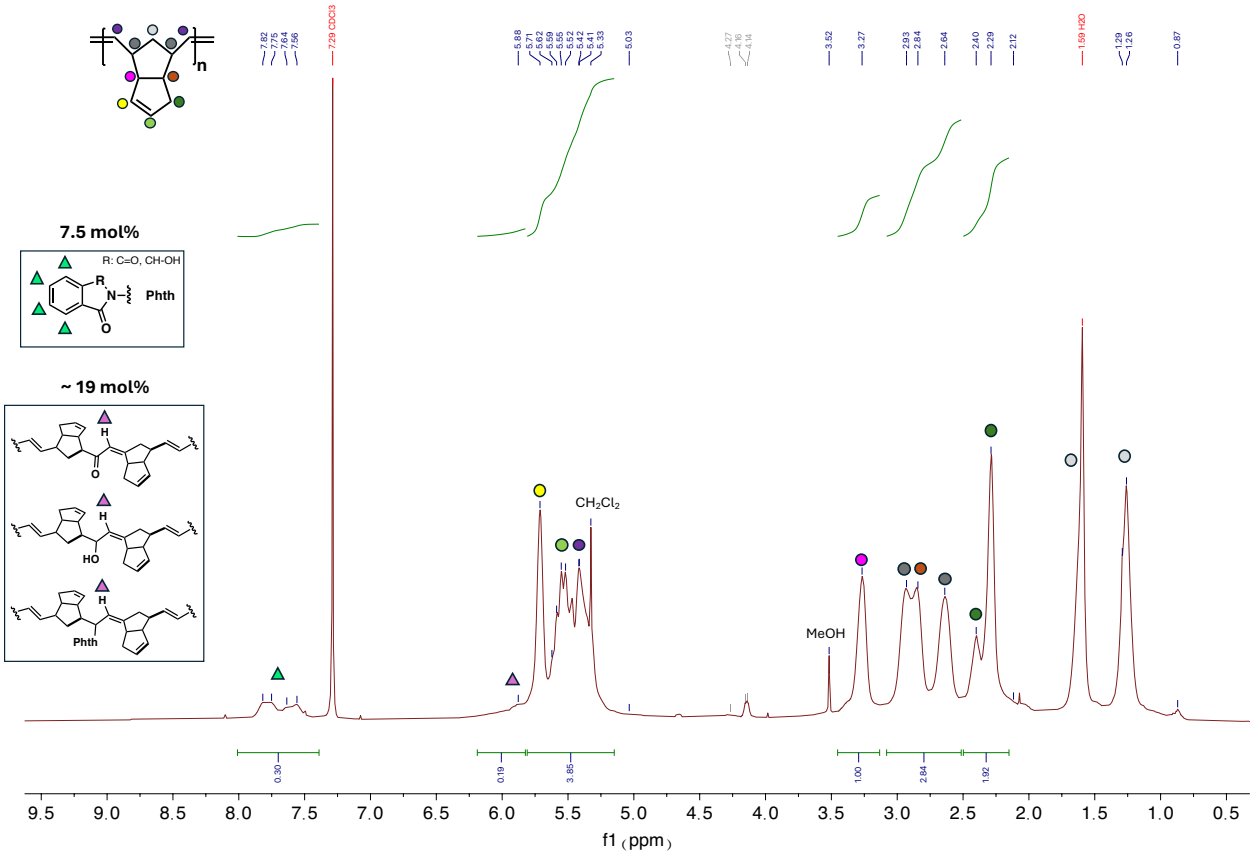

Supplementary Fig. 72 ^{1}H NMR spectrum of E-functionalized deconstructed pDCPD oligomers at t = 2h (after purification), for detailed reaction conditions, see Supplementary Table 2, Entry 2.

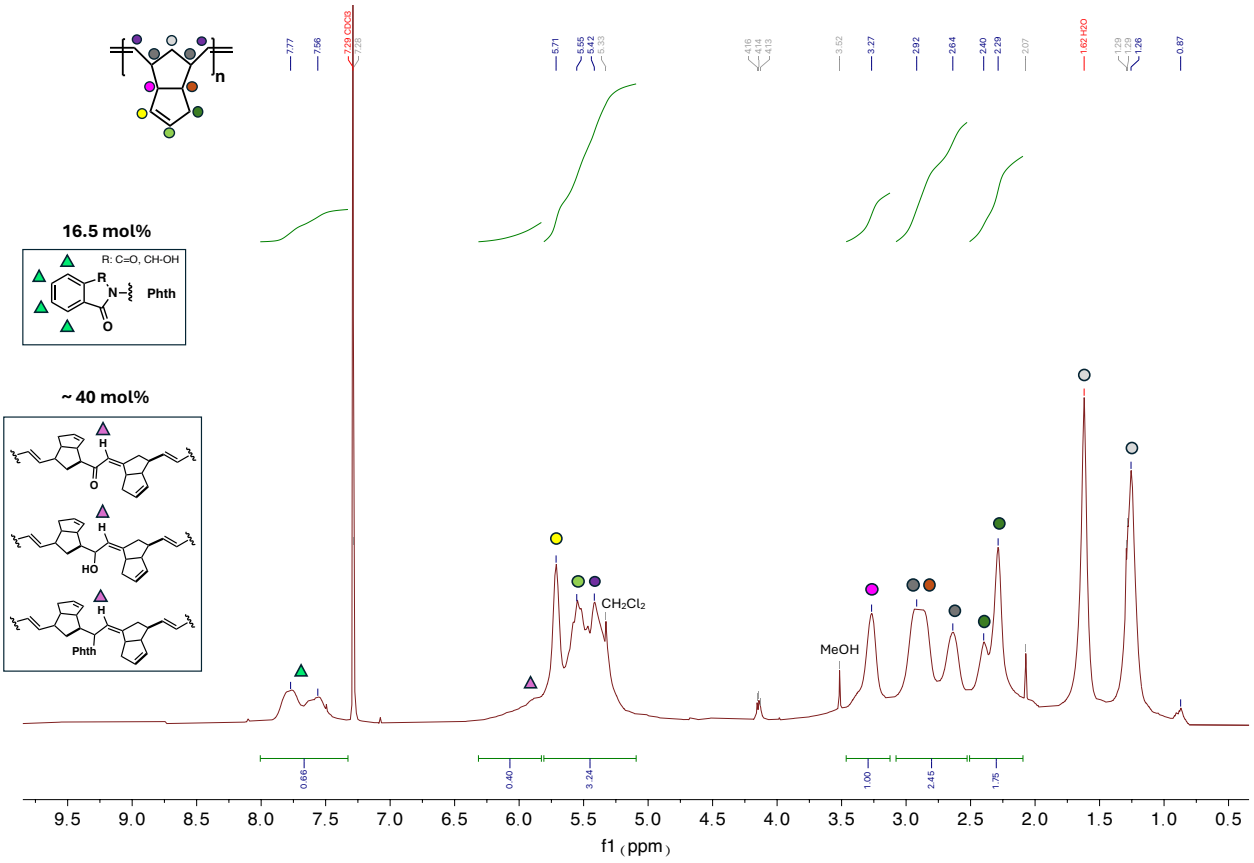

Supplementary Fig. 73 ^{1}H NMR spectrum of E-functionalized deconstructed pDCPD oligomers at t = 4h (after purification), for detailed reaction conditions, see Supplementary Table 2, Entry 2.

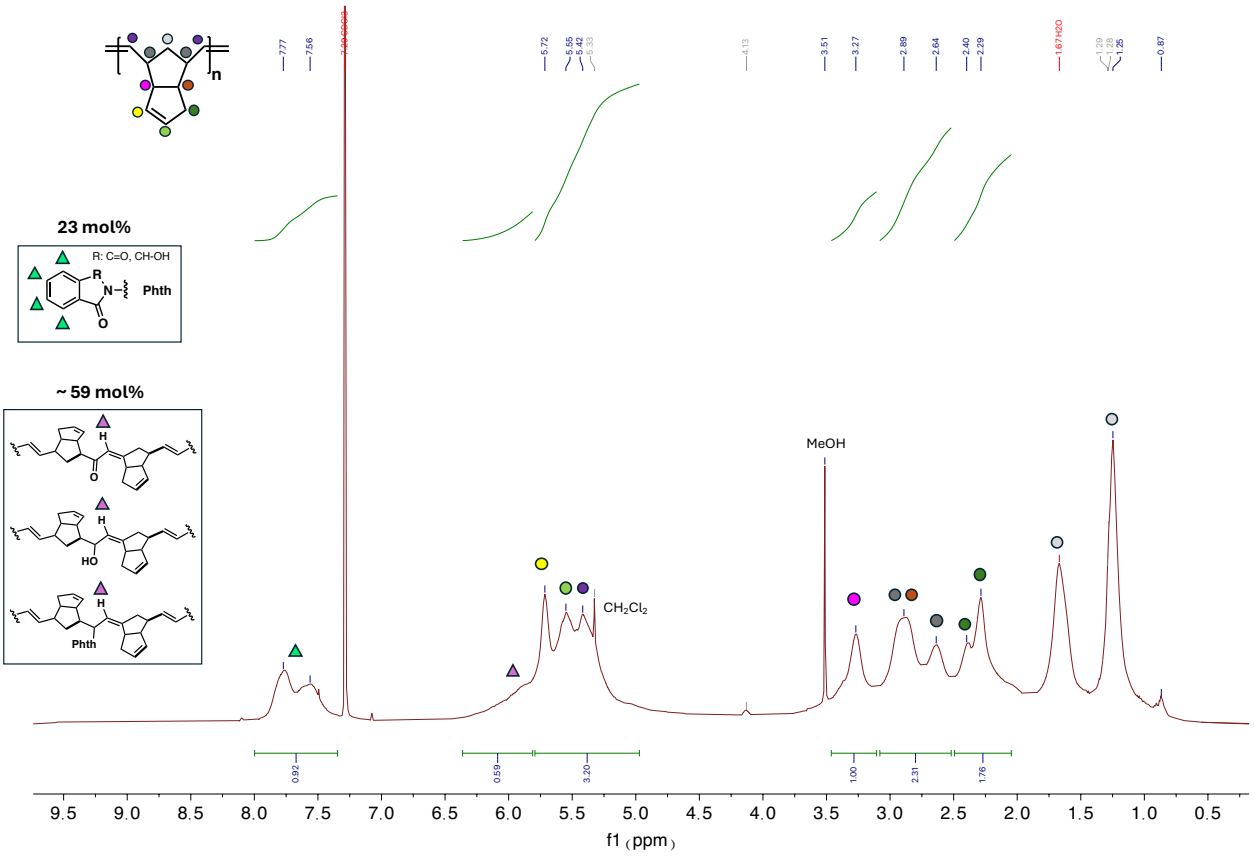

Supplementary Fig. 74 ^{1}H NMR spectrum of E-functionalized deconstructed pDCPD oligomers at t = 6h (after purification), for detailed reaction conditions, see Supplementary Table 2, Entry 2.

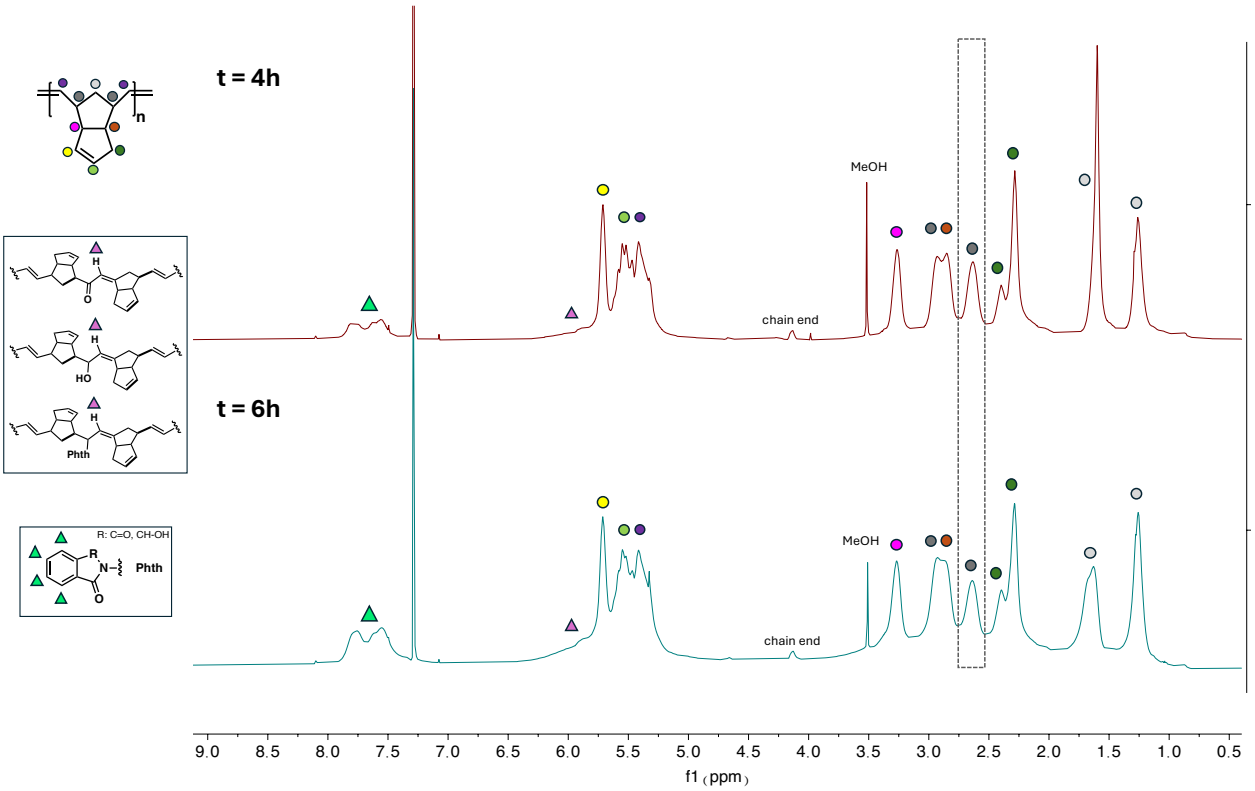

Supplementary Fig. 75 Stacked ^{1}H NMR spectra of E-functionalized deconstructed pDCPD oligomers at different reaction time point (after purification), for detailed reaction conditions, see Supplementary Table 2, Entry 3, trial I.

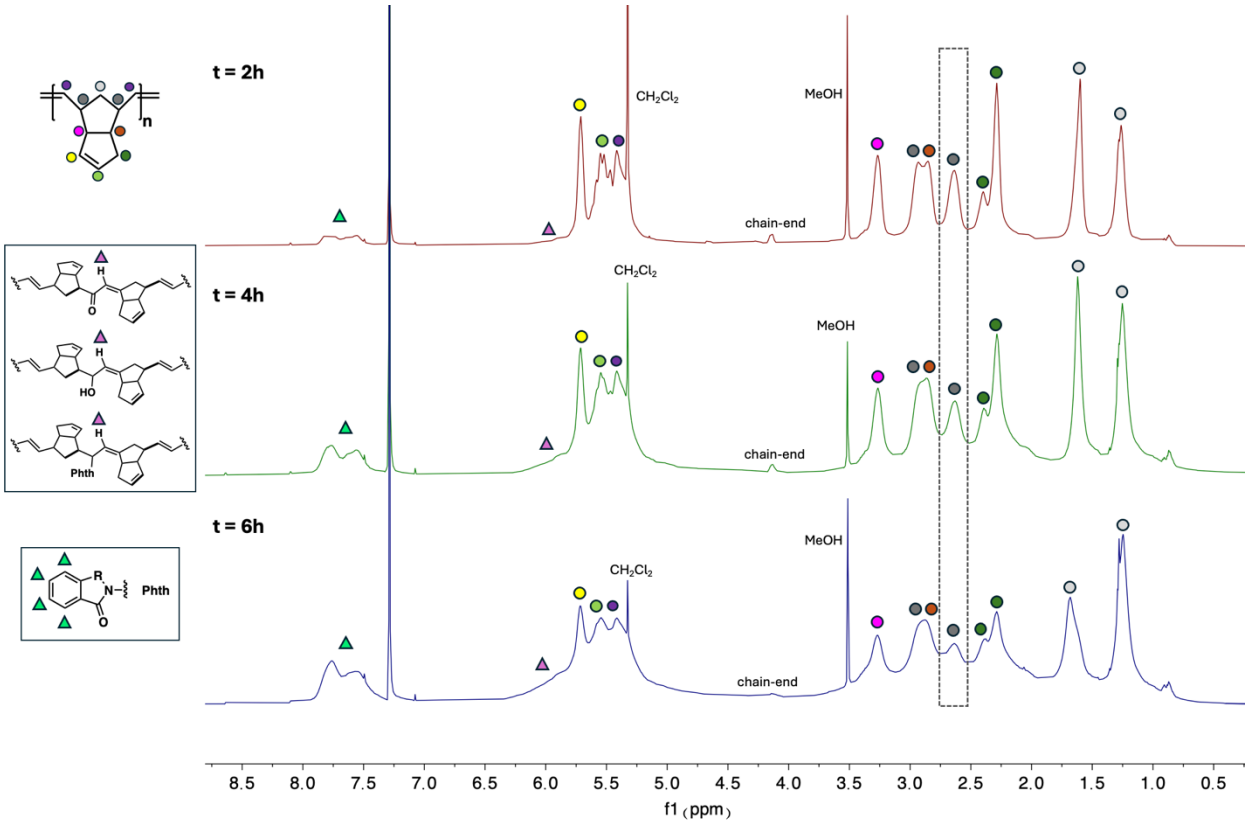

Supplementary Fig. 76 Stacked ^{1}H NMR spectra of E-functionalized deconstructed pDCPD oligomers at different reaction time point (after purification), for detailed reaction conditions, see Supplementary Table 2, Entry 3, trial II.

Table S2, Entry 3 (Trial I), 4h

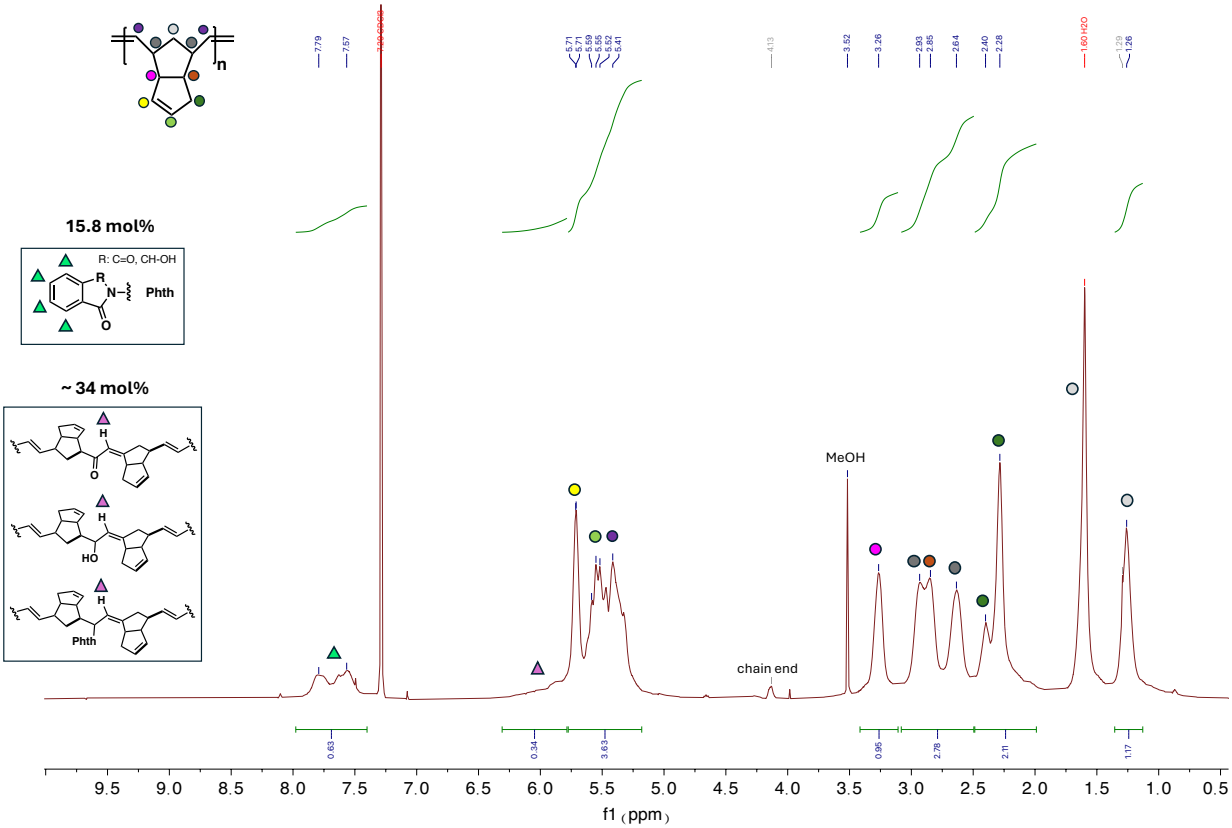

Supplementary Fig. 77 ^{1}H NMR spectrum of E-functionalized deconstructed pDCPD oligomers at t = 4h (after purification), for detailed reaction conditions, see Supplementary Table 2, Entry 3, trial I.

Table S2, Entry 3 (Trial I), 6h

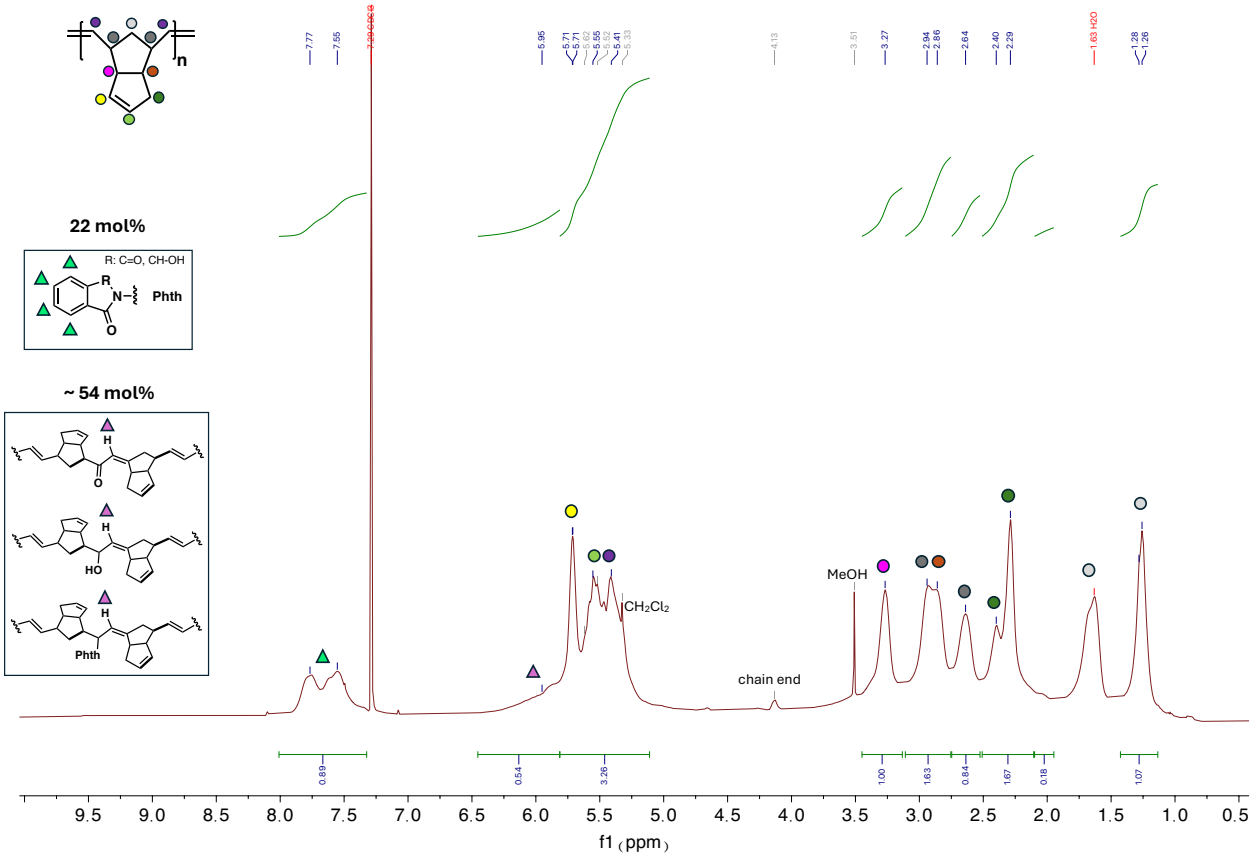

Supplementary Fig. 78 ^{1}H NMR spectrum of E-functionalized deconstructed pDCPD oligomers at t = 6h (after purification), for detailed reaction conditions, see Supplementary Table 2, Entry 3, trial I.

Table S2, Entry 3 (Trial II), 2h

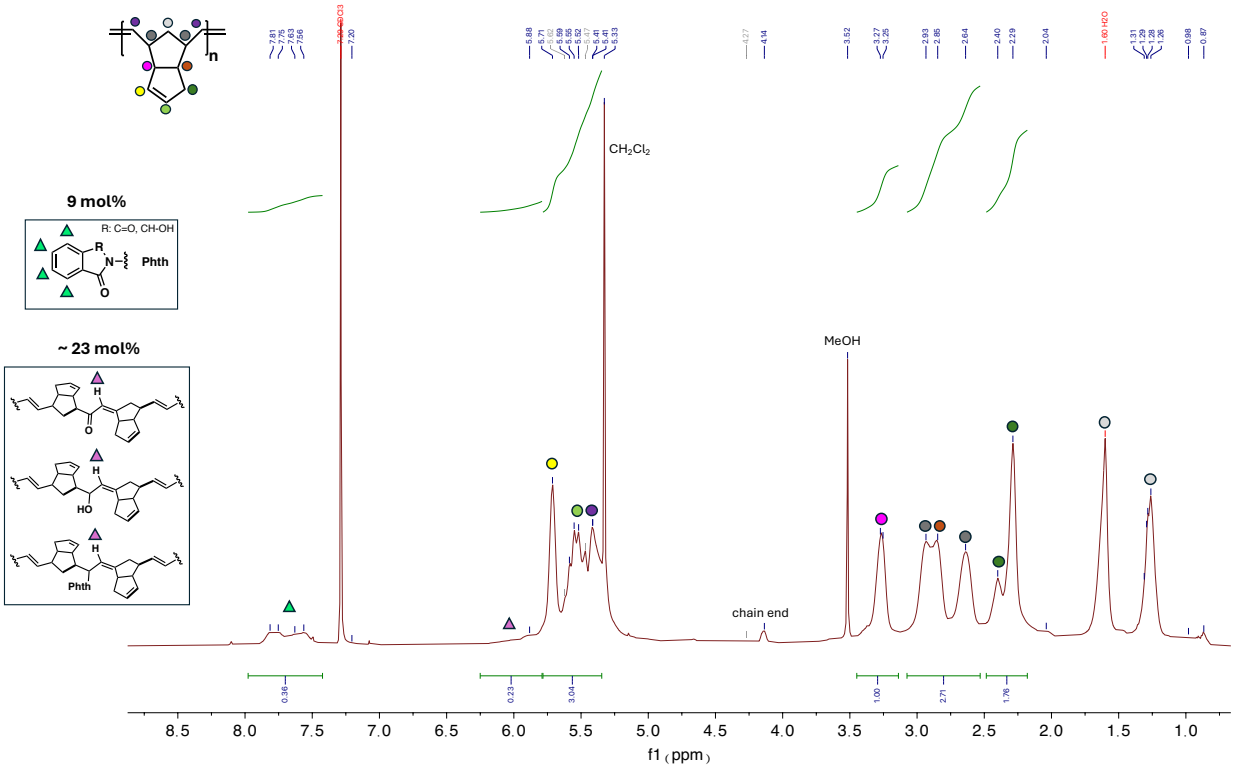

Supplementary Fig. 79 ^{1}H NMR spectrum of E-functionalized deconstructed pDCPD oligomers at t = 2h (after purification), for detailed reaction conditions, see Supplementary Table 2, Entry 3, trial II.

Table S2, Entry 3 (Trial II), 4h

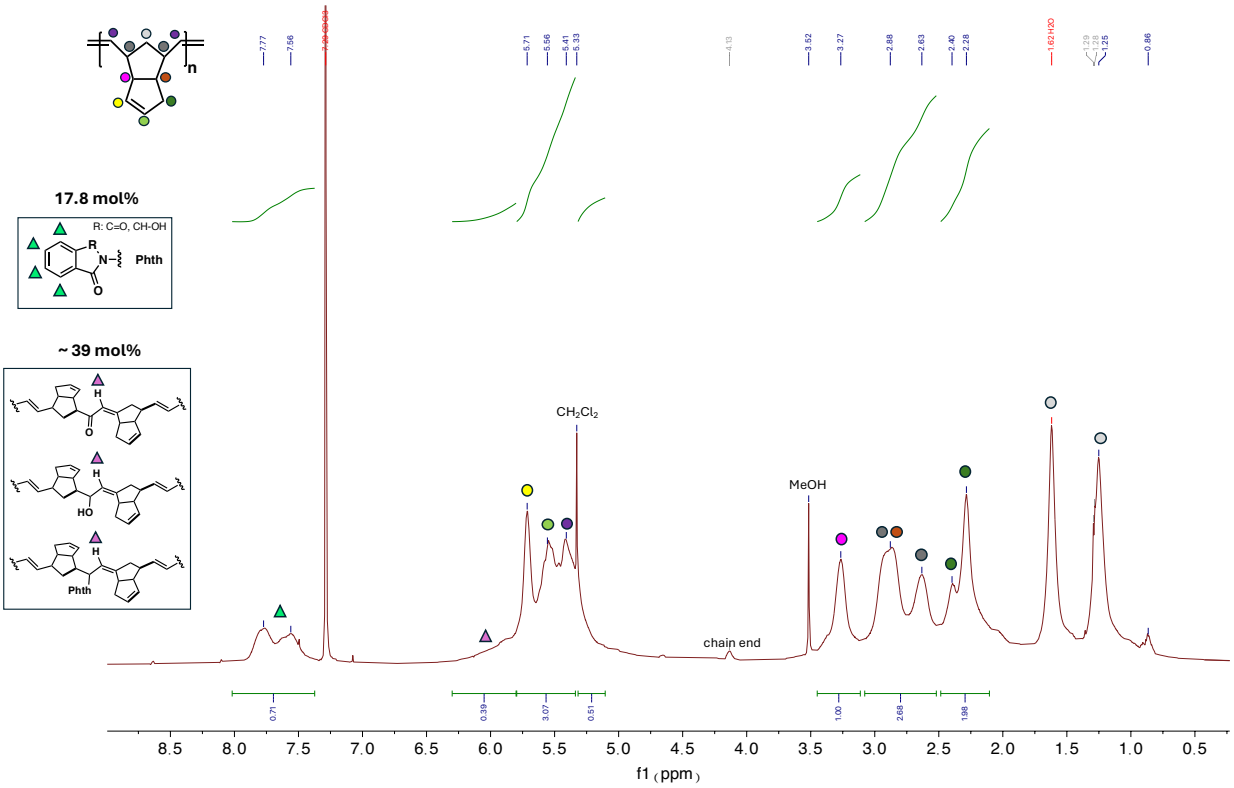

Supplementary Fig. 80 ^{1}H NMR spectrum of E-functionalized deconstructed pDCPD oligomers at t = 4h (after purification), for detailed reaction conditions, see Supplementary Table 2, Entry 3, trial II.

Table S2, Entry 3 (Trial II), 6h

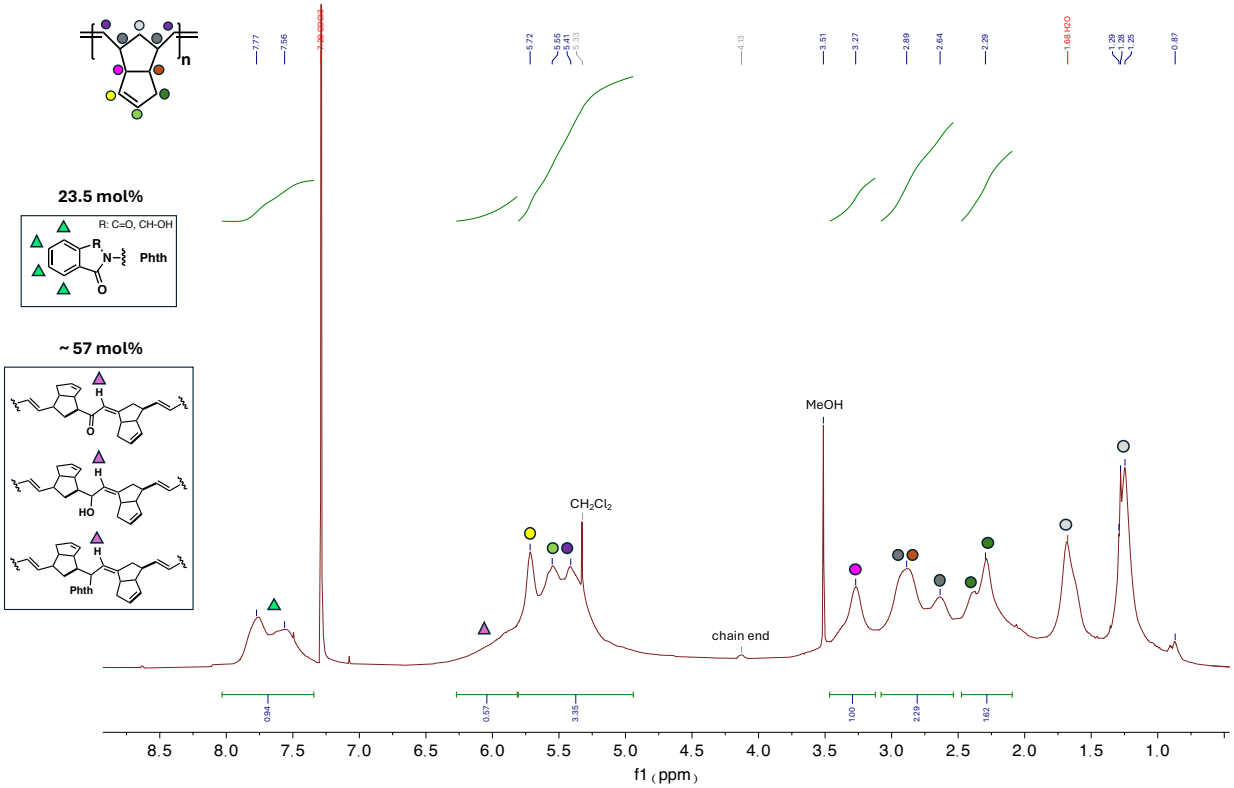

Supplementary Fig. 81 ^{1}H NMR spectrum of E-functionalized deconstructed pDCPD oligomers at t = 6h (after purification), for detailed reaction conditions, see Supplementary Table 2, Entry 3, trial II.

Supplementary Table 2, Entry 4, Stacked, Conversion Profile Over Time

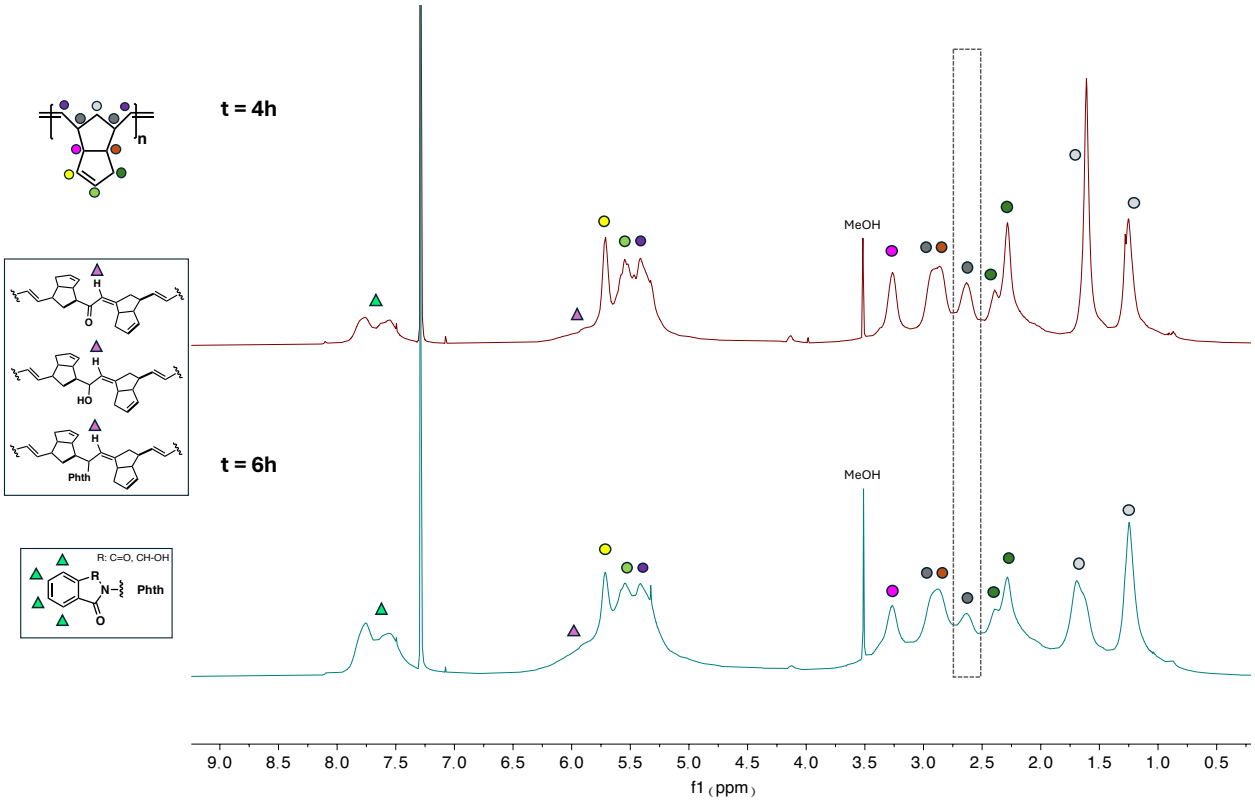

Supplementary Fig. 82 Stacked ^{1}H NMR spectra of E-functionalized deconstructed pDCPD oligomers at different reaction time point (after purification), for detailed reaction conditions, see Supplementary Table 2, Entry 4.

Supplementary Table 2, Entry 4, 4h

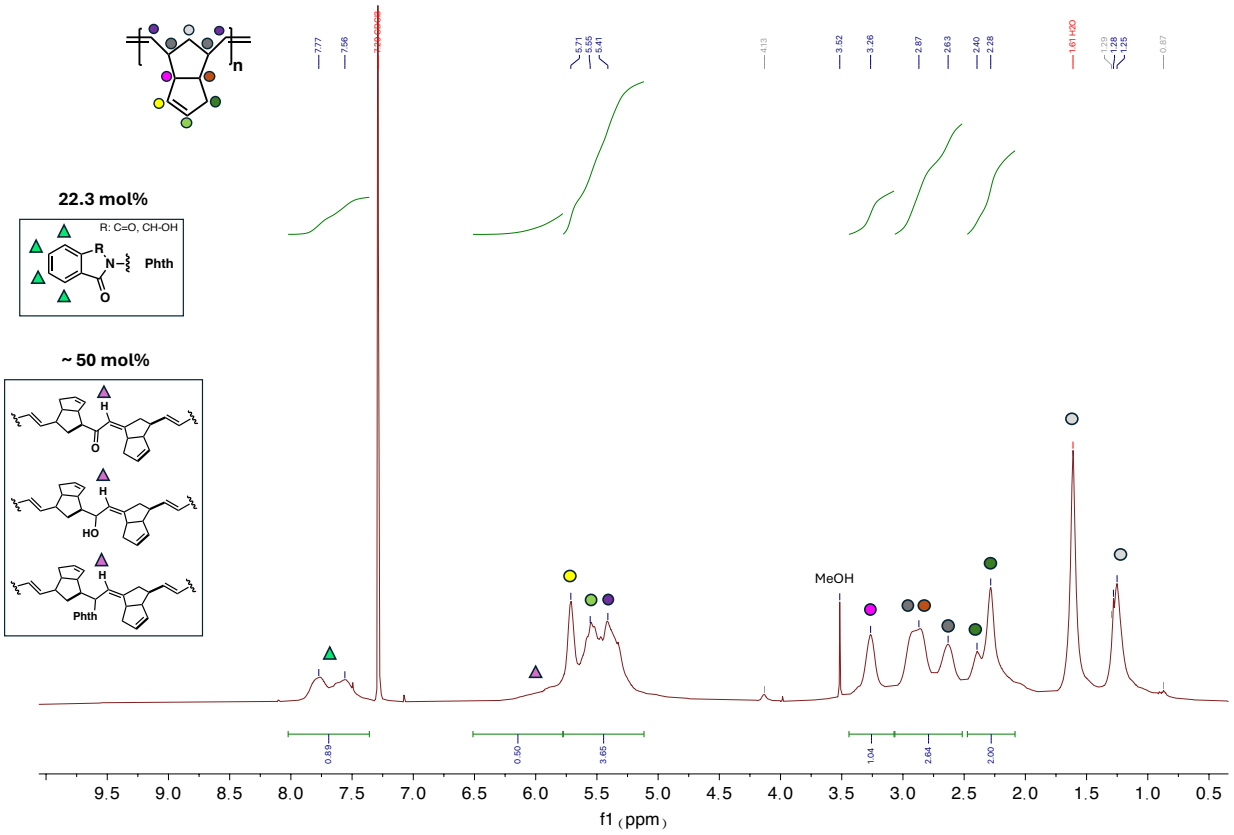

Supplementary Fig. 83 ^{1}H NMR spectrum of E-functionalized deconstructed pDCPD oligomers at t = 4h (after purification), for detailed reaction conditions, see Supplementary Table 2, Entry 4.

Supplementary Table 2, Entry 4, 6h

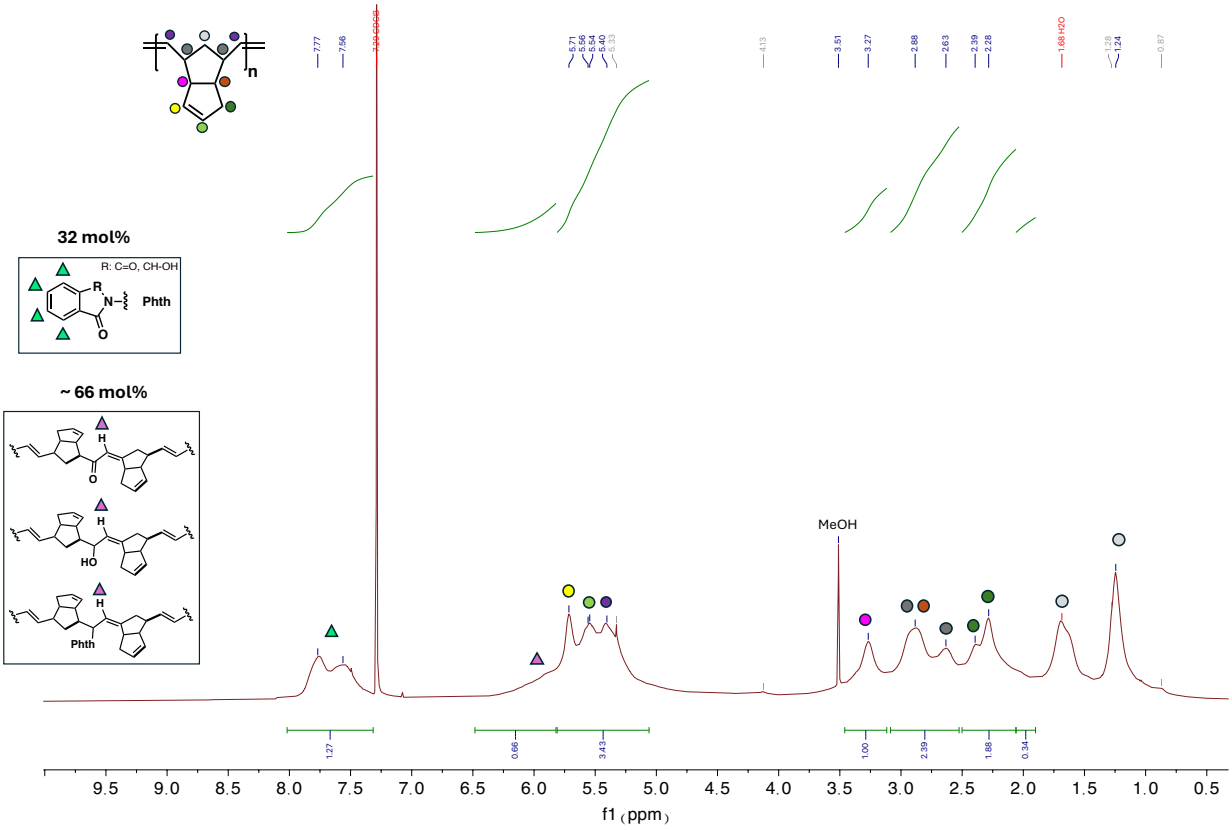

Supplementary Fig. 84 ^{1}H NMR spectrum of E-functionalized deconstructed pDCPD oligomers at t = 6h (after purification), for detailed reaction conditions, see Supplementary Table 2, Entry 4.

Supplementary Table 2, Entry 5, Stacked, Conversion Profile Over Time

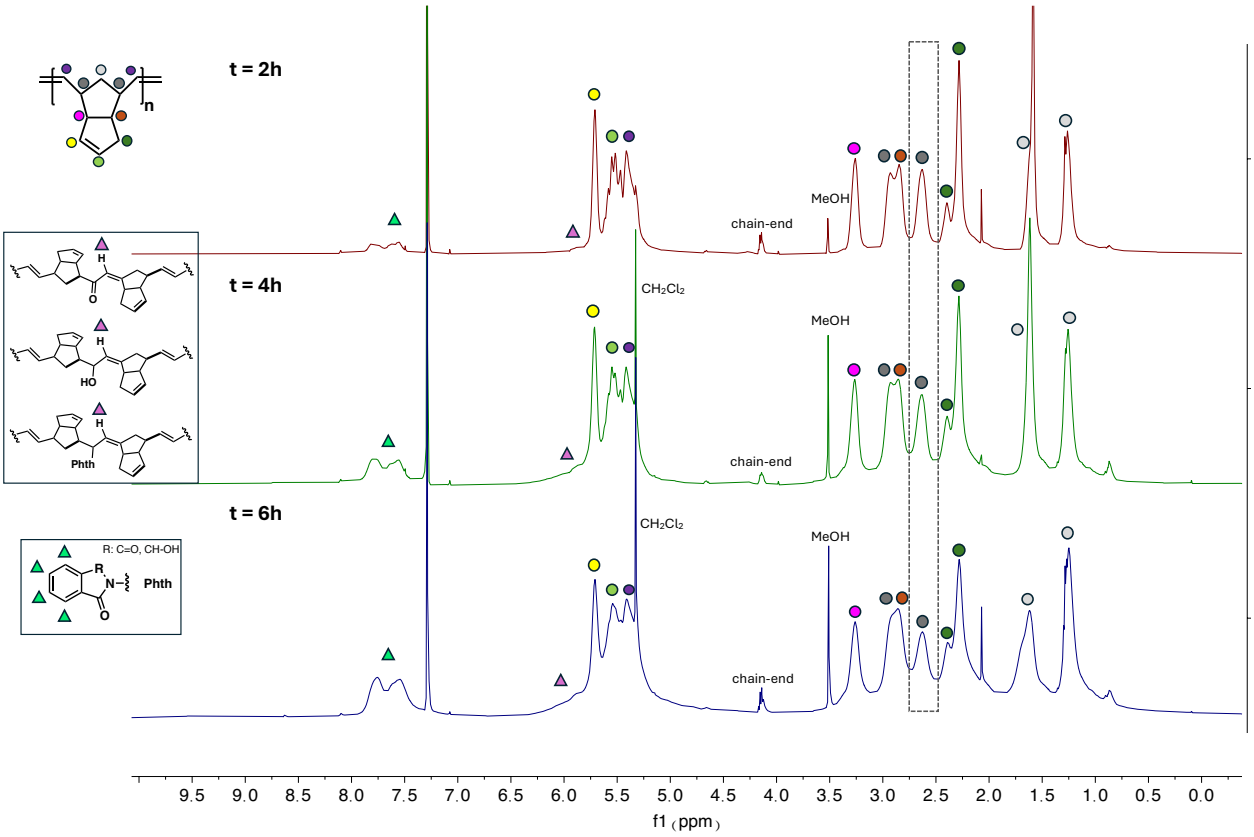

Supplementary Fig. 85 Stacked ^{1}H NMR spectra of E-functionalized deconstructed pDCPD oligomers at different reaction time point (after purification), for detailed reaction conditions, see Supplementary Table 2, Entry 5.

Supplementary Table 2, Entry 5, 2h

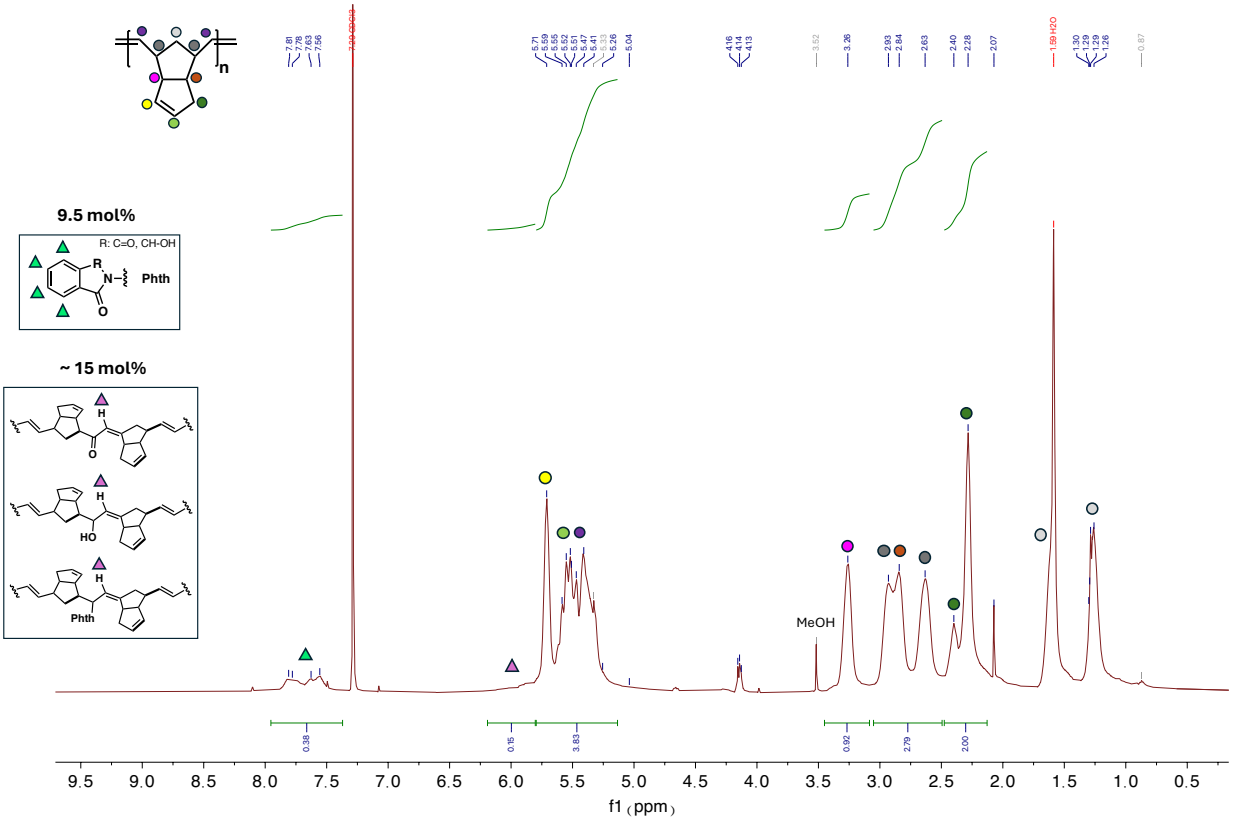

Supplementary Fig. 86 ^{1}H NMR spectrum of E-functionalized deconstructed pDCPD oligomers at t = 2h (after purification), for detailed reaction conditions, see Supplementary Table 2, Entry 5.

Supplementary Table 2, Entry 5, 4h

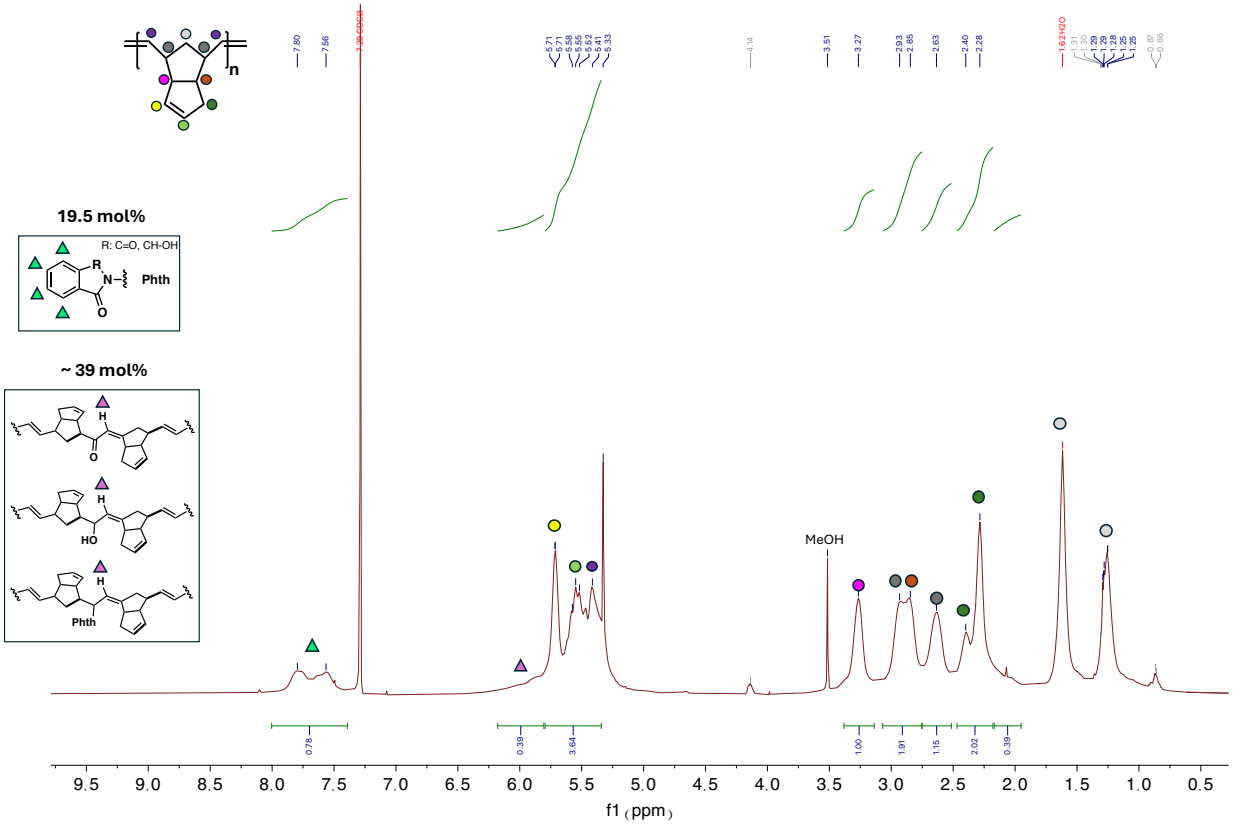

Supplementary Fig. 87 ^{1}H NMR spectrum of E-functionalized deconstructed pDCPD oligomers at t = 4h (after purification), for detailed reaction conditions, see Supplementary Table 2, Entry 5.

Supplementary Table 2, Entry 5, 6h

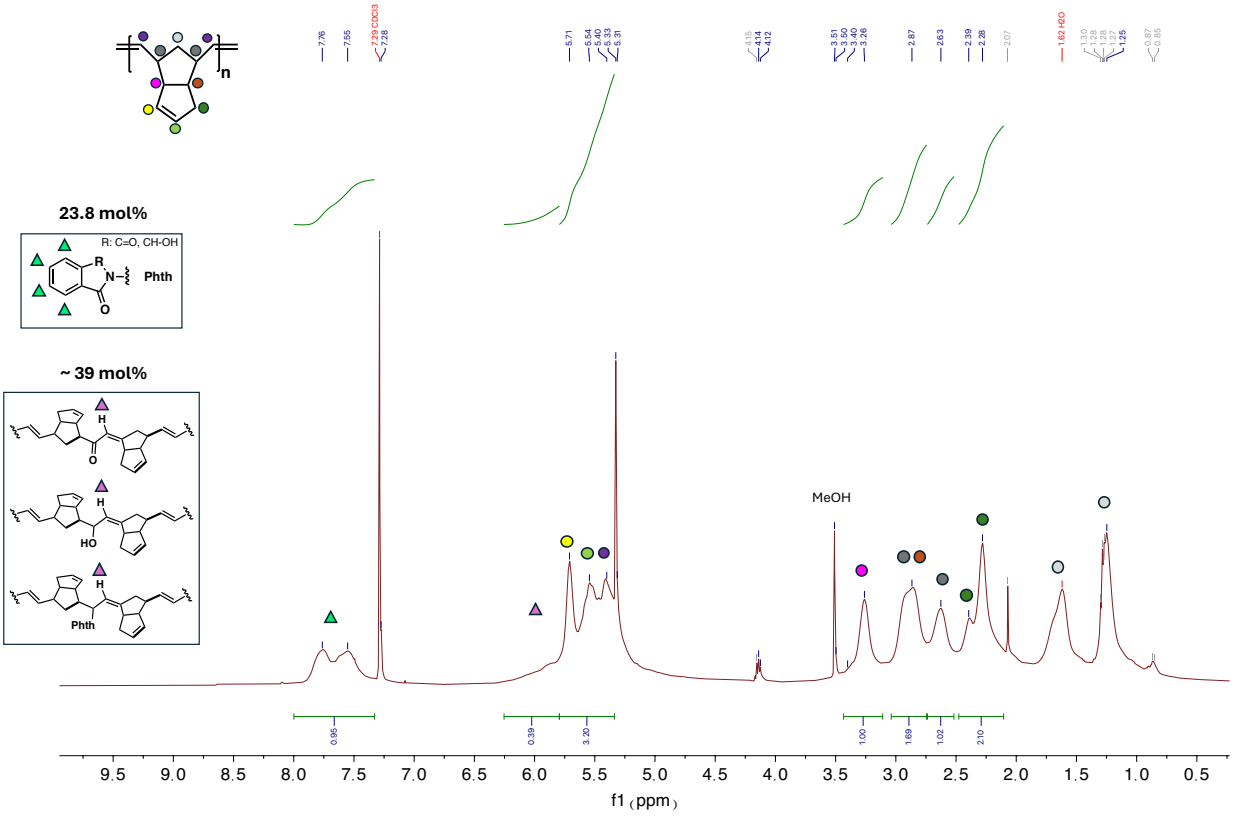

Supplementary Fig. 88 ^{1}H NMR spectrum of E-functionalized deconstructed pDCPD oligomers at t = 6h (after purification), for detailed reaction conditions, see Supplementary Table 2, Entry 5.

Supplementary Table 2, Entry 6, Stacked, Conversion Profile Over Time

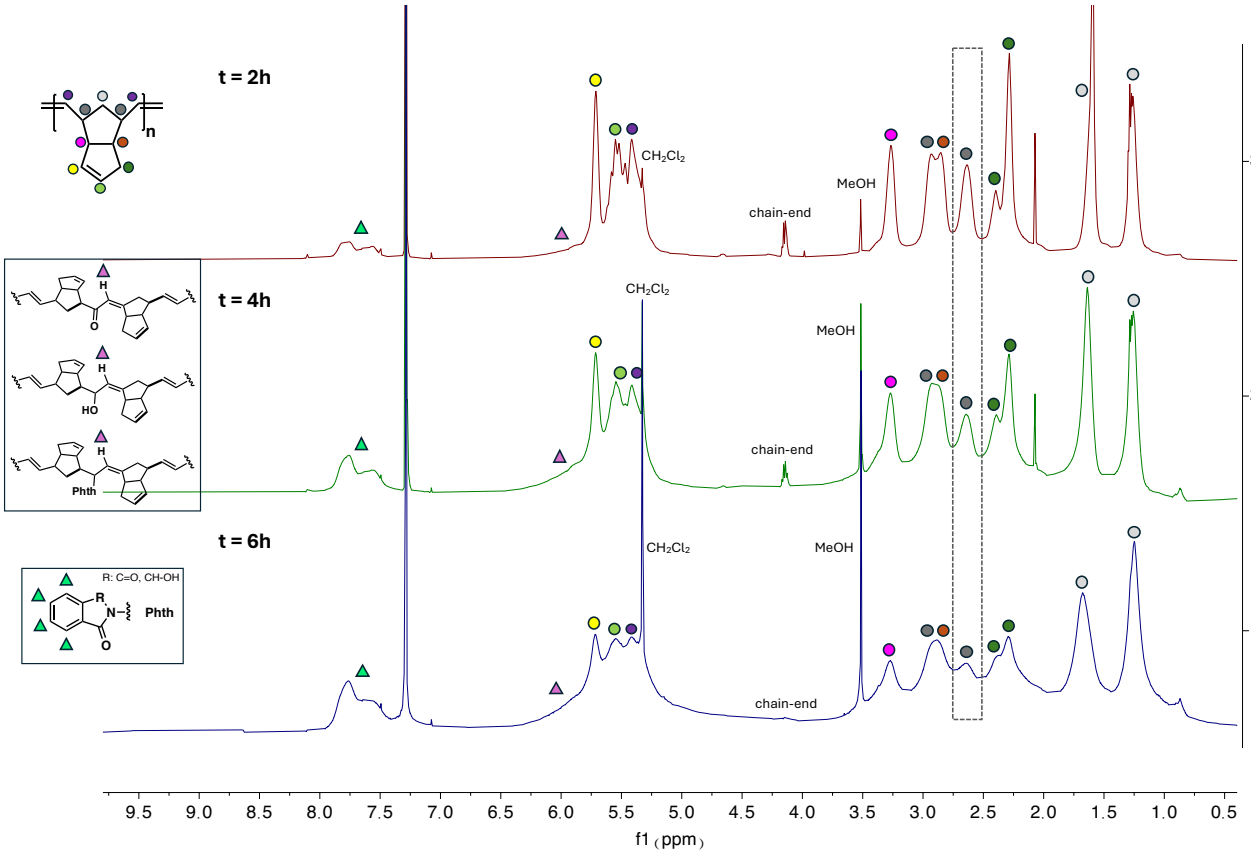

Supplementary Fig. 89 Stacked ^{1}H NMR spectra of E-functionalized deconstructed pDCPD oligomers at different reaction time point (after purification), for detailed reaction conditions, see Supplementary Table 2, Entry 6.

Supplementary Table 2, Entry 6, 2h

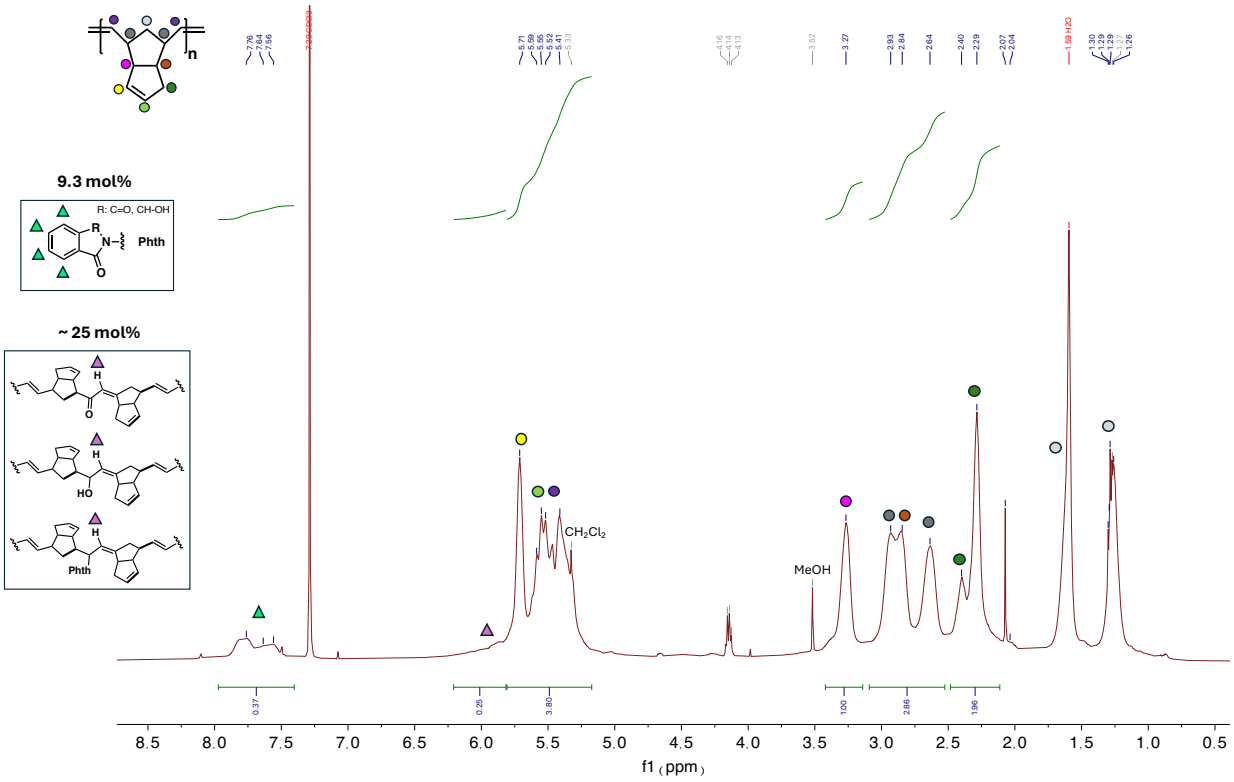

Supplementary Fig. 90 ^{1}H NMR spectrum of E-functionalized deconstructed pDCPD oligomers at t = 2h (after purification), for detailed reaction conditions, see Supplementary Table 2, Entry 6.

Supplementary Table 2, Entry 6, 4h

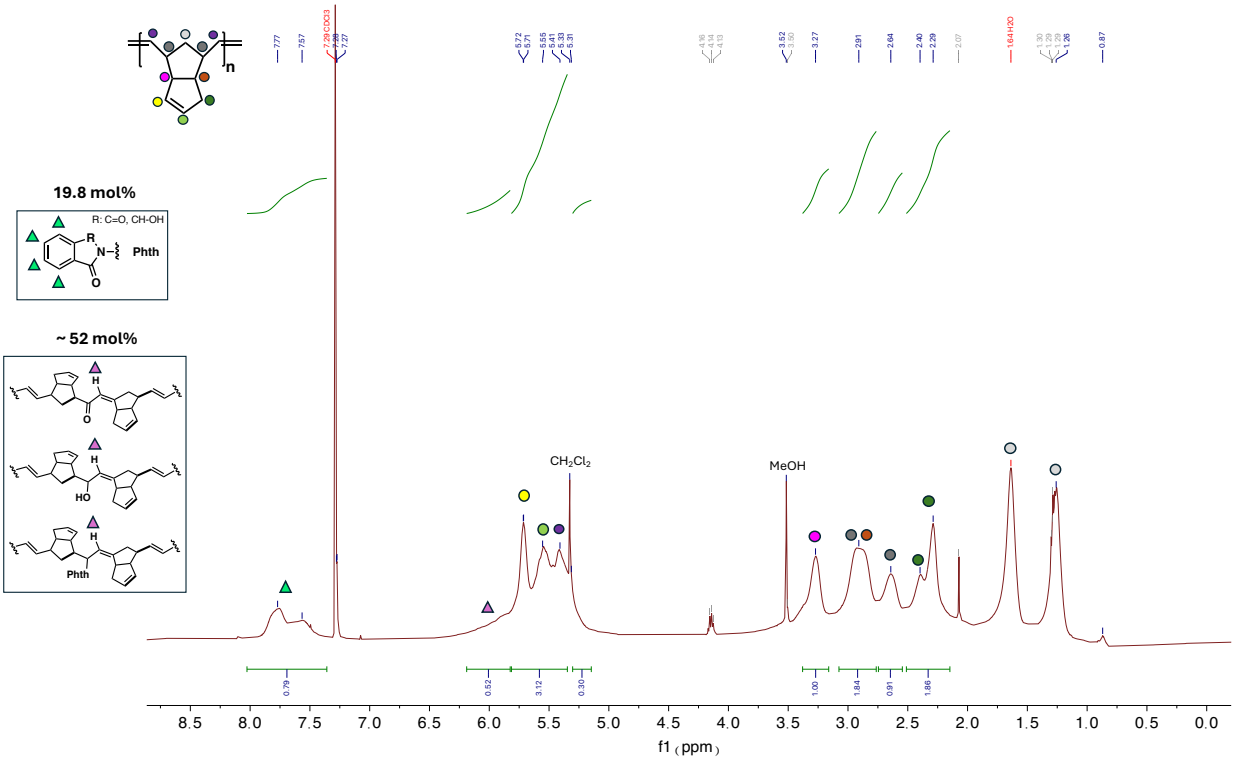

Supplementary Fig. 91 ^{1}H NMR spectrum of E-functionalized deconstructed pDCPD oligomers at t = 4h (after purification), for detailed reaction conditions, see Supplementary Table 2, Entry 6.

Supplementary Table 2, Entry 6, 6h

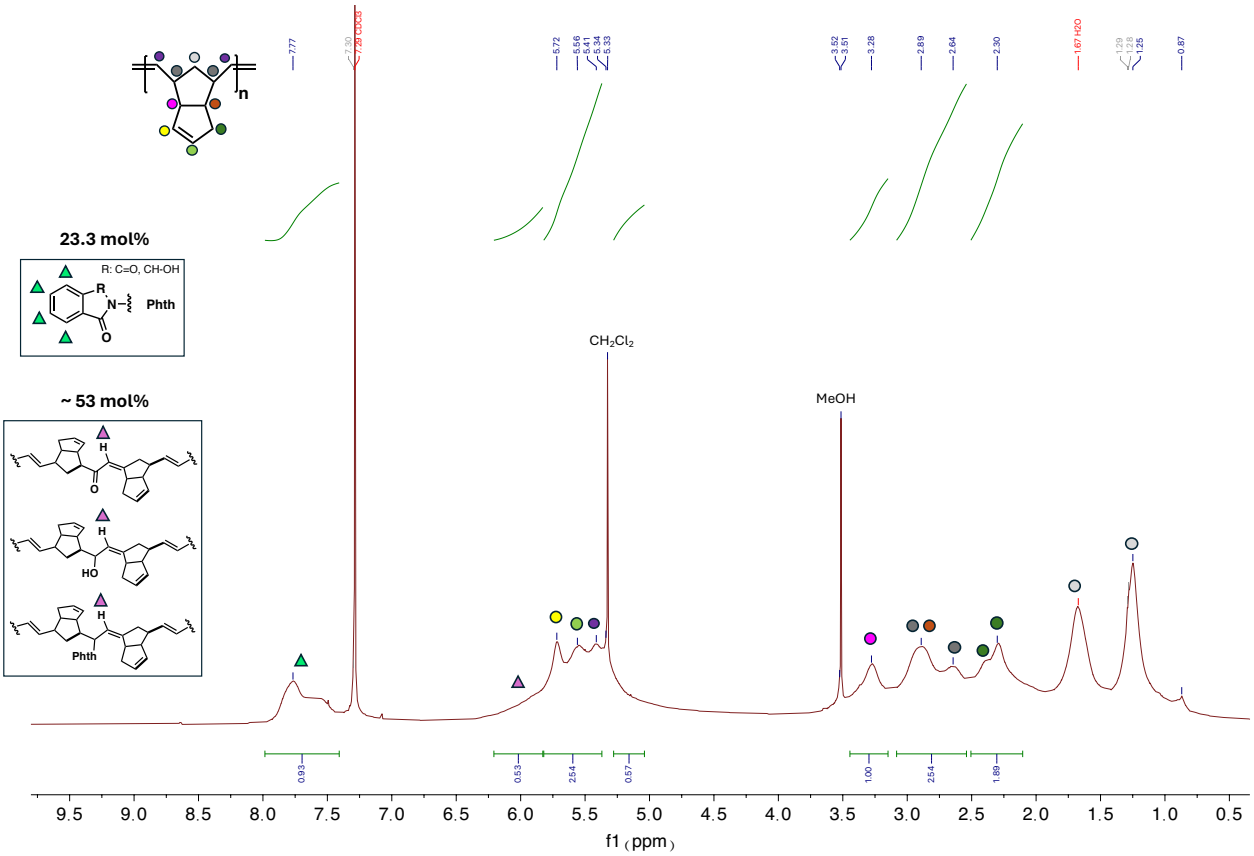

Supplementary Fig. 92 ^{1}H NMR spectrum of E-functionalized deconstructed pDCPD oligomers at t = 6h (after purification), for detailed reaction conditions, see Supplementary Table 2, Entry 6.

NMR Spectra of E-functionalization from Varying the Chain-End of the Deconstructed pDCPD Oligomers

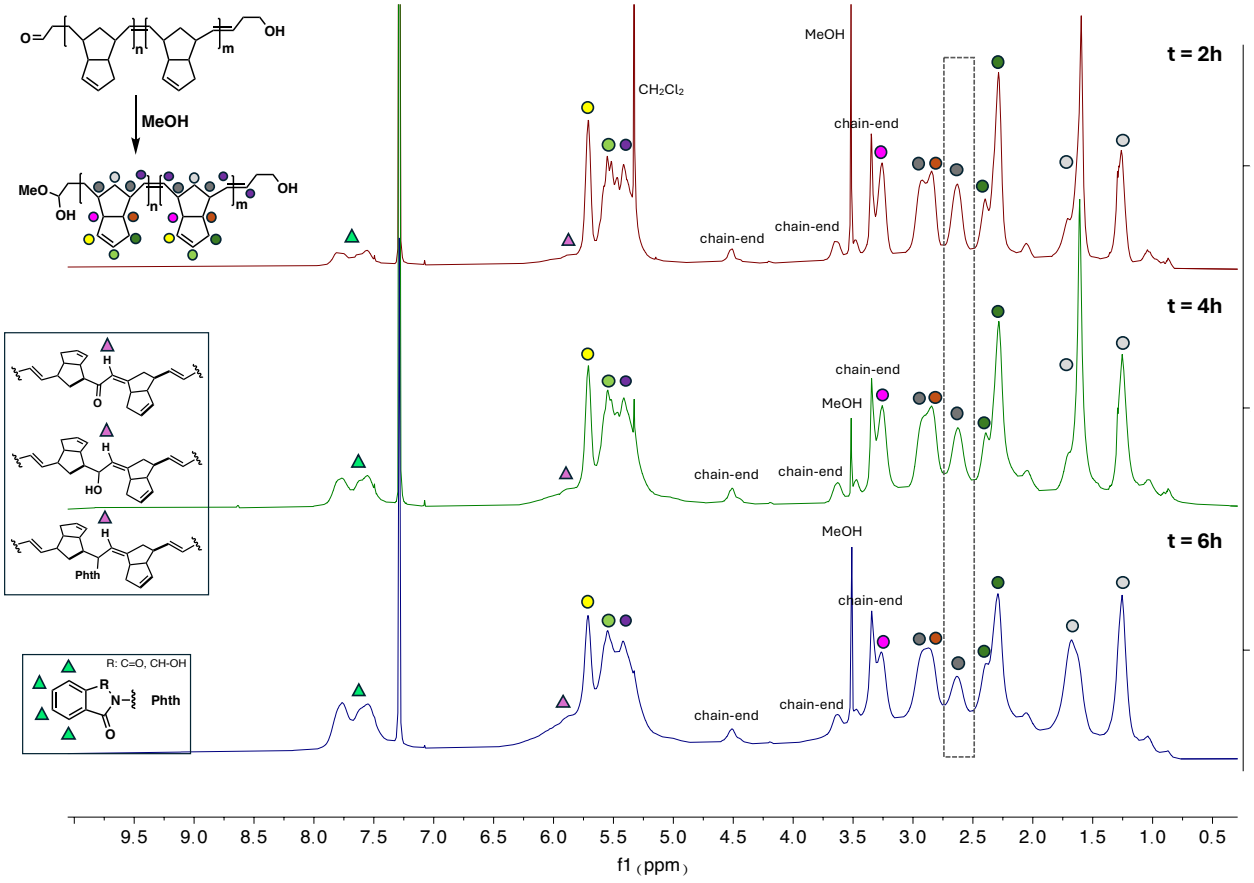

Supplementary Fig. 93 Stacked ^{1}H NMR spectra of E-functionalized deconstructed pDCPD oligomers at different reaction time point (after purification), for detailed reaction conditions, see Supplementary Table 4, Entry 2.

Supplementary Table 4, Entry 2, 2h

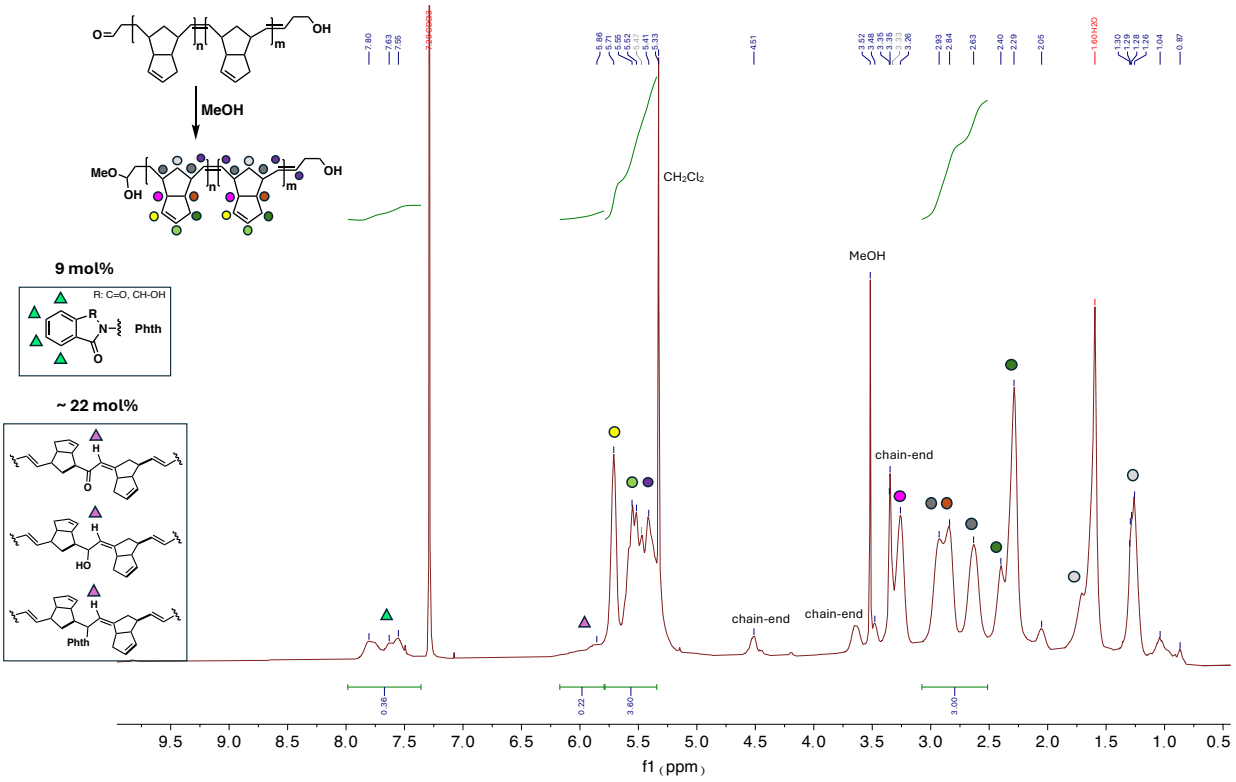

Supplementary Fig. 94 ^{1}H NMR spectrum of E-functionalized deconstructed pDCPD oligomers at t = 2h (after purification), for detailed reaction conditions, see Supplementary Table 4, Entry 2.

Supplementary Table 4, Entry 2, 4h

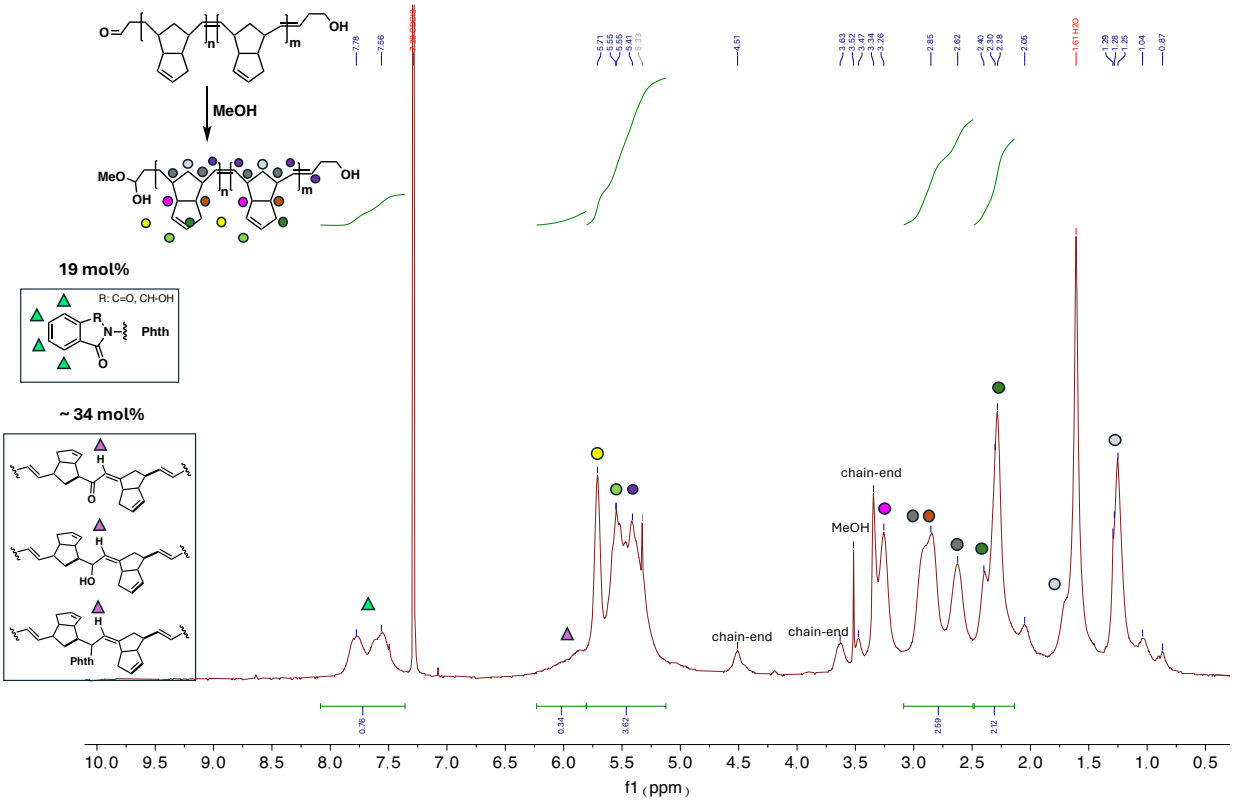

Supplementary Fig. 95 ^{1}H NMR spectrum of E-functionalized deconstructed pDCPD oligomers at t = 4h (after purification), for detailed reaction conditions, see Supplementary Table 4, Entry 2.

Supplementary Table 4, Entry 2, 6h

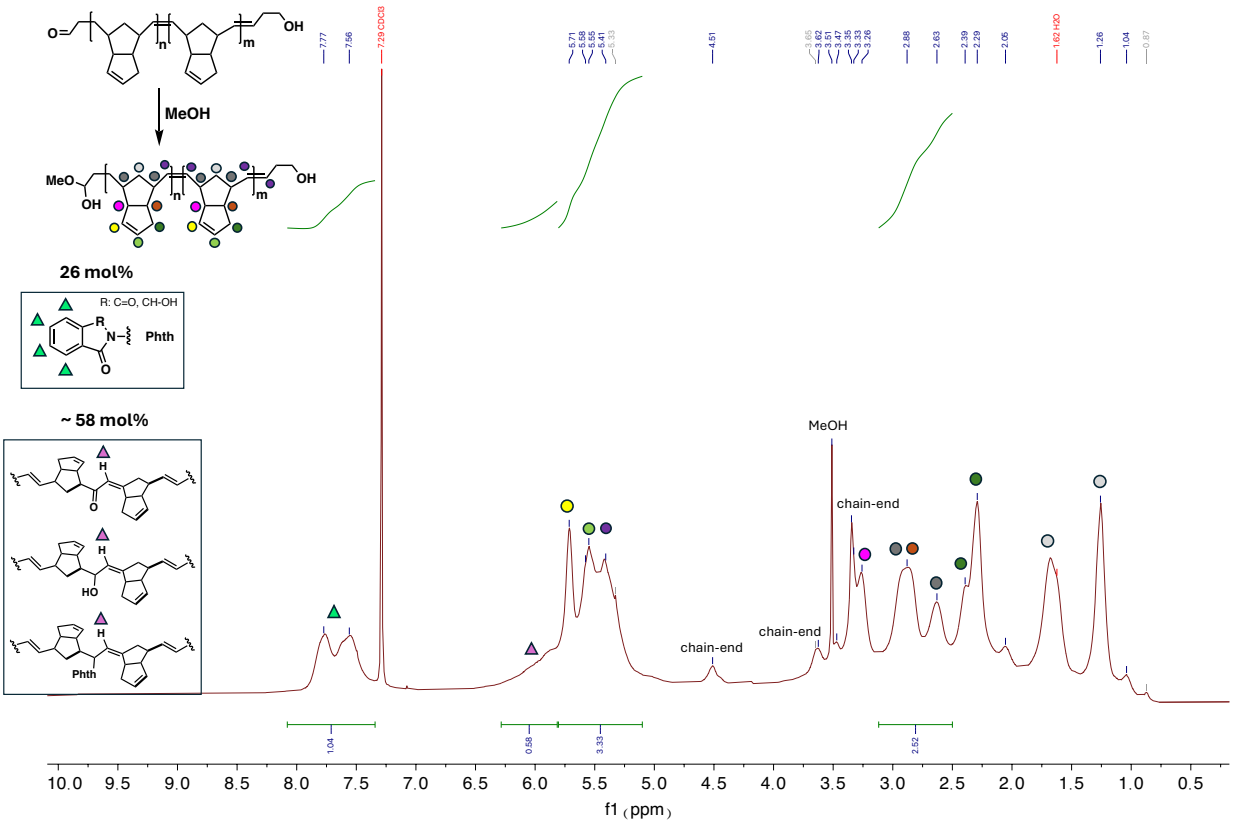

Supplementary Fig. 96 ^{1}H NMR spectrum of E-functionalized deconstructed pDCPD oligomers at t = 6h (after purification), for detailed reaction conditions, see Supplementary Table 4, Entry 2.

Supplementary Table 4, Entry 3, Stacked, Conversion Profile Over Time (DCPD:Styrene 10:1)

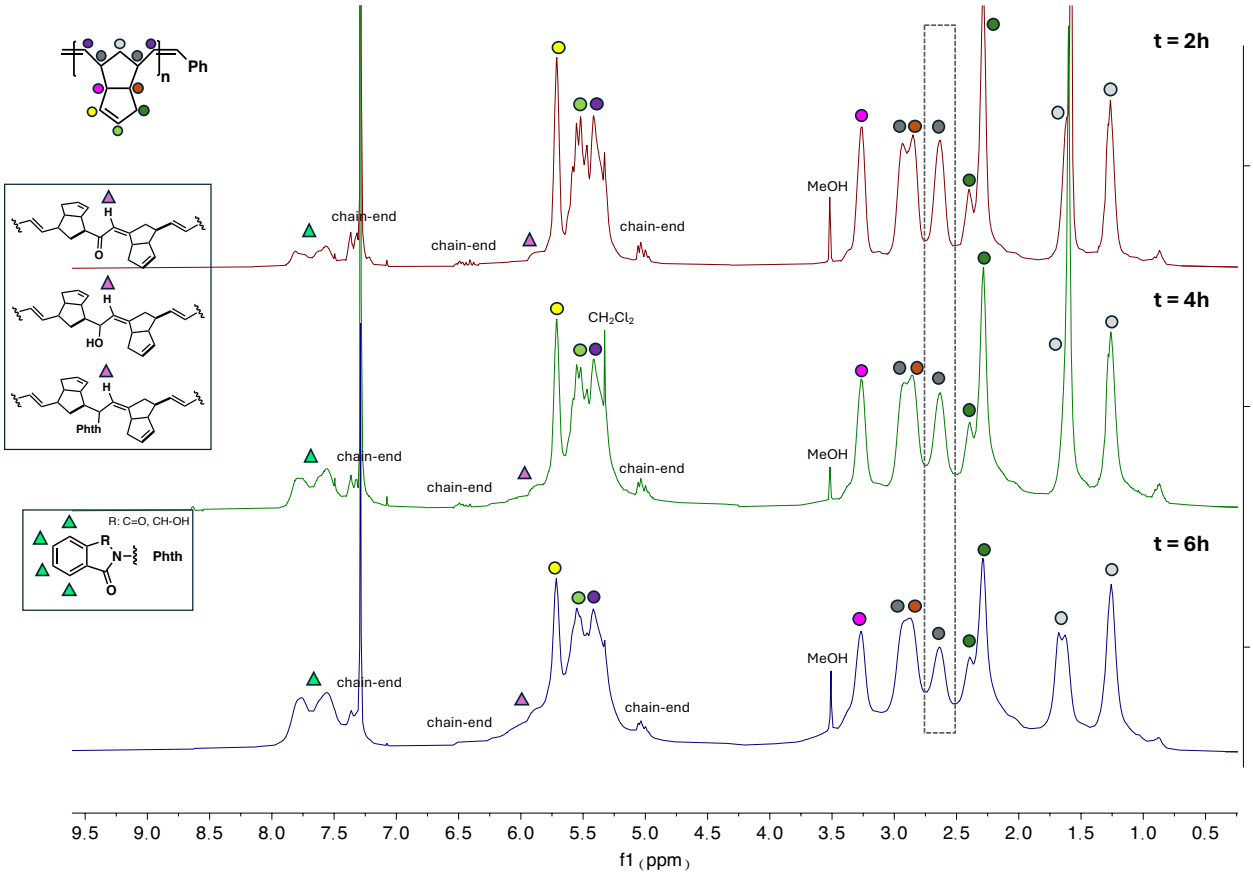

Supplementary Fig. 97 Stacked ^{1}H NMR spectra of E-functionalized deconstructed pDCPD oligomers at different reaction time point (after purification), for detailed reaction conditions, see Supplementary Table 4, Entry 3.

Supplementary Table 4, Entry 3, 2h

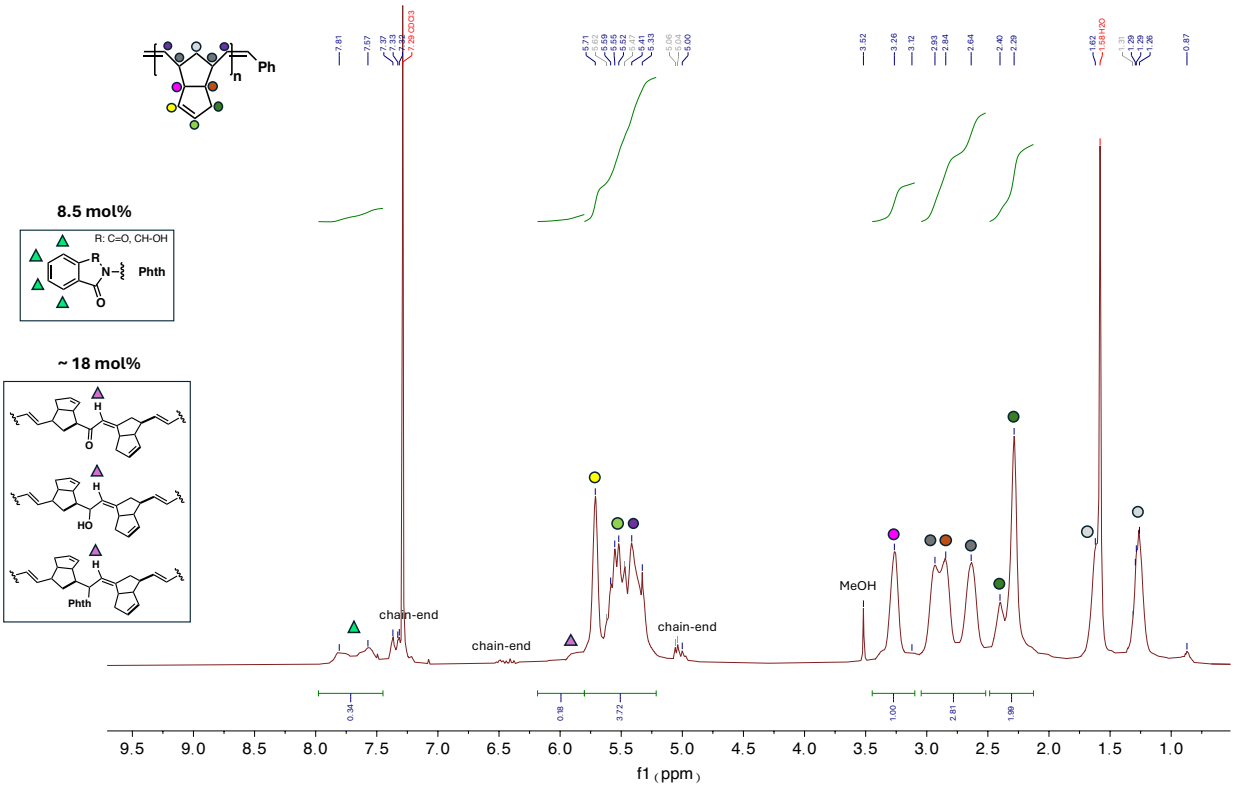

Supplementary Fig. 98 ^{1}H NMR spectrum of E-functionalized deconstructed pDCPD oligomers at t = 2h (after purification), for detailed reaction conditions, see Supplementary Table 4, Entry 3.

Supplementary Table 4, Entry 3, 4h

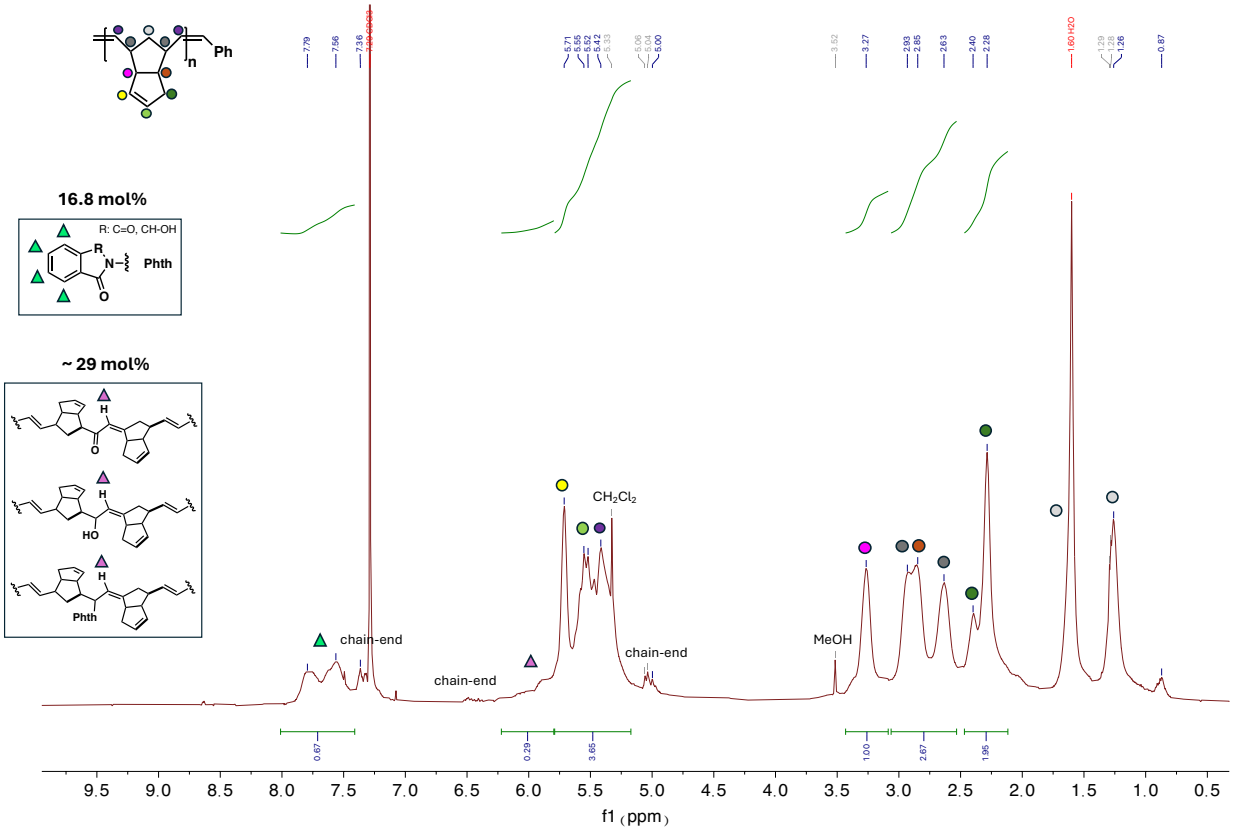

Supplementary Fig. 99 ^{1}H NMR spectrum of E-functionalized deconstructed pDCPD oligomers at t = 4h (after purification), for detailed reaction conditions, see Supplementary Table 4, Entry 3.

Supplementary Table 4, Entry 3, 6h

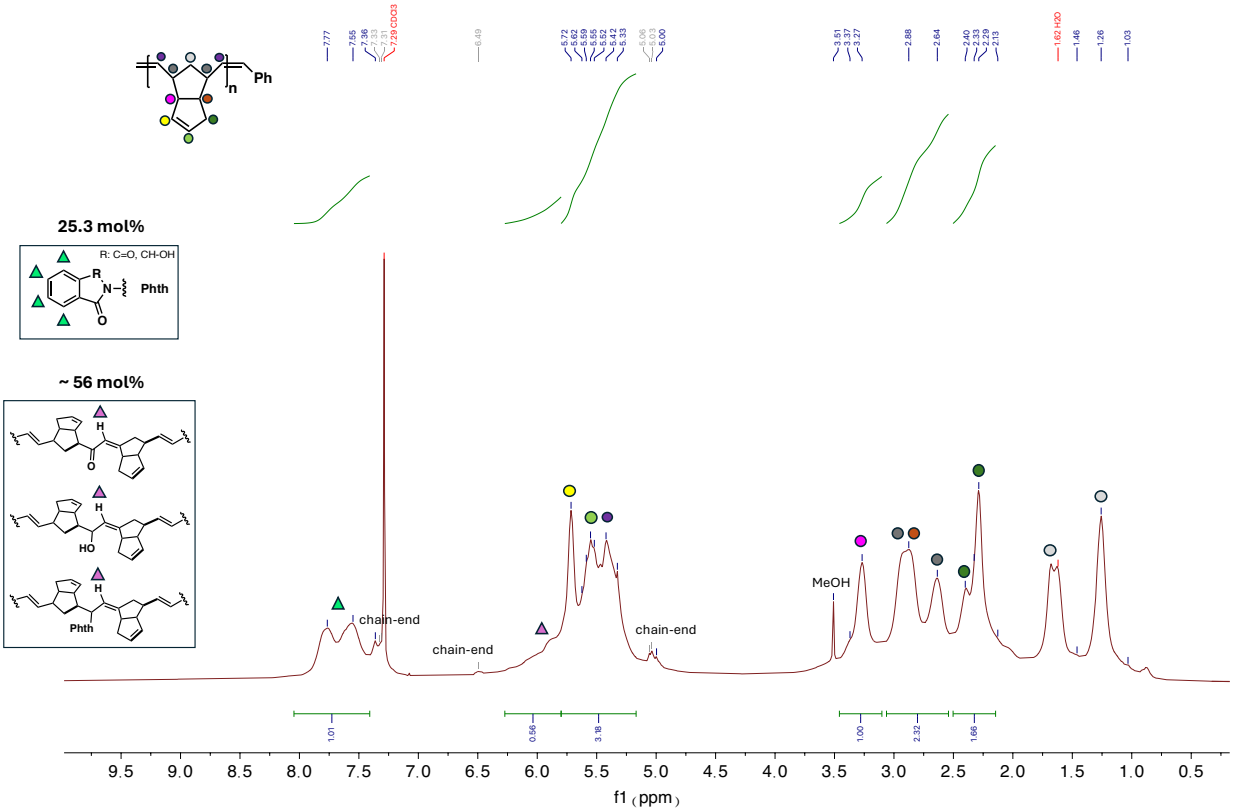

Supplementary Fig. 100 ^{1}H NMR spectrum of E-functionalized deconstructed pDCPD oligomers at t = 6h (after purification), for detailed reaction conditions, see Supplementary Table 4, Entry 3.

NMR Spectra of E-functionalization from Varying the Molecular Weight of the Deconstructed pDCPD Oligomers

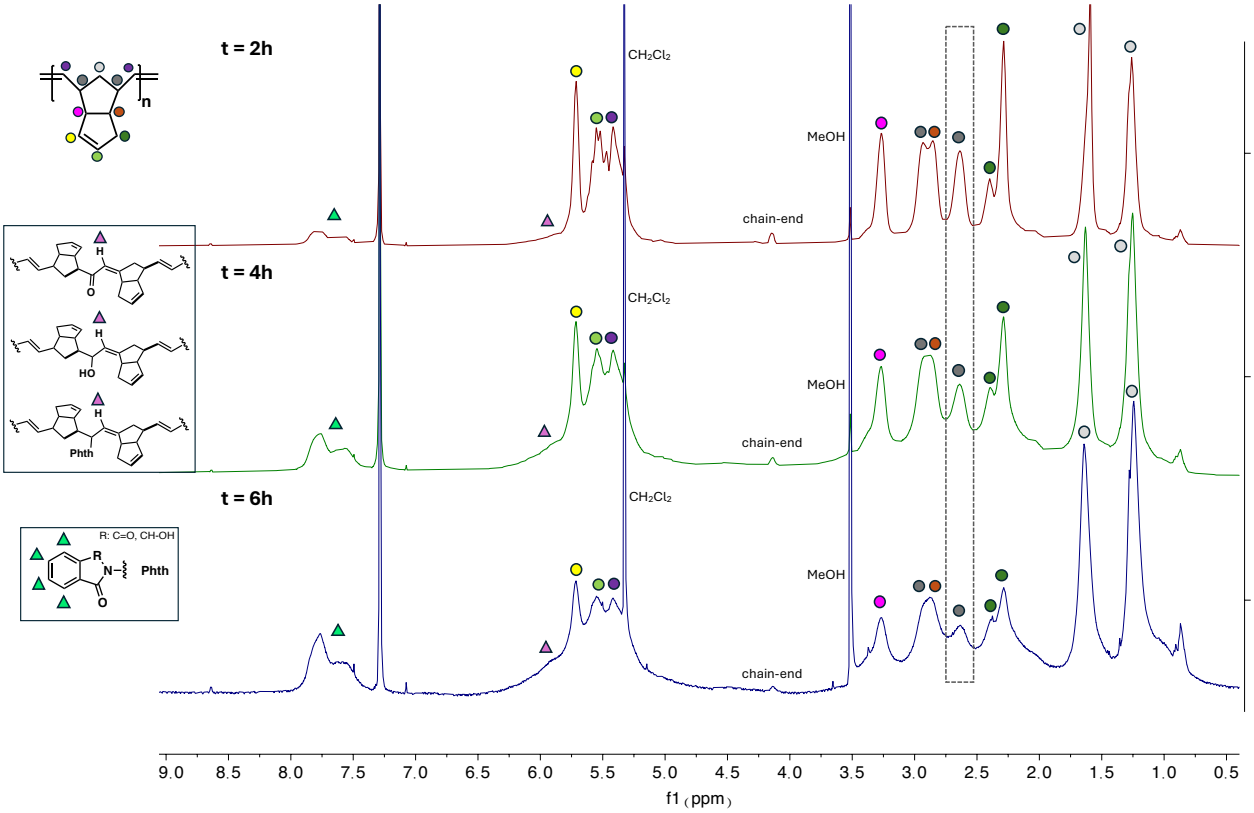

Supplementary Fig. 101 Stacked ^{1}H NMR spectra of E-functionalized deconstructed pDCPD oligomers (Mn 8.7 kDa) at different reaction time point (after purification), for detailed reaction conditions, see Supplementary Table 3, Entry 1.

Supplementary Table 3, Entry 1, 2h

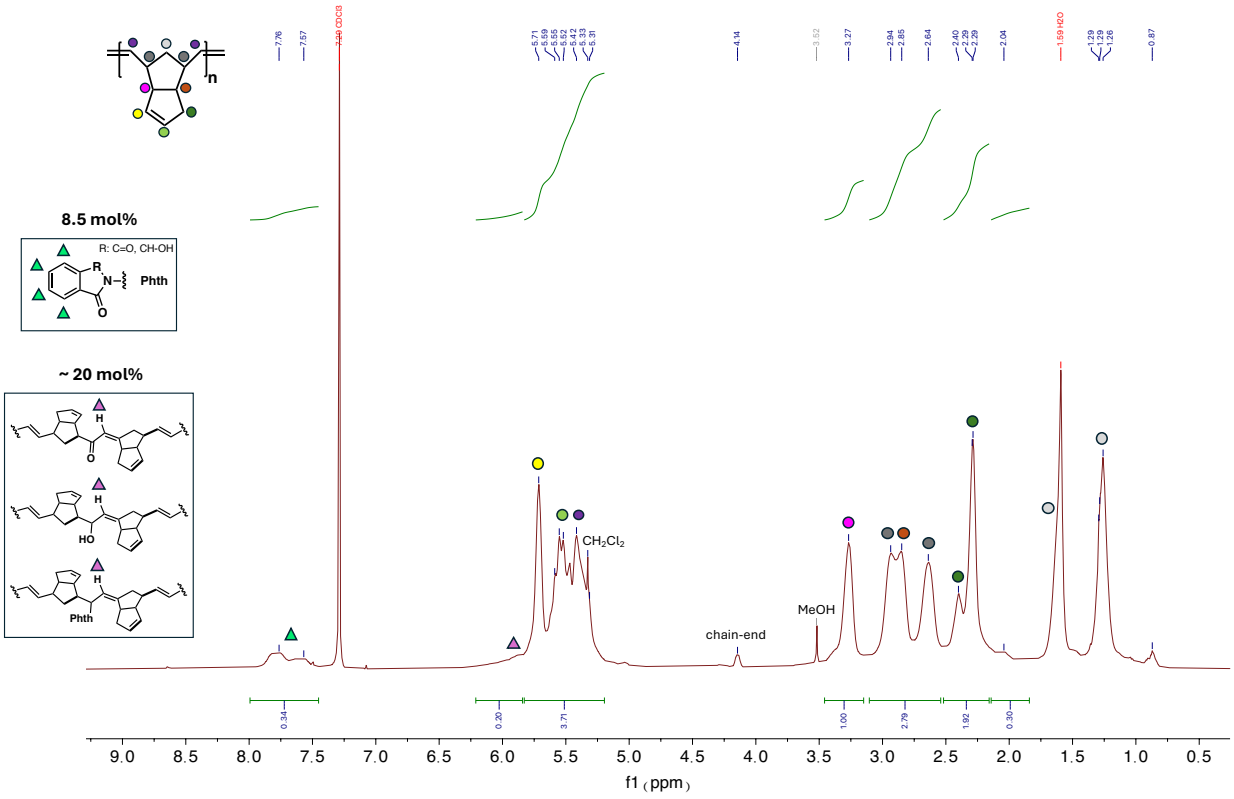

Supplementary Fig. 102 ^{1}H NMR spectrum of E-functionalized deconstructed pDCPD oligomers (Mn 8.7 kDa) at t = 2h (after purification), for detailed reaction conditions, see Supplementary Table 3, Entry 1.

Supplementary Table 3, Entry 1, 4h

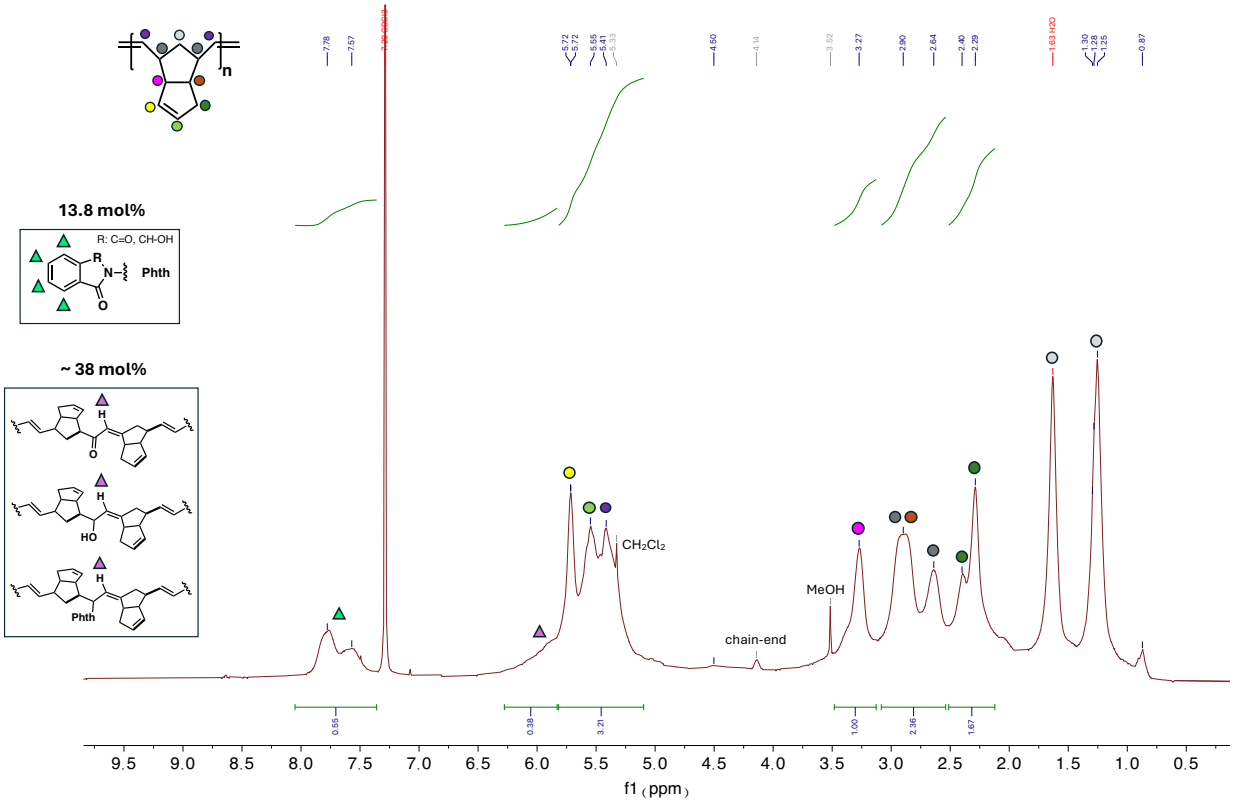

Supplementary Fig. 103 ^{1}H NMR spectrum of E-functionalized deconstructed pDCPD oligomers (Mn 8.7 kDa) at t = 4h (after purification), for detailed reaction conditions, see Supplementary Table 3, Entry 1.

Supplementary Table 3, Entry 1, 6h

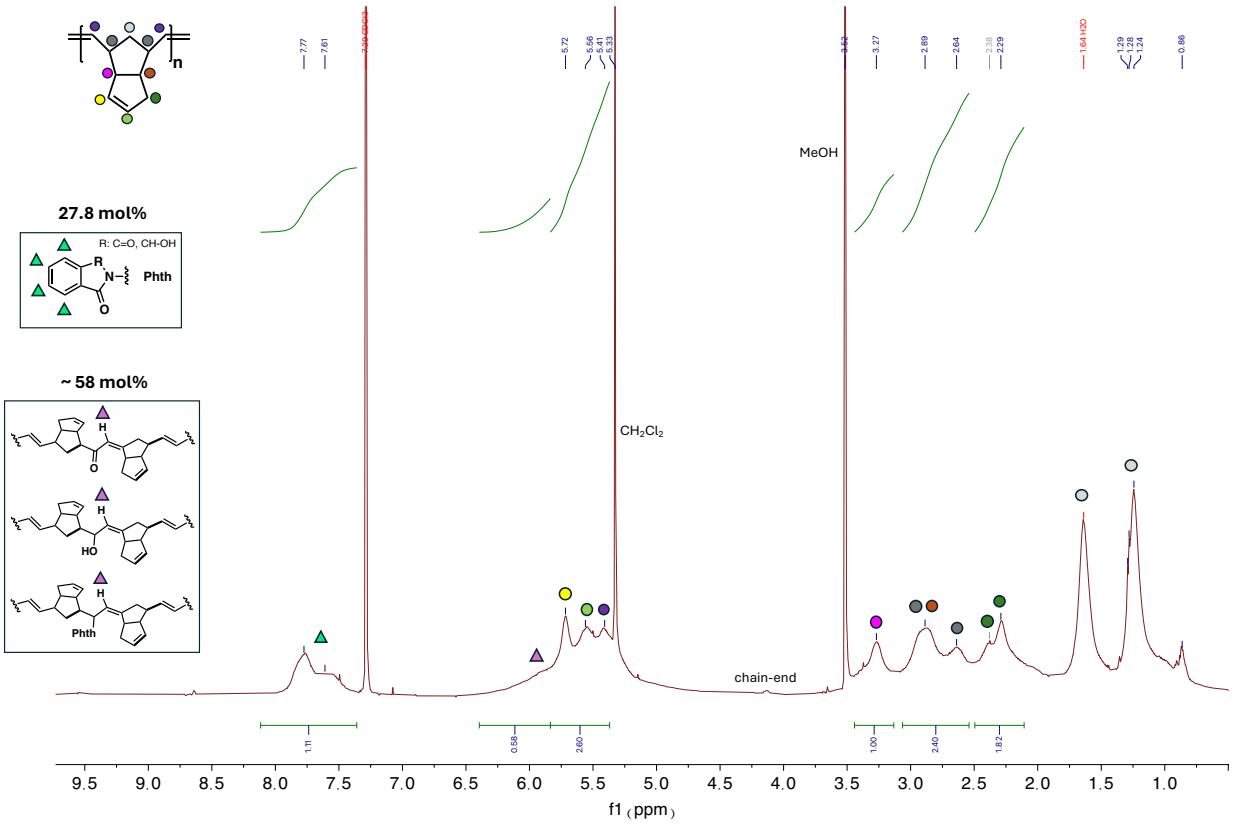

Supplementary Fig. 104 ^{1}H NMR spectrum of E-functionalized deconstructed pDCPD oligomers (Mn 8.7 kDa) at t = 6h (after purification), for detailed reaction conditions, see Supplementary Table 3, Entry 1.

Supplementary Table 3, Entry 3 (Mn 3.3 kDa), Stacked, Conversion Profile Over Time

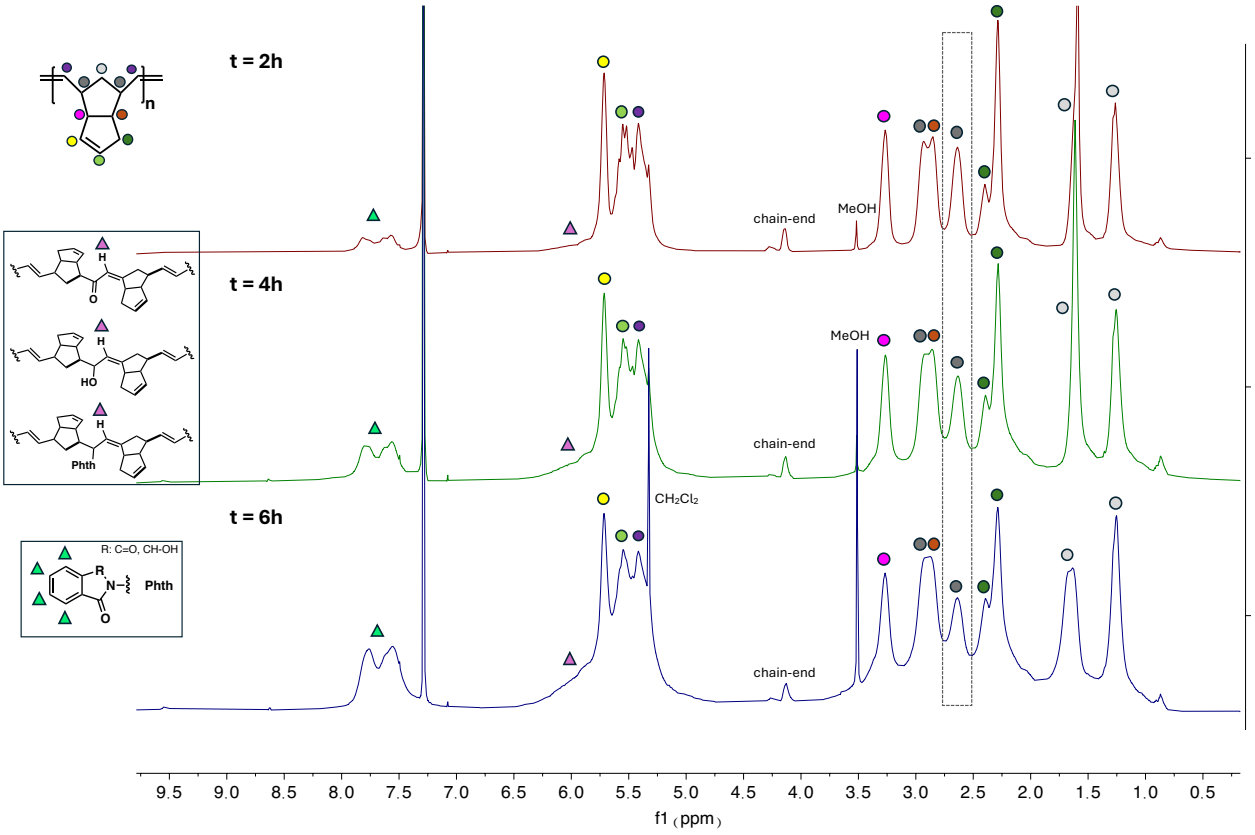

Supplementary Fig. 105 Stacked ^{1}H NMR spectra of E-functionalized deconstructed pDCPD oligomers (Mn 3.3 kDa) at different reaction time point (after purification), for detailed reaction conditions, see Supplementary Table 3, Entry 3.

Supplementary Table 3, Entry 3 (Mn 3.3 kDa), 2h

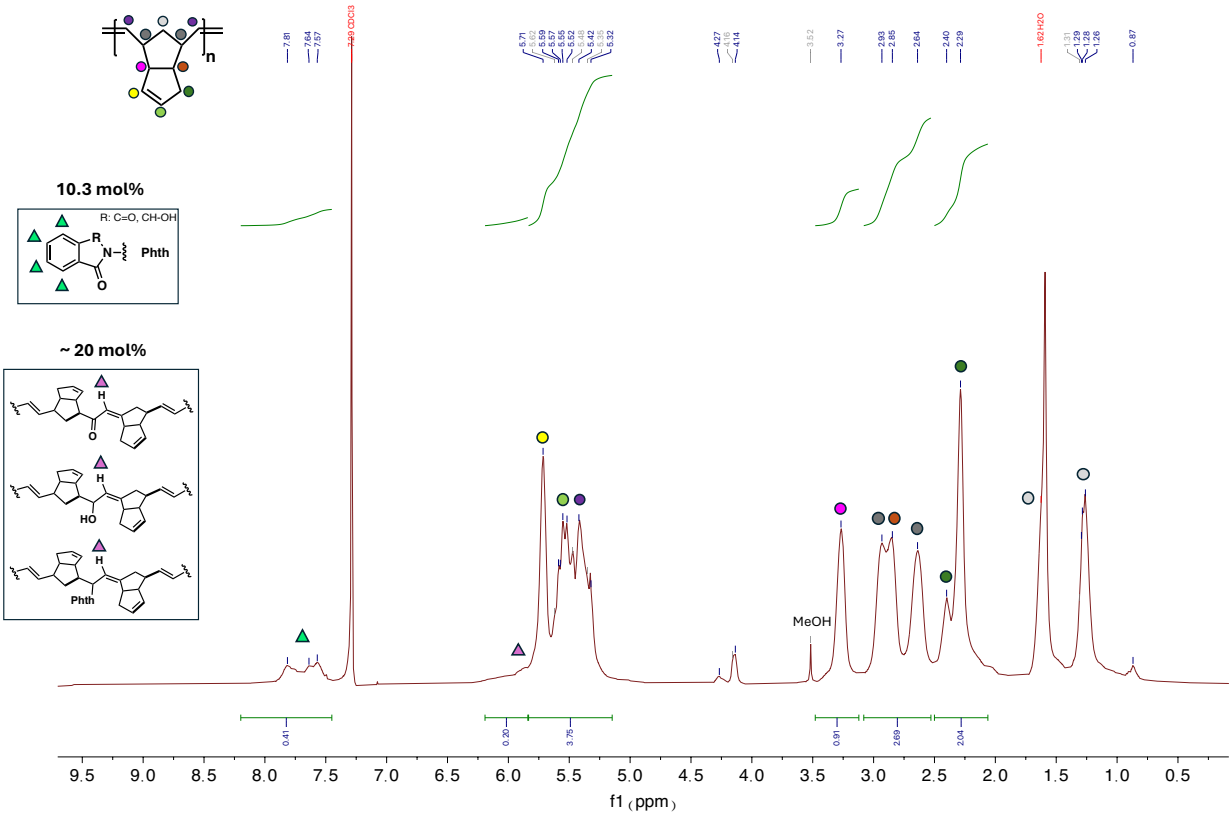

Supplementary Fig. 106 ^{1}H NMR spectrum of E-functionalized deconstructed pDCPD oligomers (Mn 3.3 kDa) at t = 2h (after purification), for detailed reaction conditions, see Supplementary Table 3, Entry 3.

Supplementary Table 3, Entry 3 (Mn 3.3 kDa), 4h

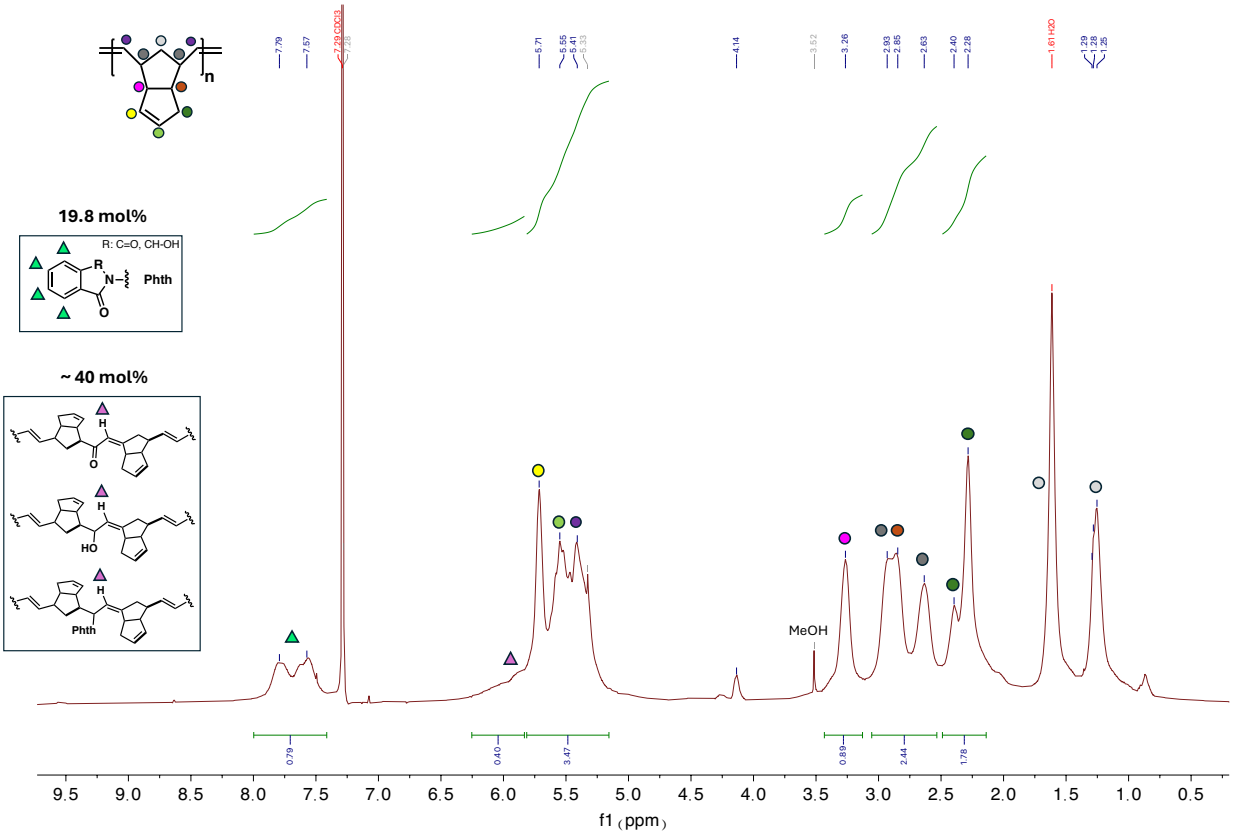

Supplementary Fig. 107 ^{1}H NMR spectrum of E-functionalized deconstructed pDCPD oligomers (Mn 3.3 kDa) at t = 4h (after purification), for detailed reaction conditions, see Supplementary Table 3, Entry 3.

Supplementary Table 3, Entry 3 (Mn 3.3 kDa), 6h

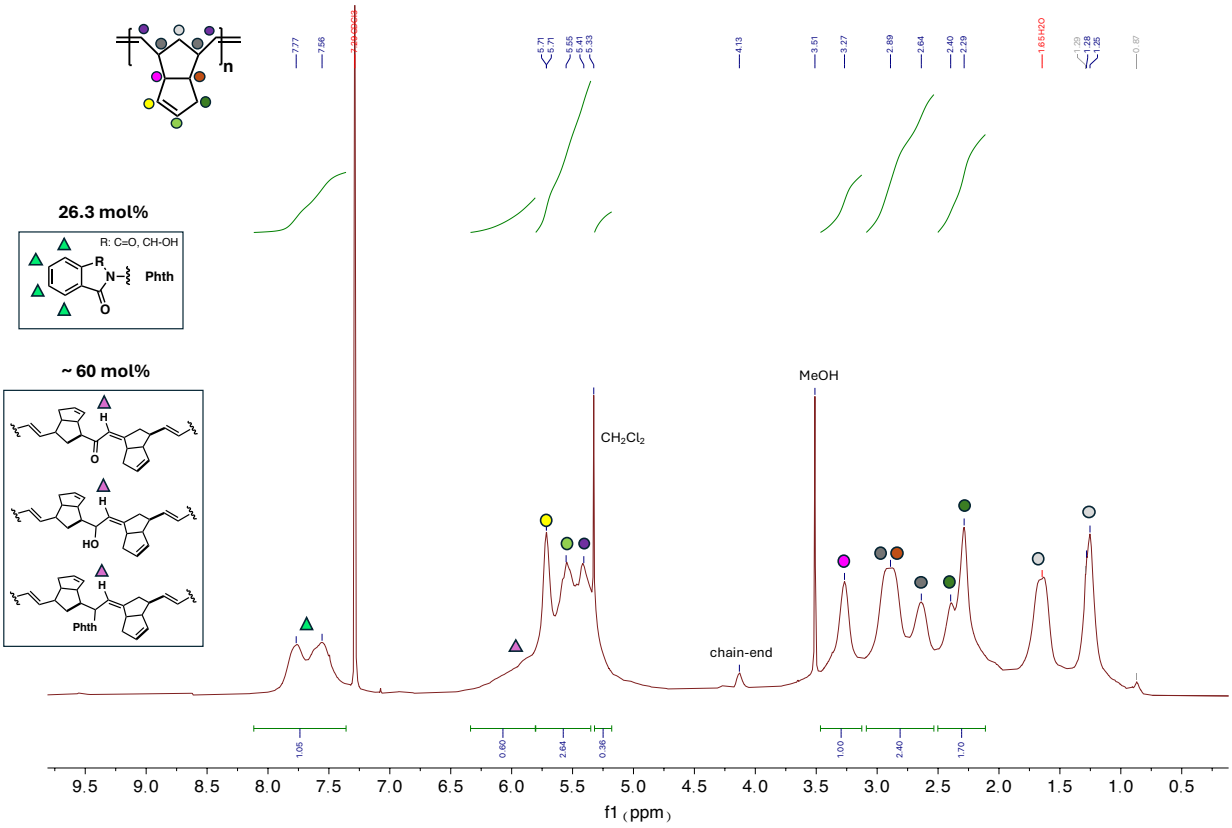

Supplementary Fig. 108 ^{1}H NMR spectrum of E-functionalized deconstructed pDCPD oligomers (Mn 3.3 kDa) at t = 6h (after purification), for detailed reaction conditions, see Supplementary Table 3, Entry 3.

NMR Spectra of E-functionalization from Varying the Choice of the Redox Mediator

Supplementary Table 5, Entry 2 (NHS), Stacked, Conversion Profile Over Time

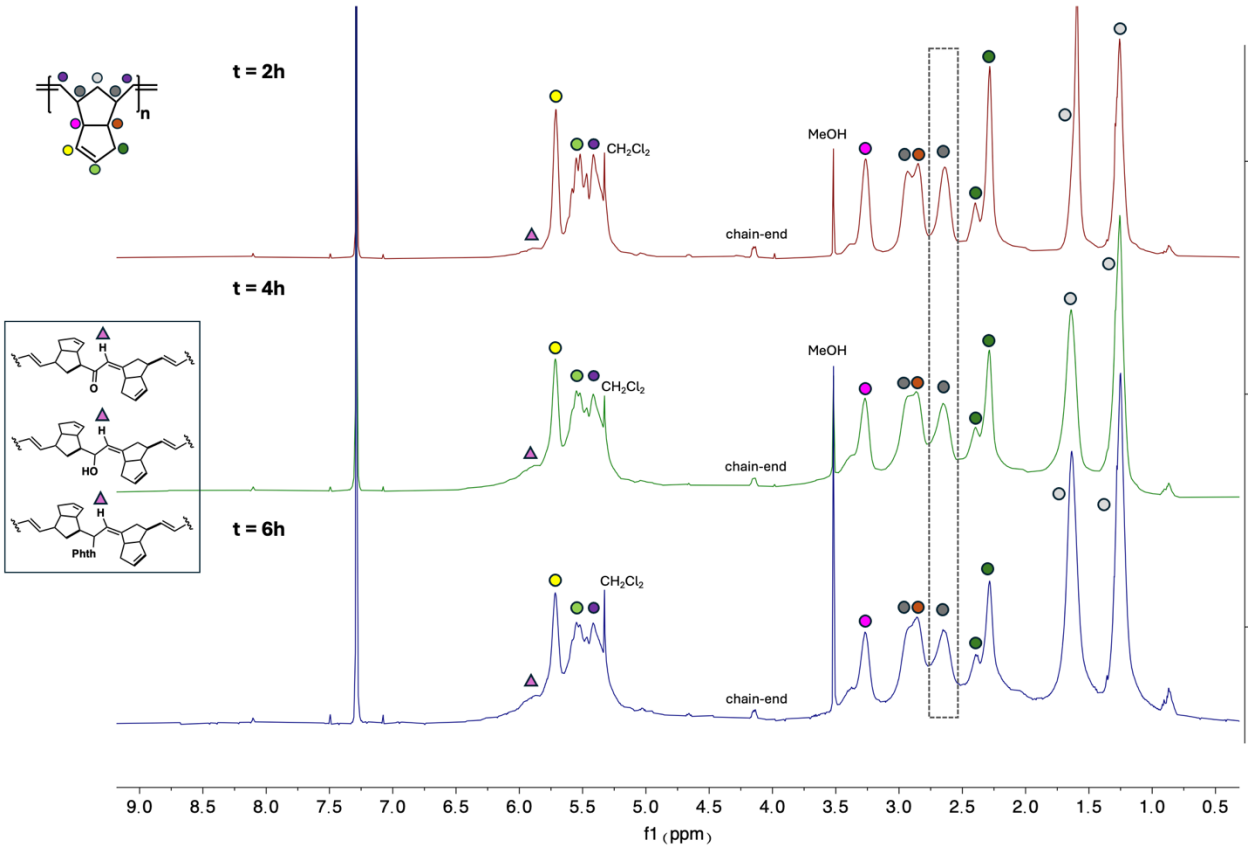

Supplementary Fig. 109 Stacked ^{1}H NMR spectra of E-functionalized deconstructed pDCPD oligomers mediated by NHS at different reaction time point (after purification), for detailed reaction conditions, see Supplementary Table 5, Entry 2.

Supplementary Table 5, Entry 2 (NHS), 2h

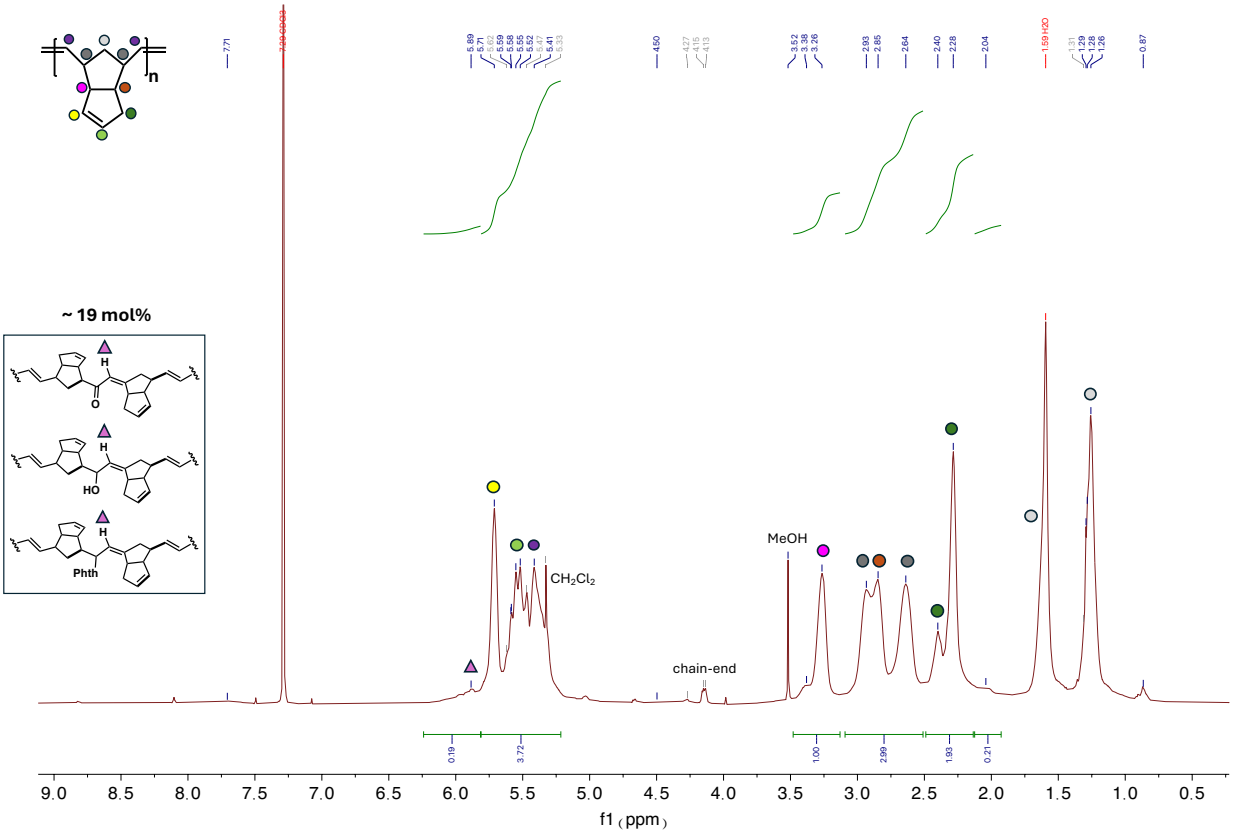

Supplementary Fig. 110 ^{1}H NMR spectrum of E-functionalized deconstructed pDCPD oligomers mediated by NHS at t = 2h (after purification), for detailed reaction conditions, see Supplementary Table 5, Entry 2.

Supplementary Table 5, Entry 2 (NHS), 4h

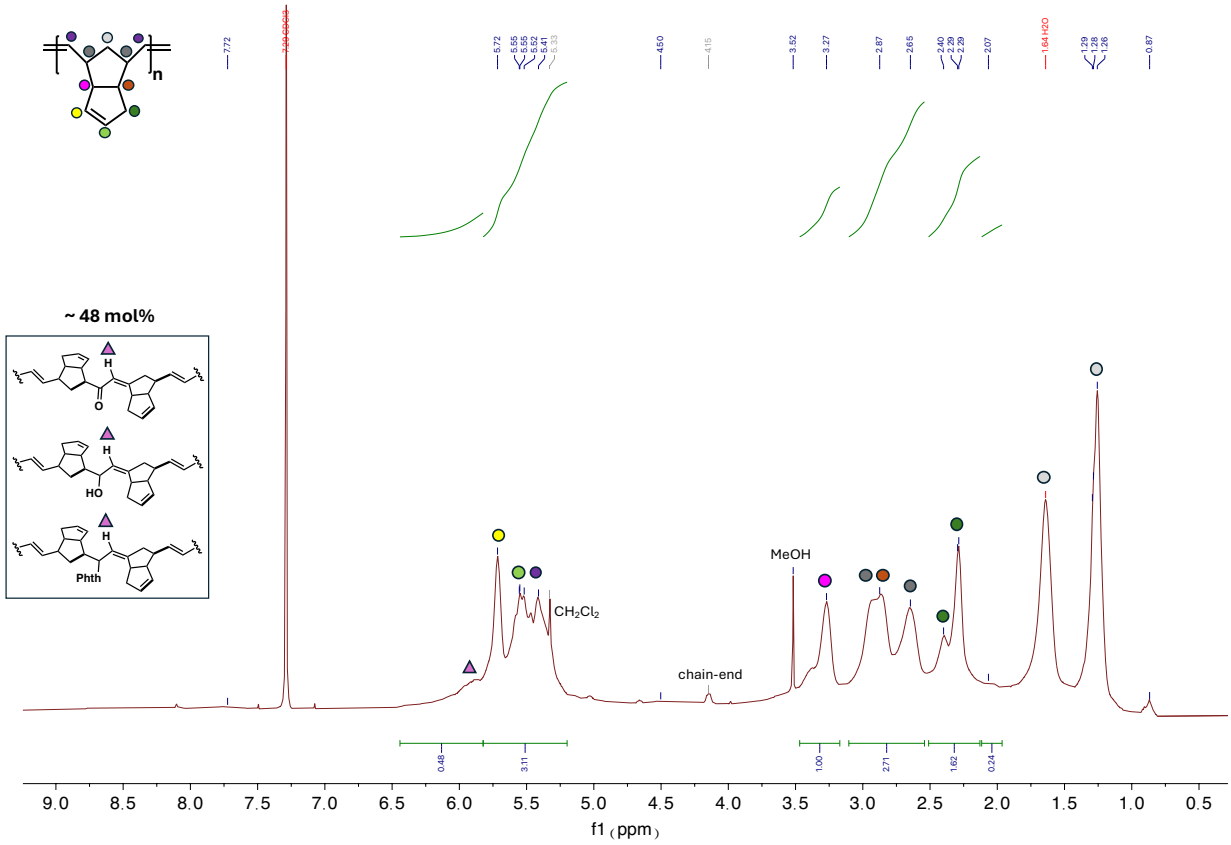

Supplementary Fig. 111 ^{1}H NMR spectrum of E-functionalized deconstructed pDCPD oligomers mediated by NHS at t = 4h (after purification), for detailed reaction conditions, see Supplementary Table 5, Entry 2.

Supplementary Table 5, Entry 2 (NHS), 6h

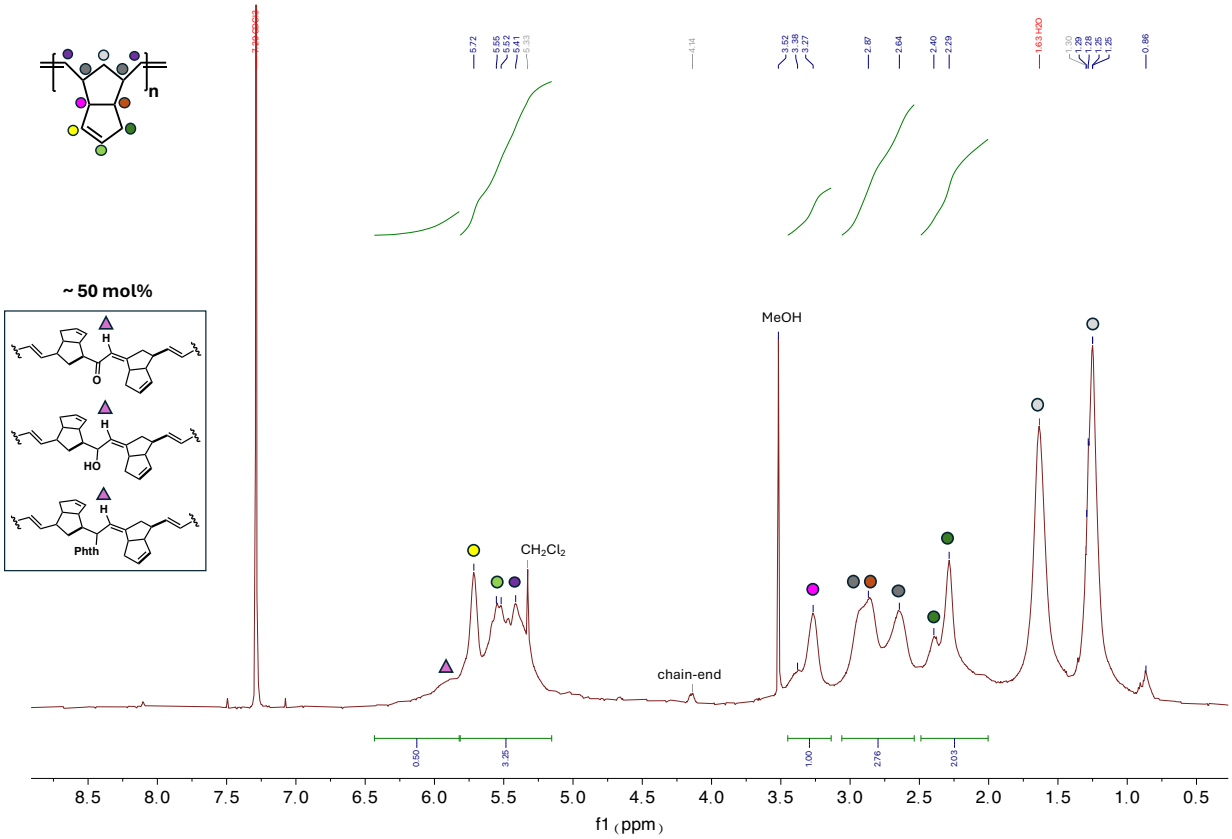

Supplementary Fig. 112 ^{1}H NMR spectrum of E-functionalized deconstructed pDCPD oligomers mediated by NHS at t = 6h (after purification), for detailed reaction conditions, see Supplementary Table 5, Entry 2.

Supplementary Table 5, Entry 3 (Cl_4NHPI), 2h

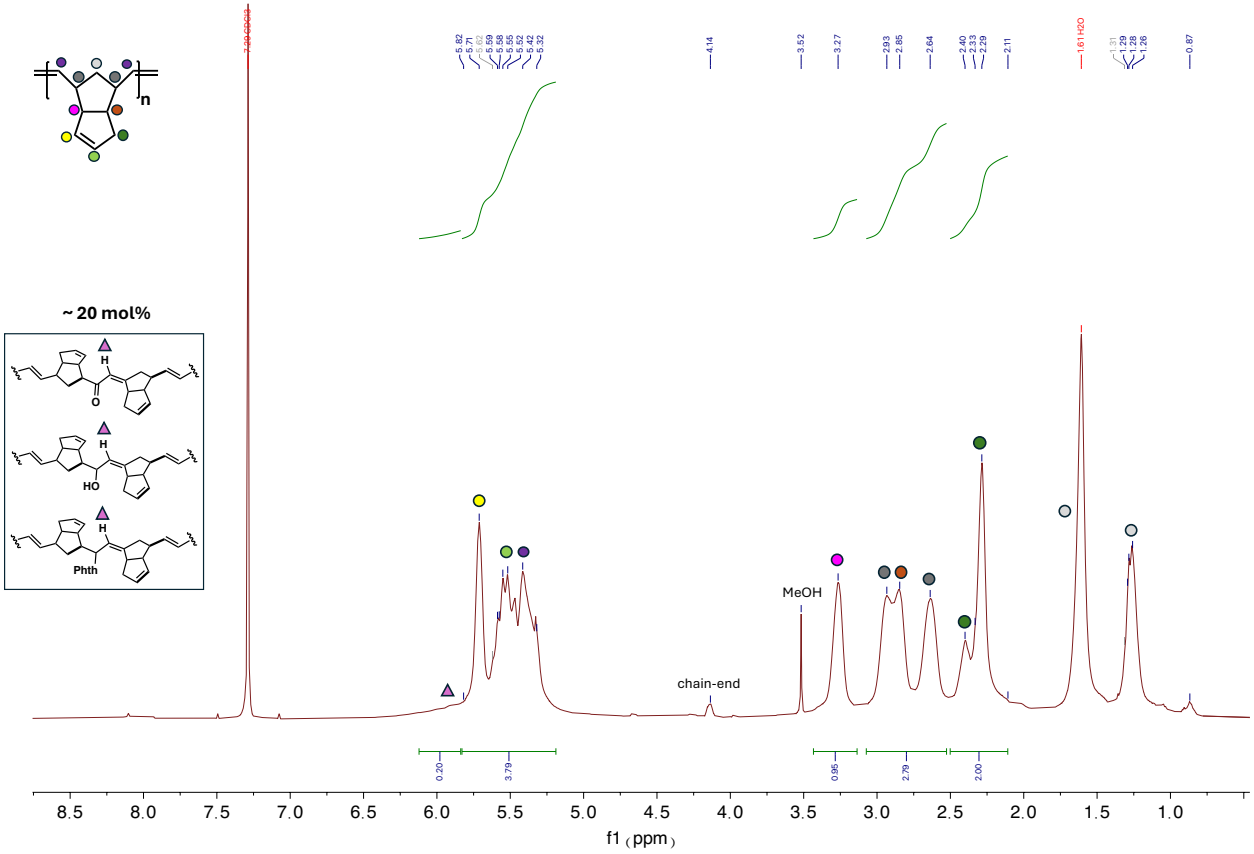

Supplementary Fig. 113 ^{1}H NMR spectrum of E-functionalized deconstructed pDCPD oligomers mediated by Cl_4NHPI at t = 2h (after purification), for detailed reaction conditions, see Supplementary Table 5, Entry 3.

Supplementary Fig. 114 Image showing insoluble solid formation during the electrochemical oxidation of deconstructed pDCPD oligomers mediated by Cl_4NHPI at t = 2 h.

References:

1. Scholl, M., Ding, S., Lee, C. W. & Grubbs, R. H. Synthesis and Activity of a New Generation of Ruthenium-Based Olefin Metathesis Catalysts Coordinated with 1,3-Dimesityl-4,5-dihydroimidazol-2-ylidene Ligands. *Org Lett* **1**, 953–956 (1999).
2. Alzate-Sanchez, D. M. *et al.* Rapid Controlled Synthesis of Large Polymers by Frontal Ring-Opening Metathesis Polymerization. *Macromolecules* **56**, 1527–1533 (2023).
3. Masjedizadeh, M. R., Dannecker-Doerig, I. & Little, R. D. Linearly fused vs bridged regioselection in the intramolecular 1,3-diyl trapping reaction. *J Org Chem* **55**, 2742–2752 (1990).
4. Husted, K. E. L. *et al.* Remolding and Deconstruction of Industrial Thermosets via Carboxylic Acid-Catalyzed Bifunctional Silyl Ether Exchange. *J Am Chem Soc* **145**, 1916–1923 (2023).
5. Wang, S. *et al.* Robust, Fire-Safe, Monomer-Recovery, Highly Malleable Thermosets from Renewable Bioresources. *Macromolecules* **51**, 8001–8012 (2018).
6. Stewart, K. A. *et al.* Biobased Polystyrene Vitrimers for Thermoset Circularity. *ACS Appl Polym Mater* **6**, 13034–13041 (2024).
7. Liu, B., Zhang, C. & Zhou, X. Access to phthalazinones via palladium-catalyzed three-component cycloamino-carbonylation of 2-formylaryl tosylates, hydrazines and CO. *Tetrahedron* **72**, 8282–8286 (2016).
8. Zhu, F., Zou, M., Shao, X. & Li, Z. On-water, catalyst-free and room-temperature construction of 2-aryl-1,3,4-oxadiazole derivatives from 1,1-dichloro-2-nitroethene and hydrazides. *RSC Adv* **5**, 61752–61758 (2015).
9. Bojaryn, K., Fritsch, S. & Hirschhäuser, C. Iterative Synthesis of Alkenes by Insertion of Lithiated Epoxides into Boronic Esters. *Org Lett* **21**, 2218–2222 (2019).
10. Yu, M., Li, G., Wang, S. & Zhang, L. Gold-Catalyzed Efficient Formation of α,β-Unsaturated Ketones from Propargylic Acetates. *Adv Synth Catal* **349**, 871–875 (2007).